2009

Specification And Function Of Early Hair Follicle Stem Cells

Jonathan Nowak

SPECIFICATION AND FUNCTION OF EARLY HAIR FOLLICLE STEM CELLS

A Thesis Presented to the Faculty of

The Rockefeller University

in Partial Fulfillment of the Requirements for

the degree of Doctor of Philosophy

by

Jonathan Nowak

June 2009

SPECIFICATION AND FUNCTION OF EARLY HAIR FOLLICLE STEM CELLS

Jonathan Nowak
The Rockefeller University 2009

In adult skin, multipotent epithelial stem cells (SCs) reside in a quiescent niche associated with each hair follicle termed the "bulge" and are essential for cyclic bouts of hair growth. Bulge stem cells can also contribute to sebaceous glands and the intefollicular epidermis when it is injured. While hair follicles begin to develop during embryogenesis, niche architecture becomes pronounced postnatally at the start of the first hair cycle. Whether SCs exist or function earlier is unknown. To determine if a stem cell population exists during follicle development, I conducted embryonic pulse-chase experiments to identify putative stem cells based on slow-cycling character. Slow-cycling cells appeared early in follicle development, where they expressed numerous SC markers, and later gave rise to the adult bulge SC population. Furthermore, early slow-cycling cells displayed a similar pattern of divisions during follicle development as activated adult bulge stem cells displayed during the postnatal hair cycle. To test whether early slow-cycling cells function as SCs, I focused on Sox9, an essential adult SC gene also expressed by early slow-cycling cells. Using *Sox9-Cre* for genetic marking and *K14-Cre* to embryonically ablate *Sox9* revealed that the progeny of Sox9-expressing cells contribute to all skin epithelial lineages and that Sox9 is required for early SC specification. In the absence of early SCs, hair follicle and sebaceous gland morphogenesis is blocked and epidermal

wound repair is compromised. To begin dissecting the molecular pathways that are required for early SC specification, a microarray screen was conducted to identify genes regulated by Sox9 during *in vivo* SC specification. Finally, purification of Sox9 expressing cells from the skin using a novel, double transgenic mouse reporter system directly demonstrated that early Sox9-positive cells display extensive colony forming ability *in vitro*, a behavior consistent with SC character. These findings establish the existence of early hair follicle SCs and reveal their physiological importance in tissue morphogenesis. Future studies of these early SCs should deepen our understanding of how SC populations are established in different tissues, and the molecular mechanisms that regulate their activity in development, adult homeostasis, and disease.

To my parents, for their continuous support and encouragement to do science

ACKNOWLEDGMENTS

First and foremost, I would like to thank Elaine Fuchs for serving as my PhD mentor. She has been generous with advice and guidance, while allowing me to independently pursue my own interests. Her remarkable work ethic and critical mindset serve as examples of her complete dedication to science and are characteristics worthy of emulation. Furthermore, she has created an ideal enviroment for scientific training. Lab members are uniformly enthusiastic, intellectually curious, and happy to share wide-ranging technical expertise.

I am especially indebted to Cedric Blanpain and Bill Lowry for helping me get started in the lab and providing encouragement and early direction for my work. Horace Rhee served as a model graduate student and taught me to be clear and concise in presenting my data. Michael Rendl and Markus Schober were always willing to discuss technical issues and the best way to do an experiment.

Valerie Horsley, Danelle Devenport, and Rui Yi provided important input on my paper and were consistently eager to talk about any aspect of biology. I am grateful to Lisa Polak for her support and technical advances in skin grafting and wound healing assays and to Nicole Stokes for tirelessly and cheerfully managing my mouse lines. Maria Nikolova's dedication to the tissue culture facility and attention to keeping the lab organized and running smoothly were appreciated on a daily basis. June Racelis also

contributed to these efforts and provided excellent technical support for *in situ* hybridizations. Amalia Pasolli contributed beautiful electron microscopy data to my work, and was a thoughtful and inquisitive colleague.

I am thankful to Benoit de Crombrugghe (Baylor University, Houston) and Andreas Schedl (INSERM, Nice) for their generosity in providing me with *Sox9-Cre* and *Sox9(fl/fl)* mice, respectively. My work relied heavily upon the technical advances of earlier lab members, and I am indebted to Cedric, Bill, Horace, Michael, and Doina Tumbar for making my experiments possible.

The Tri-Institutional MD/PhD program has been a solid base of support and guidance over the past six years, and I am especially grateful to the director, Olaf Andersen, for his commitment to maintaining the excellence of the program. I would also like to thank the members of my thesis committee, including Kathryn Anderson, David Allis, Angela Christiano and chair Alexander Tarakhovsky for their generous commitment of time, suggestions and helpful criticism to my thesis work.

Finally, I am deeply indebted to my wife, Karrie Radloff, not only for her daily support and encouragement, but also for graciously allowing me to organize my life around the schedule of mice and unpredictable demands of experiments.

TABLE OF CONTENTS

LIST OF ILLUSTRATIONS

LIST OF FIGURES

LIST OF TABLES

CHAPTER 1
INTRODUCTION

All metazoans have at least a limited ability to repair themselves after injury, and the ability of many tissues to maintain proper function and structure in the face of environmental insults has long been recognized (Birnbaum and Sanchez Alvarado, 2008; Sanchez Alvarado, 2000; Tsonis, 2000). The variable capacity of different tissues to replace themselves or respond to injury has long been correlated with the proliferative behavior of cells that comprise each tissue (Bullough, 1962b; Leblond, 1964; Pelc, 1964). More recently, such regeneration and repair has been shown to depend upon populations of stem cells resident within each tissue (Pellettieri and Sanchez Alvarado, 2007; Rando, 2006). Although some tissues appear capable of repair in response to injury without utilizing stem cells (Dor et al., 2004; Michalopoulos, 2007), strong evidence suggests that discrete stem cell populations exist in almost all mammalian tissues that undergo continual self-renewal as a part of normal function (Joseph and Morrison, 2005; Rando, 2006).

Architecture of the skin

Mammalian skin performs several critical roles for an organism, including protecting against fluid loss, physical trauma, radiation, temperature changes, and invasion by pathogens (Blanpain and Fuchs, 2006). To accomplish these tasks, the epithelial component of the skin undergoes a continual process of self-renewal, and this long-

recognized feature makes the mammalian epidermis one of the better model systems in which self-renewal can be studied (Blanpain et al., 2007; Bullough, 1962a).

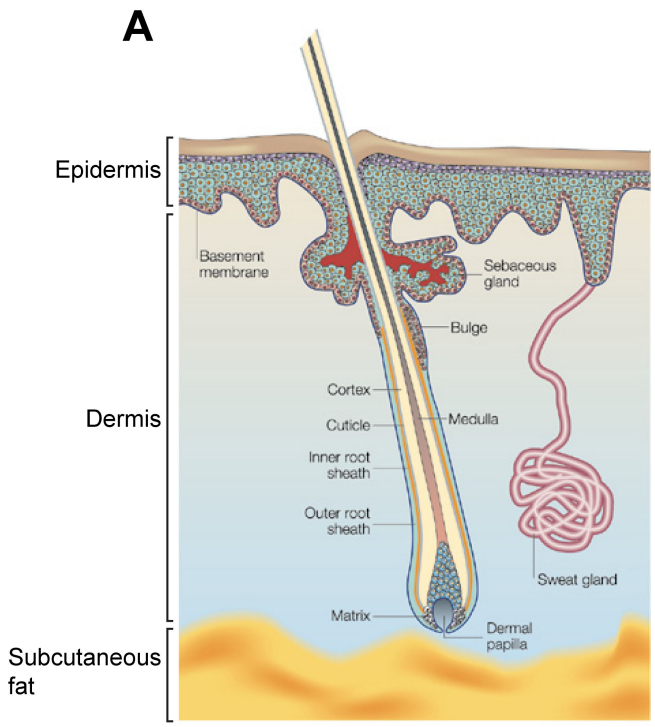

Illustration 1.1. Schematic of mammalian skin. (**A**) Adult skin contains multiple cell types and has a complex morphology. The overlying epidermis is a stratified epithelial tissue that functions as a physical barrier at the skin surface. The dermis, rich in collagen and other extracellular matrix molecules, provides a platform for epidermal organization and contributes mechanical strength to the skin. Beneath the dermis, subcutaneous fat helps skin function as an insulator to minimize heat loss. Specialized epithelial structures, such as hair follicles and sweat glands, extend downwards from the epidermis into the dermis, and generate products that help skin function. The bottom (basal) layer of the epidermis is contiguous with the outer layer of cells surrounding the hair follicle, and a basement membrane separates these epithelial cells from the dermis. Illustration adapted from Fuchs and Raghavan, 2002.

Adult skin is an architecturally complex tissue containing many specialized structures and approximately twenty different cells types derived from multiple embryonic origins (Blanpain and Fuchs, 2006). The epidermis, an ectodermal derivative, lies on the

surface of the skin and is composed of stratified epithelial cells that provide the skin's barrier function (Illustration 1.1). Below the epidermis, mesenchymal cells secrete collagen and other extracellular matrix components to form the dermis, which provides a physical support for the epidermis and gives mechanical strength to the skin. Specialized structures such as hair follicles and sweat glands are epithelial in origin and extend downwards from the epidermis into the surrounding dermis.

Within the epidermis, the bottom layer of basal cells is proliferative, and produces a flux of cells which migrate upward and continually renew the epidermis (Fuchs, 2008). Also referred to as keratinocytes, these cells are typified by expression of keratin intermediate filament proteins, such as keratin 5 and keratin 14, which are specific to the basal layer. As epidermal cells exit the basal layer and cease to proliferate, they progress upwards through three distinct differentiation stages distinguished morphologically as the spinous layer, granular layer and stratum corneum of the epidermis (Illustration 1.2). A complex series of transcriptional and metabolic alterations accompany this differentiation program, which culminates in the formation of a cross-linked protein scaffold and lipid bi-layer responsible for the skin's barrier function (Fuchs and Raghavan, 2002). In humans, the turnover time of the epidermis is approximately one month. Mouse epidermis is thinner, consistent with the abundant hair coat providing the bulk of physical protection rather than the epidermal surface, and displays a turnover time of 10-14 days (Potten, 1975). While the precise organization of cells within the basal layer

remains under investigation, it appears that many if not all basal cells can function as unipotent progenitors for renewal of the epidermis (Clayton et al., 2007).

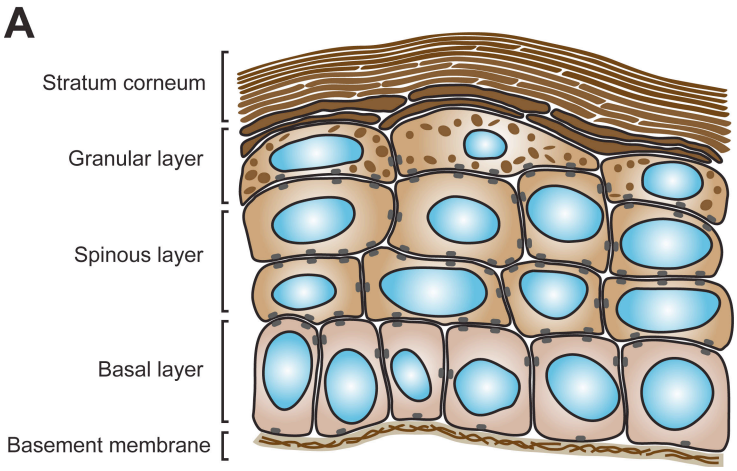

Illustration 1.2. The cellular architecture of the epidermis. (**A**) The process of epidermal differentiation is shown in this schematic, illustrating the basement membrane, separating the epidermis from the underlying dermis, the proliferative basal layer, and the three differentiation stages: spinous layer, granular layer and outermost stratum corneum. Progenitor cells within the basal layer undergo continuous division to generate a flux of cells that move upwards and undergo a series of stepwise transcriptional, cytoskeletal and metabolic changes. This process culminates in production of a protein and lipid barrier that renders the skin impermeable to liquids and pathogens.

Underscoring its essential physiological role, the epidermis begins stratification during embryonic development and is a completely functioning barrier by the time animals are born (Fuchs, 2007). Basal cells are known to undergo both symmetric and asymmetric division during the initial embryonic stratification process and also during adult homeostasis (Clayton et al., 2007; Lechler and Fuchs, 2005). Numerous positive and negative regulatory pathways function to control the balance of proliferation and

differentiation in the epidermis, allowing wounds to heal quickly while minimizing the chance that excessive proliferation leads to cancer (Fuchs and Raghavan, 2002).

Morphogenesis of the hair follicle

Beyond forming a stratified epithelial barrier, the mammalian epidermis gives rise to a wide variety of specialized epithelial appendages, including mammary glands, apocrine and eccrine sweat glands, nails, and hair follicles. Notably, while all of these appendages seem quite distinct, they all begin development in a similar way (Mikkola, 2007), and knowledge of this process has been gained by studying the embryonic skin at a stage when it exists as a single layered epithelium.

Prior to hair follicle morphogenesis, a uniform layer of epithelial cells overlies a disperse population of dermal cells. At ~E14.5 of mouse development, mesenchymal-epithelial interactions result in the formation of the first wave of hair placodes, which appear as small epidermal invaginations extending from the basal layer into the dermis (Illustration 1.3A). Once specified, signals from the epithelium cause dermal cells to aggregate and form a dermal condensate under each placode (Schmidt-Ullrich and Paus, 2005). This specification process occurs in four overlapping waves, with rare primary guard hairs being specified at E14.5 and the remainder of follicles being specified from E15.5 to P0. Soon after specification, proliferative placodes transform into hair germs, which grow more deeply into the dermis, and subsequently become hair pegs. Beginning at the peg stage, regional variations in proliferative status appear in the follicle, with the

most proliferative cells localizing to the bottom leading edge of the follicle, where they are in direct contact with the dermal condensate. These highly proliferative leading edge cells give rise to the hair follicle matrix population as they surround the dermal condensate, which then becomes the dermal papilla (DP). While the matrix is transient, proliferating and differentiating only during the growth (anagen) phase of the hair cycle, the DP remains permanently associated with each follicle.

The matrix produces two main differentiating structures: a three-layered (Henle, Huxley, cuticle) inner root sheath (IRS) and a three-layered (cuticle, cortex, medulla) central hair shaft (HS) (Muller-Rover et al., 2001). The IRS forms first, providing the channel for the emerging hair. Both of these structures are internal to the outer root sheath (ORS), whose cells are in direct contact with the basement membrane and are topologically contiguous with the basal layer of the interfollicular epidermis. Reciprocal signaling between the DP and transit amplifying (TA) matrix cells in the bottom portion of the hair follicle, or bulb, is important for instructing the matrix progeny to engage in the distinct programs of gene expression that generate the full complement of differentiated cells lineages in the hair follicle. As the hair shaft elongates, neural crest-derived melanocytes, located in a region of the matrix just above the dermal papilla, provide pigment to the differentiating cells of the hair shaft, giving them their color (Slominski et al., 2005).

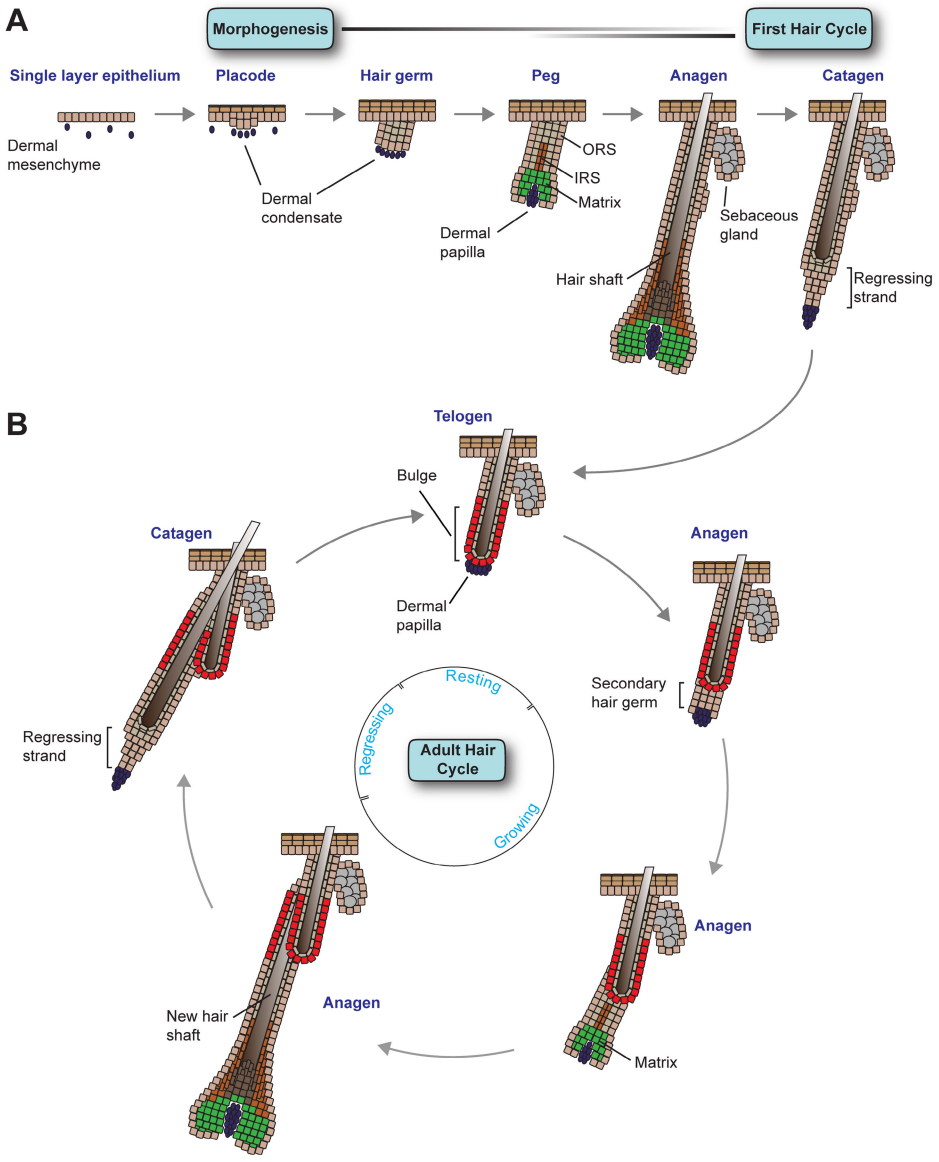

Illustration 1.3. Embryonic hair follicle morphogenesis and the adult hair hair cycle. (**A**) The process of follicle morphogenesis begins at ~E14.5 when small invaginations termed placodes appear in the basal layer of the epidermis. Follicle morphogenesis reaches completion at ~P9, when follicles reach maximum length, marking full entrance into anagen. After hair coat production, follicles transition to catagen, where the matrix degenerates into a regressing epithelial strand which draws the dermal papilla (DP) upwards to rest below the newly formed adult bulge niche. (**B**) Direct contact between the DP and adult bulge indicates the onset of telogen. Soon thereafter, bulge stem cells are activated and a secondary hair germ grows downwards, signaling entry into the next anagen. After several weeks of growth, anagen ceases and follicles again enter catagen. After a variable period of time, bulge stem cells are again activated to initiate a new hair growth cycle.

At birth, sebaceous gland precursor cells appear in the upper portion of the ORS, and the sebaceous gland forms shortly thereafter (Horsley et al., 2006; Schmidt-Ullrich and Paus, 2005). The major role of the sebaceous gland is to generate terminally differentiated sebocytes, which degenerate to release lipids and sebum and lubricate the skin surface as they are expelled from the sebaceous gland into the hair canal (Alonso and Rosenfield, 2003; Stewart, 1992).

For most backskin follicles of the mouse, maturation is completed towards the end of the first postnatal week, when follicle downgrowth stops and the upward-moving, terminally differentiated hairs break through the skin surface (Schmidt-Ullrich and Paus, 2005). Follicles then remain in a growing, anagen state for another 7-9 days before they synchronously cease growing and enter into a destructive phase of the hair cycle (catagen), followed by a resting phase (telogen) before a new cycle of hair growth begins. While new hair follicles may form under certain wound condition in the skin, the number and location of hair follicles is generally set during embryogenesis and does not change throughout the lifetime of an organism (Ito et al., 2007; Schmidt-Ullrich and Paus, 2005).

Molecular regulation of hair follicle morphogenesis

The developmental decision to form a hair follicle is the result of mesenchymal-epithelial cross-talk which integrates multiple instructive signals necessary to initiate hair

follicle morphogenesis. These signaling cues include Wnt/β-catenin, sonic hedgehog (Shh), fibroblast growth factors (FGFs) and bone morphogenic proteins (BMPs).

Several lines of evidence suggest that activation of Wnt/β-catenin signaling in epithelial cells is a key initial step in placode formation (Schmidt-Ullrich and Paus, 2005). β-catenin is localized at cell-cell adherens junctions in a complex with E-cadherin and α-catenin. Excess β-catenin in the cytoplasm is normally rapidly degraded by a proteasome-mediated pathway. Upon receipt of a Wnt signal by transmembrane Frizzled receptors, the degradation of excess β-catenin is inhibited, and stabilized β -catenin can then translocate into the nucleus where it partners with members of the Lef/Tcf family of DNA binding proteins and functions as an activating transcription factor complex (Logan and Nusse, 2004). The transcription factor Lef1 can be readily detected in the nuclei of developing placode cells (DasGupta and Fuchs, 1999; van Genderen et al., 1994; Zhou et al., 1995). Transgenic mice harboring the "Wnt reporter" gene *TOPGAL*, containing an enhancer element composed of multimerized Lef1 binding sites, have confirmed the specific transcriptional activity of the bipartite transcription factor complex composed of Lef1 and stabilized β-catenin in the placode (DasGupta and Fuchs, 1999; Millar, 2002). Notably, when the Wnt inhibitor Dickoff 1 (Dkk1) was expressed ectopically or when *β-catenin* was conditionally targeted for ablation in epithelial cells, hair follicle morphogenesis was blocked altogether, while mice lacking Lef1 displayed a reduced number of follicles (Andl et al., 2002; Huelsken and Birchmeier, 2001; van

Genderen et al., 1994). Strong evidence for Wnt signaling as a sufficient, instructive cue for placode formation came from experiments expressing excessive Lef1 or stabilized β-catenin in the epithelium, which resulted in mice exhibiting ectopic hair follicle formation (Gat et al., 1998; Zhou et al., 1995). Recently Cotsarelis and colleagues (Ito et al., 2007) showed that when the skin of normal mice is severely wounded, endogenous Wnt signaling is elevated in the regenerating epithelium and this leads to the induction of hair follicle formation from epidermal stem cells. Taken together, these findings underscore the role for Wnt signaling and stabilized β-catenin in governing the choice of whether to become epidermis or hair follicle.

In contrast to Wnt signaling, which is activated during placode formation, BMP signaling must be inhibited for placode morphogenesis to progress. One dermal cue which appears to be particularly critical is the BMP inhibitory protein Noggin, whose absence severely impairs hair follicle morphogenesis (Botchkarev et al., 1999) as well as hair cycling (Botchkarev et al., 2001). When skin is genetically engineered to overexpress Noggin, genes controlling cell-cycle progression are enhanced (Sharov et al., 2006). Consistent with these findings, mice conditionally null for the *BMPR1a* receptor in the epithelium form the correct number of hair follicles, which are later blocked in differentiation of the inner root sheath and hair shaft (Andl et al., 2004; Kobielak et al., 2003; Ming Kwan et al., 2004; Yuhki et al., 2004). The interplay between the Wnt and BMP pathways is highlighted by the requirement of BMP inhibition for proper Lef1

expression in the placode (Andl et al., 2004; Jamora et al., 2003; Kobielak et al., 2003). More recently, it was found that inhibition of BMPs also contributes to stabilization of β-catenin (Kobielak et al., 2007; Zhang et al., 2006)

Interestingly, while this paradigm serves the bulk of follicle morphogenesis, the external cues that trigger these internal regulatory processes differ for the formation of the large primary guard hairs. The guards are the first hair follicles to appear in embryonic backskin, and they are uniquely dependent upon a ligand-receptor complex composed of the TNF-related ectodysplasin (Eda) and the Eda receptor (EdaR) (Schmidt-Ullrich and Paus, 2005). Notably, Eda/EdaR signaling results in induction of two BMP inhibitors different from Noggin, namely Ccn2/Ctgf and Follistatin (Pummila et al., 2007). *Eda* is itself a target of Wnt signaling (Laurikkala et al., 2001), which is already active at this time, as judged by *TOPGAL* reporter activity and Lef1/β-catenin (DasGupta and Fuchs, 1999). Thus, while the initiating events may differ, the recipe for hair follicle morphogenesis has many common ingredients across different hair types.

In order to drive hair follicle morphogenesis, signaling pathways ultimately have to elicit changes in the expression and dynamics of the extracellular matrix (ECM), cytoskeleton, and cell-matrix and cell-cell junctions in order to remodel the epithelium from its single layer to a hair placode. Several changes which accompany this process involve downregulation of some adhesion proteins, such as E-cadherin, and upregulation of others, such as P-cadherin (Hirai et al., 1989). One intriguing intersection between

signaling and cytoskeletal organization is that the *E-cadherin* gene itself harbors a functional Lef1 binding site and is downregulated concomitant with the appearance of Wnt reporter activity in developing placodes (Jamora et al., 2003). Consistent with direct regulation by Wnt signaling, this shift in cadherin expression is one of the earliest visible signs of hair follicle specification and occurs even before placodes adopt their distinct morphological appearance.

Once the placode forms, signaling events downstream of Wnts/BMPs drive the downgrowth and maturation of hair follicles. Sonic hedgehog (Shh) is an early gene expressed downstream of Wnt/BMP receptor signaling (and Eda/EdaR in the case of guard hairs) once placodes have formed (Gat et al., 1998; Morgan et al., 1998; Oro et al., 1997; St-Jacques et al., 1998). Without *Shh*, hair follicles arrest at the placode stage and fail to form a dermal condensate, suggesting critical roles for Shh in proper epithelial-mesenchymal signaling and the dramatic expansion of cells involved in the transition from a placode to a mature follicle (Hardy, 1992; Levy et al., 2007b; Oro and Higgins, 2003; St-Jacques et al., 1998). That said, many facets of Shh's role in skin appendage formation remain mysterious. This is perhaps best exemplified by recent studies showing that abrogation of Shh responsiveness in the epithelium by *K14-Cre* mediated conditional targeting of the transmembrane protein Smoothened leads to hair follicles which adopt features of mammary glands during development (Gritli-Linde et al., 2007).

One recurring theme in hair follicle biology is re-use of the same signaling pathways at successive stages in follicle morphogenesis and cycling. Thus, while Wnt, BMP, and Shh signaling are all necessary for proper follicle specification and early development, they also play spatially and temporally distinct roles in the differentiation program required for matrix cells to produce a differentiated hair shaft in more developed follicles. All of these pathways exert additional effects on stem cell activation and maintenance in the adult hair cycle. Thus, the role of any given signaling pathway in the hair follicle is highly dependent upon location of activity and developmental timing. This overlap and re-use of signaling pathway activity poses a molecular challenge to hair follicle cells which must not only integrate signals received from multiple pathways, but respond in a manner appropriate to their location and developmental fate.

Homeostasis in adult skin

The postnatal hair cycle

As a normal feature of skin homeostasis, the hair follicle undergoes cyclic bouts of degeneration and regeneration, producing a new hair with each cycle (Illustration 1.3B). During the hair growth phase of the cycle (anagen), the DP acts as a signaling center for the epithelial–mesenchymal cross-talk that regulates the balance between matrix cell proliferation and hair production (Alonso and Fuchs, 2006; Schmidt-Ullrich and Paus, 2005). TA matrix cells proliferate rapidly during anagen, but then disappear when follicle growth ceases. After the anagen phase of the first hair cycle in postnatal mice, which is

an extension of initial follicle morphogenesis, follicles enter a destructive phase (catagen) (Illustration 1.3B). Beginning at ~P16, this stage is initially characterized by massive apoptosis of matrix cells. Over the ensuing 3 days, the hair bulb of each follicle degenerates into an epithelial strand which regresses, dragging the DP upwards to the base of the permanent, non-cycling portion of the follicle.

In mice, backskin follicles have all entered telogen by P19, and they remain in this resting phase for several days (Illustratin 1.3B). After this time, bulge stem cells are activated and a secondary hair germ grows downwards from the base of the bulge niche, signaling entry into the anagen phase of the next hair cycle. The emergence of a new hair follicle from the side of the original club hair lends the stem cell niche its characteristic "bulge" morphology and divides the CD34-positive stem cells in the bulge into two populations based on high or low integrin expression levels and adherence to the basement membrane. In a process which has many similarities to initial hair follicle morphogenesis, the highly proliferative secondary germ expands and gives rise to a new matrix, which begins to produce the differentiated lineages first of the inner root sheath and then of the hair shaft (Schmidt-Ullrich and Paus, 2005). This new hair shaft then exits from the same channel as the existing club hair. After several weeks of growth, anagen ceases and follicles enter catagen, again drawing the DP upwards to rest below the bulge stem cell niche. After telogen, bulge stem cells are again activated to initiate a new hair growth cycle.

As mice age, the anagen and catagen phases remain relatively constant in length. In contrast, the telogen phase of the hair cycle increases in length during later hair cycles. While the first several rounds of the hair cycle are synchronized and occur at very predictable times, individual follicles become more asynchronous as animals age. The ability of old club hairs to remain in their socket through several rounds of hair cycling means that only a portion of the hair coat is replaced during each cycle.

Identification of adult hair follicle stem cells

The ability of the postnatal hair follicle to regenerate has long been recognized to require a reservoir of epithelial stem cells (Chase, 1954). Given their close proximity to the dermal papilla and obvious involvement in hair shaft production, it was long believed that matrix cells were the stem cells that allowed the follicle to regenerate over multiple hair cycles (Kligman, 1959). However, functional experiments which either used X-ray irradiation to ablate matrix cells or microdissection and transplantation assays to assess the regenerative capacities of different portions of whisker follicles both demonstrated that the matrix is dispensable for hair regeneration activity, and that this ability instead rests in cells within the ORS (Jahoda et al., 1984; Montagna and Chase, 1956; Oliver, 1966a, b, 1967). Further evidence suggestive of a stem cell population in the ORS was provided by pulse-chase studies which showed that cells within the "bulge" region of the ORS specifically retain nucleotide label (Cotsarelis et al., 1990). While by no means an absolute indication of stem cell functionality, slow-cycling behavior has been detected in

many subpopulations of cells within epithelial and other regenerative tissues and appears to be a relatively common feature of stem cell populations (Bickenbach, 1981; Blanpain et al., 2007; Potten, 1974). Notably, the bulge region that contains label retaining cells (LRCs) is located at the lowest permanent, non-cycling portion of the hair follicle, an anatomic niche ideally suited to protecting stem cells from injury for the lifetime of an organism.

Although much circumstantial data implicated label retaining bulge cells as the stem cells of the hair follicle, direct testing of this hypothesis only recently became possible with the development of methods to prospectively mark and purify bulge cells. These methods specifically identify bulge cells based upon either a) bulge cell surface markers α6-Integrin and CD34 coupled with *K14-GFP* transgene expression (Blanpain et al., 2004); b) specific *K15*-promoter activity driving GFP or Cre recombinase expression in the bulge (Morris et al., 2004) or c) a tetracycline-regulatable H2B-GFP *in vivo* pulse chase system which labels slow-cycling cells in the skin epithelum (Tumbar et al., 2004). All of these methods are compatible with isolation of viable bulge cells by fluorescence-activated cell sorting (FACS), making it possible to perform experiments on pure bulge cell populations.

Lineage tracing experiments using a bulge-preferred *K15*-promoter expressing an inducible Cre recombinase demonstrated that cells in the bulge can contribute to all epithelial lineages in the skin, including hair follicles, sebaceous glands and interfollicular

epidermis, confirming the previously hypothesized potential for these cells (Morris et al., 2004; Pinkus, 1981). This result was consistent with analysis of H2B-GFP label retaining bulge cells which suggested that the progeny of label retaining bulge cells can exit the niche, proliferate and contribute to the interfollicular epidermis during wound repair and growing hair follicles during normal homeostasis (Tumbar et al., 2004). Remarkably, when the progeny of a isolated genetically marked rodent bulge cells are expanded in culture and then grafted onto host recipients, they give rise to all skin epithelial lineages and even regenerate the bulge stem cell niche (Blanpain et al., 2004). This result was later corroborated by similar transplantation experiments using single, genetically marked cells isolated from the bulge region of rat whiskers and passaged for more than 100 generations (Claudinot et al., 2005). Together, these clonal studies provided the first evidence that individual bulge cells are multipotent. Importantly, these studies further revealed that normally slow-cycling bulge cells display hallmark epidermal stem cell behavior (Barrandon and Green, 1987) in culture and can retain functional multipotency when removed from their native niche (Blanpain et al., 2004; Claudinot et al., 2005; Morris et al., 2004). The extent to which the bulge is homogeneous is still unknown, as clonal analysis of bulge stem cells prior to culturing has not yet been achieved.

Multipotency of adult hair follicle stem cells

Although transplantation and lineage tracing studies on bulge stem cells definitively demonstrated that individual bulge stem cells can give rise to all three epithelial lineages of the skin under some conditions, it has been considerably more challenging to define the normal homeostatic lineage contributions of bulge cells residing in their native niche.

Consistent with the early hypothesized role of bulge stem cells (Cotsarelis et al., 1990), strong evidence supports the notion that bulge cells give rise to the temporary portion of the hair follicle responsible for producing a new hair shaft during the hair cycle (Illustration 1.4). *K15-CrePR* lineage tracing studies (Morris et al., 2004) support the anatomic observation that the temporary portion of hair follicles grows out of the base of the bulge niche during the anagen phase of the hair cycle, while label retaining studies (Taylor et al., 2000; Tumbar et al., 2004) suggest that follicle growth is accompanied by migration of cells out of the bulge. Measurement of cycling rates in the bulge itself demonstrates an increase in bulge cell proliferation specifically during anagen, consistent with bulge cells contributing to follicle growth (Blanpain et al., 2004; Waghmare et al., 2008).

Finally, some evidence suggests that the secondary hair germ, a small population of cells positioned between the base of the bulge and the dermal papilla, contributes to the lower, cycling portion of the hair follicle (Panteleyev et al., 2001). However, pulse-chase

studies suggest that the bulge itself gives rise to the cells of the secondary hair germ at the end of each hair cycle (Ito et al., 2004), and that matrix cells are transient and do not survive catagen (Ito et al., 2004; Tumbar et al., 2004). Notably, ablation of the bulge and secondary hair germ in adult mice using a thymidine kinase suicide gene expressed by the *K15*-promoter shows that hair follicles completely degenerate and cease hair production when the bulge and secondary hair germ populations are lost (Ito et al., 2005).

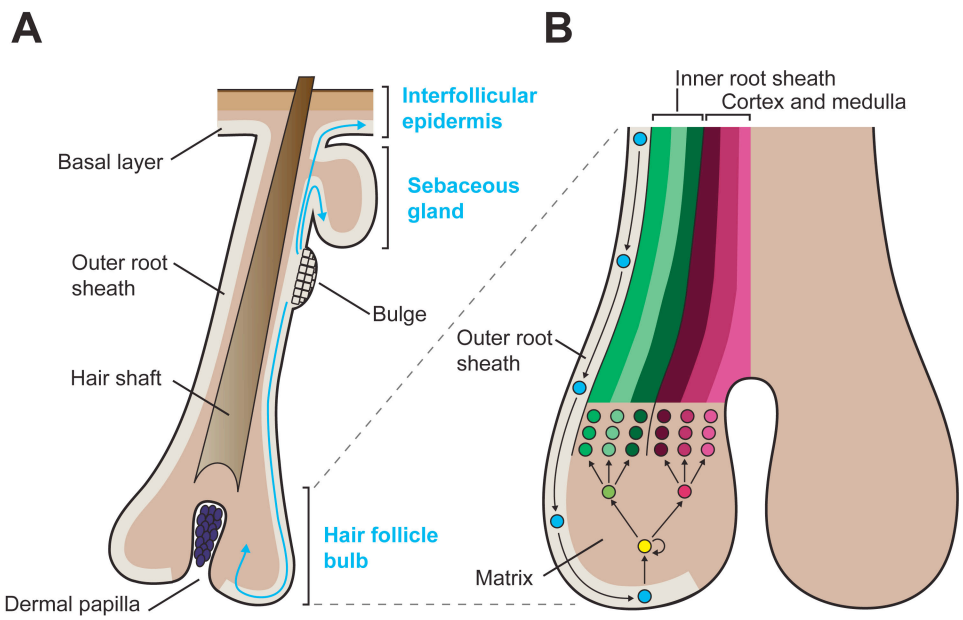

Illustration 1.4. Multipotency of adult bulge epithelial stem cells. (**A**) Epithelial stem cells reside in a specialized niche in the upper outer root sheath of each hair follicle and can give rise to all three epithelial lineages of the skin. During normal homeostasis, bulge stem cells are periodically activated to form a new hair follicle. During the hair follicle growth period (anagen), bulge cells migrate down the lower ORS towards the matrix, which is a specialized population of highly proliferative transit-amplifying cells responsible for producing a new hair. Bulge stem cells can also migrate to and differentiate along a sebaceous gland lineage when sebaceous progenitors are absent or impaired. In a wound environment, bulge stem cells can migrate upwards and out of the hair follicle to contribute to regeneration of the interfollicular epidermis. (**B**) As bulge progeny migrate down the ORS, they subsequently detach from the basement membrane and enter the matrix. Matrix cells then differentiate along one of six hair lineages, three of which comprise the inner root sheath and three of which comprise the cortex and medulla of the hair shaft. Intimate contact with the dermal papilla is essential for maintaining the high proliferative capacity of the matrix and driving lineage decisions.

Although bulge cells are clearly necessary to form the cycling hair follicle lineage, whether they proliferate continuously throughout anagen or merely undergo a transient burst of proliferation to initiate anagen is less clear. While transit-amplifying matrix cells

are highly proliferative throughout all of anagen (Potten et al., 1971), the majority of bulge cell proliferation has been reported to occur in a burst within the first four days of anagen initiation (Ito et al., 2004; Wilson et al., 1994). These results suggest that a transient burst of bulge proliferation at the beginning of anagen is sufficient to form a matrix population which then self-renews throughout the rest of anagen independent of bulge input. In contrast, lineage tracing experiments using transplanted bulge cells from rat whisker follicles demonstrate a continuous, progressive flux of cells from the bulge region down the ORS towards the matrix, consistent with ongoing bulge cell division throughout anagen (Illustration 1.4) (Oshima et al., 2001). These lineage tracing studies are supported by the finding that many cells in the bulge can be labeled by a three day BrdU pulse administered beginning at P28 when follicles are in mid-anagen (Lowry et al., 2005). The ability of bulge cells to exit their niche throughout anagen provides an explanation for how the size of the bulge remains constant during the hair cycle despite the continuous slow division of bulge cells during anagen. Dissecting the relative contributions of the bulge and secondary hair germ to hair follicle growth, as well as determining whether bulge cell proliferation is a discrete, transient event at the beginning of anagen or a continuous process that occurs throughout anagen has major implications for the types of molecular mechanisms that can be expected to regulate bulge cell activation and the adult hair cycle in general (Blanpain and Fuchs, 2006; Stenn and Paus, 2001).

While bulge stem cells clearly have the ability to regenerate sebaceous glands in transplantation assays (Blanpain et al., 2004; Claudinot et al., 2005; Morris et al., 2004; Oshima et al., 2001), the extent to which they normally contribute to sebaceous gland homeostasis is unknown. Because of the holocrine nature of sebaceous gland secretions, in which dead, differentiated cells filled with lipids and sebum are constantly being lost, sebaceous gland homeostasis necessitates a population of progenitor cells. Consistent with this notion, lineage tracing by retroviral mediated gene transfer suggests that a small population of cells near or at the base of the SG might be long-lived progenitor cells (Ghazizadeh and Taichman, 2001).

Recently, the transcriptional repressor protein Blimp1 was shown to mark a small population of cells at the SG base (Horsley et al., 2006). These Blimp1-positive cells appeared to be in close association with the basement membrane that surrounds the gland and genetic lineage tracing experiments revealed that the Blimp1-positive SG cells can regenerate the entire gland, including the differentiated sebocytes. When *Blimp1* was conditionally targeted for ablation, SGs became larger, a phenotype likely due to Blimp1's ability to transcriptionally repress *c-myc*, a gene known to induce SG hyperplasia and sebocyte differentiation (Arnold and Watt, 2001; Waikel et al., 2001). Notably, Blimp1-negative bulge cells show signs of active cycling and reduced label retention in the absence of Blimp1-marked SG progenitors (Horsley et al., 2006). This result suggests

that bulge cells can be recruited to maintain the sebaceous lineage when resident sebaceous gland progenitor cells are defective (Illustration 1.4).

Similar to the sebaceous gland, the interfollicular epidermis appears to contain a distinct reservoir of unipotent progenitor cells. While nucleotide double labeling experiments in non-wounded skin suggested that cells from the upper portion of neonatal follicles can migrate into the interfollicular epidermis (Taylor et al., 2000), more comprehensive studies using a *Shh-Cre* transgene to genetically mark the majority of cells in the hair follicle, including the bulge, failed to show a substantial contribution of hair follicle cells to the interfollicular epidermis either during skin morphogensis or adult homeostasis (Levy et al., 2005). The *Shh-Cre* study supported an earlier study using inducible *K15-CrePR* to mark adult bulge cells which suggested that the bulge rarely contributes to normal interfollicular homeostasis (Morris et al., 2004). Direction functional evidence for a progenitor population in the interfollicular epidermis came from studies which ablated hair follicles and the bulge in adult skin by either conditional deletion of *β-catenin* or a *K15*-promoter regulated thymidine kinase suicide gene (Ito et al., 2005; Lowry et al., 2005). In both of these cases, hair follicles were quantitatively lost while the epidermis remained unhindered in its ability to renew.

While the presence of a unipotent progenitor population in the interfollicular epidermis is now well established, the organization of these cells and the level of heterogeneity within the basal layer are less well understood. Numerous genetic marking

methods shows that labeled cells can persist in the interfollicular epidermis after many rounds of epidermal turnover and multiple hair cycles, suggestive of a long-term self-renewing poplation of cells (Ghazizadeh and Taichman, 2001; Ro and Rannala, 2004). In addition, BrdU-based pulse-chase experiments have demonstrated the persistence of label retaining cells in the interfollicular epidermis after 140 days of chase (Braun et al., 2003). While some proliferation studies and investigations into the clonal organization of the epidermis suggest that the epidermis is composed of discrete epithelial proliferative units (EPUs), containing a single central stem cell, surrounded by 9-10 transit-amplifying cells which continuously give rise to differentiated suprabasal cells (Potten, 1974), a more recent study which examined the size of epithelial clones over time concluded that all basal cells might be functionally equivalent SCs (Clayton et al., 2007). Consistent with this notion, no known markers in the interfollicular epidermis of mice prospectively identify a discrete population of stem cells.

In contrast to the lack of hair follicle input to the interfollicular epidermis during normal homeostasis, cells from the hair follicle are clearly able to participate actively in regeneration of the interfollicular epidermis during wound healing (Illustration 1.4) (Levy et al., 2007a; Morris et al., 2004; Tumbar et al., 2004). However, it appears that the ability of hair follicle derived cells to differentiate along the interfollicular lineage during wound healing is somewhat imperfect, because most traces of the hair follicle contribution to the regenerated IFE disappear several weeks after wound closure (Ito et

al., 2005). In this regard, the hair follicle contribution to the IFE acts as a transit-amplifying population that promotes rapid wound healing but not subsequent IFE maintenance. Nevertheless, IFE wound healing is delayed in the absence of hair follicles, underscoring the physiological importance of the transient hair follicle contribution to regenerating IFE (Langton et al., 2008).

In summary, while transplantation assays and lineage tracing show that bulge cells can give rise to all three epithelial lineages of this skin, unipotent progenitor populations within the sebaceous gland and interfollicular epidermis appear to have substantial capacity to maintain these structures in the absence of bulge input. Intriguingly, in severe wound environments, elevated Wnt signaling appears capable of directing *de novo* hair follicle formation within regenerated epidermis (Ito et al., 2007), hinting at a possible plasticity within the unipotent progenitor populations. With the identities of the distinct stem and progenitor populations in the skin just now becoming clear, more investigation will undoubtedly be necessary to define the molecular mechanisms which regulate self-renewal, lineage decisions and differentiation within and between these populations.

Molecular regulation of adult hair follicle stem cells

The isolation and transcriptional profiling of bulge SCs has shed a great deal of light on the mechanisms which regulate the characteristics and behavior of follicle SCs. These studies suggested that numerous signaling pathways act on the bulge and its direct

progeny to influence stem cell activation and lineage commitment (Illustration 1.5). Chief among these pathways is Wnt signaling. Bulge cells are known to express several Frizzled Wnt receptor proteins, as well as Tcf3 and Tcf4, two of the four key terminal effectors of Wnt signaling. However, bulge cells appear to generally be in a state of repressed Wnt signaling, as suggested by the bulge-preferred expression of numerous Wnt-inhibitory molecules (sFRP1, Dkk3, Wif1) and minimal expression of Wnt ligands by bulge stem cells (Tumbar et al., 2004). Consistent with this notion, bulge cells in telogen follicles lack nuclear β-catenin and are negative for *TOPGAL* Wnt reporter gene activity (DasGupta and Fuchs, 1999; Lowry et al., 2005). In the absence of Wnt-dependent nuclear β-catenin, Tcf3 appears to function as a transcriptional repressor, and transgenic mice expressing Tcf3 outside of the bulge niche display inhibition of differentiation along all three skin lineages and induction of bulge stem cell markers in cells where Tcf3 is ectopically expressed, suggesting that Tcf3 may function as a key regulator for maintaining bulge stem cells by preventing activation of differentiation programs (Merrill et al., 2001; Nguyen et al., 2006).

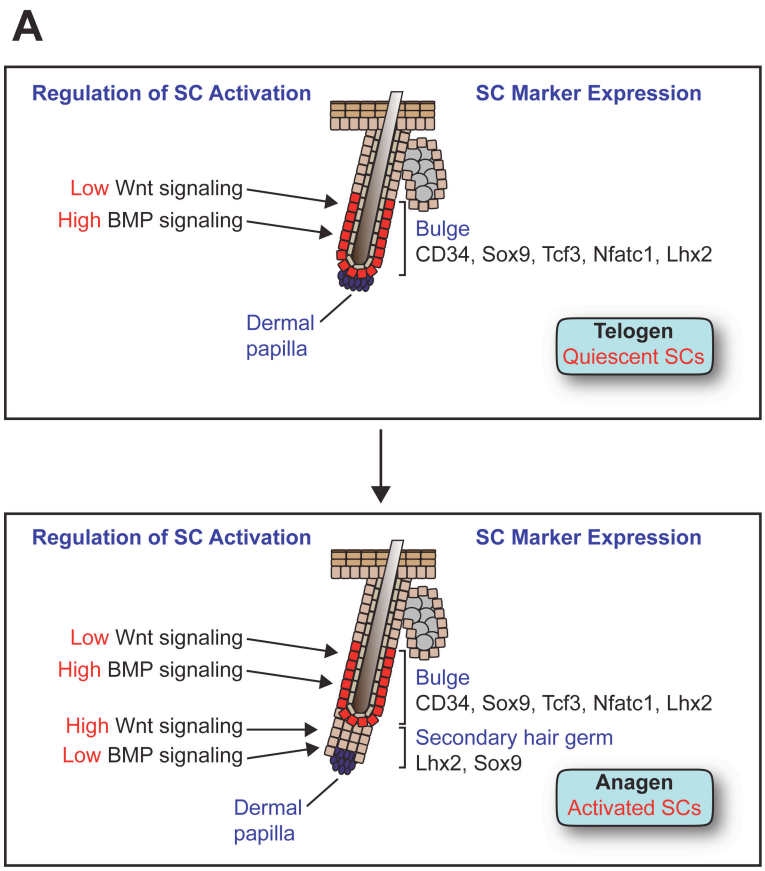

Illustration 1-5. Regulation of stem cell identity and activity in the adult bulge niche. (A) In telogen phase hair follicles, stem cells residing in the bulge are quiescent and express the markers CD34, Sox9, Tcf3, Nfatc1, and Lhx2. High levels of BMP signaling maintain stem cells in a quiescent state, while low levels of Wnt signaling may help to maintain stem cell identity but are insufficient to drive SC activation. In early anagen phase hair follicles, stem cells in the bulge proliferate and give rise to a secondary hair germ, which loses most SC markers but still retains Sox9 and Lhx2 expression. In contrast to the bulge, BMP signaling is downregulated and Wnt signaling is upregulated in the germ, allowing cells to proliferate rapidly in order to produce a new hair follicle.

While bulge cells are normally in a Wnt-inhibited state, periodic elevations of Wnt signaling appear to regulate bulge cell activation and contribution to the hair follicle lineage. Transgenic expression of a stabilized form of β-catenin in bulge cells mimics elevated Wnt signaling and results in bulge cell proliferation and premature entry into the

anagen phase of the hair cycle (Lo Celso et al., 2004; Lowry et al., 2005; Van Mater et al., 2003). Consistent with a positive role for Wnt signaling in activating stem cells to proliferate and differentiate along a hair follicle lineage, the secondary hair germ which emerges from the bulge niche and gives rise to the growing follicle displays nuclear β-catenin and Lef1 expression as well as positive *TOPGAL* Wnt reporter gene activity (Lowry et al., 2005; Merrill et al., 2001).

In contrast to signs of Wnt signaling, which are usually low in the bulge, but are elevated in the secondary hair germ at the start of the new hair cycle, high levels of BMP signaling in the bulge help to maintain quiescence and SC identity. While both telogen phase bulge cells and the surrounding dermis express BMP ligands (Blanpain et al., 2004; Plikus et al., 2008), dermal papilla cells express a number of inhibitors of BMP signaling (Rendl et al., 2005). Bulge cells are known to constitutively express BMP receptor genes, and nuclear phospho-SMAD-1,5,8 staining, indicative of active BMP signaling, can be detected in quiescent telogen follicles (Andl et al., 2004). However, this nuclear phospho-SMAD expression disappears shortly prior to the onset of anagen, and then does not reappear until the next telogen, suggesting that BMP signaling functions as a brake to inhibit bulge activation, and that competing levels of BMP ligands and inhibitors produced by bulge cells, DP, and dermis dynamically balance the level of BMP signaling occurring in the bulge throughout the hair cycle (Plikus et al., 2008).

Consistent with the notion of BMP signaling promoting quiescence, cultured bulge cells remain sensitive to BMP treatment, which causes them to transiently reduce their cycling rate (Blanpain et al., 2004). When the BMP receptor 1A gene is conditionally ablated in adult skin, otherwise quiescent bulge stem cells begin to proliferate rapidly, expanding the size of the SC niche and expressing early hair follicle lineage markers, including Sox4 and Shh (Kobielak et al., 2007). However, these abnormally activated stem cells are blocked in later terminal differentiation stages because they can no longer receive the BMP signals necessary for IRS and hair shaft differentiation (Andl et al., 2004; Kobielak et al., 2003; Yuhki et al., 2004). Although the *BMPr1a*-deficient bulge cells are no longer slow cycling, and do not express appreciable CD34, follicle cells lacking *BMPr1a* still appear able to repair epidermis in a wound response, suggesting that they maintain some aspects of stem cell functionality (Kobielak et al., 2007).

Beyond the well-established roles of Wnt and BMP signaling in modulating bulge stem cell activity, several transcription factors have recently been shown to be specifically involved in bulge regulation. Interestingly, and in contrast to CD34, their expression begins early in HF morphogenesis, with Lhx2 and Sox9 appearing at the placode stage and Nfatc1 appearing during the peg stage (Horsley et al., 2008; Rhee et al., 2006; Vidal et al., 2005). Skin grafts from *Lhx2* and *Nfatc1* null embryos, which die during late embryogenesis, develop HFs which contain functional SC niches but display reduced SC

quiescence, with *Lhx2* null HFs also displaying reduced CD34 expression in the bulge (Horsley et al., 2008; Rhee et al., 2006). *Y10:Cre/Sox9(fl/fl)* mice target *Sox9* ablation to postnatal skin via a human WT1 YAC construct expressing Cre recombinase, and reveal hair cycle defects that include a failure of adult bulge SCs to function and to express CD34 (Vidal et al., 2005).

While the molecular mechanisms that regulate Lhx2 and Sox9 activity in bulge stem cells remain largely unknown, the Nfatc1 gene appears to be a downstream target of BMP signaling, since *BMPr1a* conditionally null mice fail to express Nfatc1. Furthermore, nuclear Nfatc1, which requires calcium for nuclear translocation, appears to function as a direct transcriptional repressor for the G_1/S regulatory kinase Cdk4 in the bulge, providing a partial explanation for how BMP signaling and Nfatc1 might act coordinately to maintain bulge quiescence (Horsley et al., 2008). Now that the expression profile and lineage contributions of bulge stem cells are finally becoming clear, it should be possible to begin dissecting the rest of the molecular mechanisms which regulate bulge cell identity and activity.

Specific Aims

In mammalian hair follicles, stem cells reside in a relatively quiescent state within a permanent, anatomically distinct region of the follicle known as the bulge. In adult mice, bulge SCs can contribute to all three epithelial lineages of skin (Blanpain et al., 2004; Morris et al., 2004; Oshima et al., 2001). During normal homeostasis, bulge SCs

are periodically activated to fuel postnatal hair cycles. These multipotent SCs can also provide a cellular input to the interfollicular epidermis and sebaceous gland lineages in a wound environment. While all HFs have initiated development by P0 when mice are born, bulge niche architecture is not pronounced until three weeks after birth (~P20-P21) when mice already have a full hair coat (Cotsarelis, 2006; Schmidt-Ullrich and Paus, 2005). This timing also coincides with CD34 upregulation and bulge-specific *K15 promoter* activity. Where these adult bulge SCs come from and how they first organize within a niche remains unknown. It has been widely assumed that bulge SCs are not needed for embryonic morphogenesis, where HFs develop from epidermis rather than the base of preexisting bulge niches. Consistent with this notion, the existence of stem cells in the hair follicle before the appearance of the adult bulge niche has never been reported.

In order to investigate the developmental origins of bulge stem cells, I have adapted an existing strategy designed to detect adult bulge cells based on their relative quiescence and used it to identify a previously unrecognized population of slow-cycling cells which appears early in hair follicle development. While these early label retaining cells do not express CD34, they do express numerous markers of adult bulge stem cells. They also directly give rise to the adult bulge cell population. Furthermore, the pattern of label retention in early slow-cycling cells suggests that they participate actively in hair follicle growth.

By studying an established adult stem cell gene, Sox9, which I found to be expressed by early LRCs, I was able to assess the function of the early LRC population (Nowak et al., 2008). Expression and genetic marking studies showed that Sox9-positive cells act as a stem cell population during skin morphogenesis and can give rise to all three epithelial lineages. Conditional ablation of *Sox9* in embryonic skin revealed that *Sox9* is required for initial stem cell specification. In the absence of early SCs, hair follicle and sebaceous gland morphogenesis is blocked and epidermal wound repair is compromised. These findings established the existence of early hair follicle SCs and revealed their physiological importance in tissue morphogenesis.

Finally, I pursued two strategies to begin dissecting the molecular requirements for stem cell specification. Because Sox9 is absolutely required for initial stem cell specification, I conducted a microarray expression screen on developing hair follicles from WT and *Sox9* cKO mice to generate a list of genes which are regulated by Sox9 and likely to be important for initial stem cell specification. Additionally, I developed a transgenic mouse system that allows for FACS purification of Sox9-expressing cells from the skin. Analysis of Sox9-positive cells purified from developing follicles revealed that these cells display functional properties and expression characteristics consistent with a stem cell population. The ability to purify Sox9-expressing cells and uncover the transcriptional network which regulates hair follicle stem cell specification should provide important new insight into both skin morphogenesis and epithelial stem cell regulation.

CHAPTER 2
QUIESCENCE IN SKIN MORPHOGENESIS AND HAIR FOLLICLE CYCLING

Cells in the bulge region of adult hair follicles are known to function as multipotent epithelial stem cells (Blanpain et al., 2004; Claudinot et al., 2005; Morris et al., 2004). While all hair follicles have initiated development by P0 when mice are born, bulge niche architecture is not pronounced until three weeks after birth (P20) when mice already have a full hair coat (Cotsarelis, 2006; Schmidt-Ullrich and Paus, 2005). The distinctive appearance of the bulge at this age coincides with the onset of the growth phase (anagen) of the first postnatal hair cycle. Where the adult bulge SCs come from and how they organize within a niche remains unknown. It has been widely assumed that bulge SCs are not needed for embryonic morphogenesis, where HFs develop from epidermis rather than the base of preexisting bulge niches. In support of this notion, two widely used bulge SC markers, CD34 and a *keratin 15-LacZ* reporter gene, are both upregulated at ~P20 (Blanpain et al., 2004; Liu et al., 2003; Trempus et al., 2003). Additionally, while many studies using postnatal nucleotide tracer pulse-chase experiments have demonstrated the quiescence of adult bulge SCs (Cotsarelis et al., 1990; Morris and Potten, 1999; Taylor et al., 2000), the existence of a quiescent cell population within developing HFs has never been reported.

Furthermore, even though quiescent adult bulge cells are periodically activated to proliferate and form a new hair follicle during each hair cycle, the kinetics and timing of the adult stem cell activation process remain poorly characterized. Throughout the entire anagen phase of the hair cycle, many cells in the hair follicle matrix are highly proliferative (Potten et al., 1971). However, the majority of bulge cell proliferation has been reported to occur in a burst within the first four days of anagen (Ito et al., 2004; Wilson et al., 1994), implying that matrix proliferation is maintained independently of bulge input throughout most of anagen. In contrast, lineage tracing experiments using transplanted bulge cells from whisker follicles demonstrate a continuous, progessive flux of cells from the bulge region down the ORS towards the matrix, consistent with ongoing bulge cell division throughout anagen (Oshima et al., 2001). Determining whether bulge cell proliferation is a discrete, transient event at the beginning of anagen or a continuous process that occurs throughout anagen has major implications for the relationship between bulge and transit-amplifying matrix cells as well as the types of molecular mechanisms that can be expected to regulate bulge cell activation.

To determine when quiescent bulge stem cells might first be established, I conducted a time course of embryonic pulse-chase experiments using an inducible H2B-GFP label retention system previously shown to identify slow-cycling adult bulge cells (Tumbar et al., 2004). These experiments revealed that label retaining cells are specified at the earliest stages of hair follicle morphogenesis, yet participate actively in hair follicle

growth. Notably, these early label retaining cells express numerous markers characteristic of adult bulge cells and specifically give rise to the adult bulge stem cell population.

In order to provide a detailed point of comparison for the morphogenesis time course, I also conducted an H2B-GFP pulse-chase time course across the first adult hair cycle. This experiment directly demonstrated that adult bulge stem cells divide continuously throughout anagen. Furthermore, this data provided a quantitative measurement of how many times bulge cells divide during the hair cycle and the level of proliferative heterogeneity within the bulge cell population. The kinetics of cell division in the embryonic pulse-chase and the adult hair cycle pulse-chase are notably similar, highlighting the manner in which a discrete stem cell population could be utilized to drive both processes.

Results

Label retaining cells in hair follicle morphogenesis

In order to determine when the quiescent bulge SC population is first specified, I modified an *in vivo* pulse-chase experimental strategy previously employed for labeling adult bulge cells with histone H2B-GFP (Tumbar et al., 2004) (Illustration 2.1). Use of a genetically encoded label ensured that all cells started out with a very similar amounts of label prior to the chase period and avoided the known deleterious effects of nucleotide analog label incorporation in dividing cells (Waghmare et al., 2008). Similar to the previous strategy, I used *K5-tetVP16* mice to control keratin 5 (K5)-positive skin epithelial

expression of histone H2B-GFP driven by a tetracycline regulatable enhancer, but in this case, I began my chase at embryonic day 18.5 (E18.5). At this early time, most hair follicles have been specified, but are still in the early stages of morphogenesis.

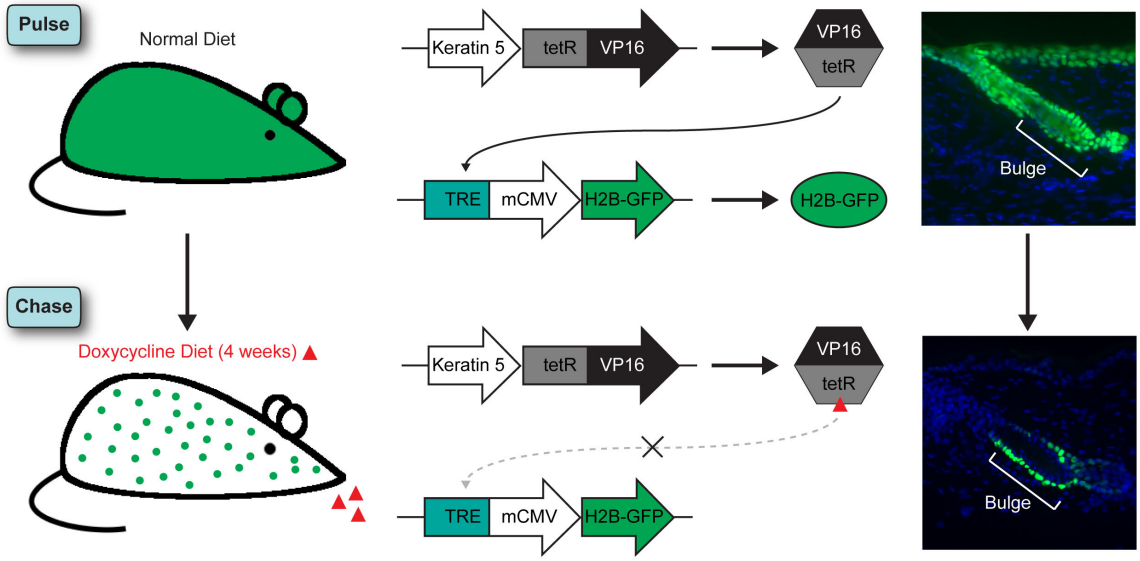

Illustration 2.1. The H2B-GFP genetically encoded pulse-chase system. Mice harboring either *K5-tetVP16* or *TRE-H2BGFP* transgenes were bred together to produce doubly transgenic mice. The *keratin 5* promoter directs skin specific expression of a tetracycline-regulatable transactivator protein (tetVP16). In the absence of the tetracycline-derivative doxycycline, this activator can bind to the tetracycline-regulator response element (*TRE*), thereby driving expression of GFP-tagged histone H2B (top) and fluorescently labeling all skin epithelial cells. When mice are then fed doxycycline to initiate a chase, the transcriptional activator is inhibited from binding to the *TRE* element, and H2B-GFP expression is shut off (bottom). Then, as cells divide, they progressively dilute their H2B-GFP label, with only slow-cycling cells, such as those in the adult bulge, retaining appreciable label after a chase period of four weeks.

In unchased embryos, all skin epithelial cells displayed H2B-GFP epifluorescence, consistent with strong *K5* promoter activity by E13.5 (Byrne et al., 1994) (Figure 2.1). After 3d of chase (P2), the brightest H2B-GFP cells in the epidermis were in non-

proliferative suprabasal layers, as expected from the upward mode of terminal differentiation in this tissue. Surprisingly, the brightest cells in the hair follicle were concentrated in a relatively narrow zone (bracketed) of outer root sheath (ORS) (Figure 2.1). After 9d of chase, when HF downgrowth was nearly complete (P8), H2B-GFP label retaining cells (LRCs) clustered prominently within this upper ORS zone. Marking completion of the pilosebaceous unit (Schmidt-Ullrich and Paus, 2005), SGs had emerged just above these LRCs (Figure 2.1).

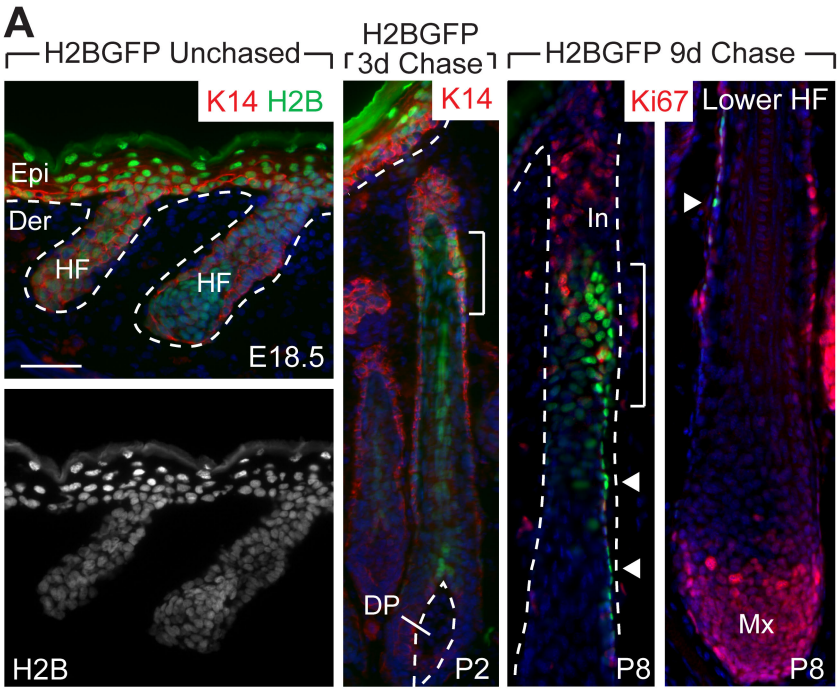

Figure 2.1. Label retaining cells appear early in hair follicle morphogenesis. *K5-tetVP16/TRE-H2BGFP* double transgenic mice were chased at E18.5 to shut off H2B-GFP expression and identify label retaining cells (LRCs) within the early postnatal skin epithelium (P2-P8). (**A**) Appearance of LRCs during hair follicle (HF) morphogenesis. Shown are representative skin sections with green H2B-GFP epifluorescence and counterlabeling with indicated antibodies (red). After 3d of chase, the brightest H2B-GFP LRCs in the hair follicle reside in a narrow zone of the upper outer root sheath (brackets) and are distinct from rapidly proliferating (Ki67-positive) cells, abundant in the infundibulum (In) and matrix (Mx). Arrowheads indicate a trail of slightly dimmer H2B-GFP LRCs extending down the outer root sheath. Dotted lines denote the basement membrane that separates the interfollicular epidermis (Epi) and hair follicle from the underlying dermis (Der) and dermal papilla (DP). Scale bar, 50 μm.

Consistent with their relatively slow-cycling nature, these early follicle LRCs were largely negative for proliferative nuclear protein Ki67, which instead marked many cells located both above (infundibulum) and below (matrix) this zone (Figure 2.1). In mature follicles, a thin trail of H2B-GFP-positive cells (arrowheads) extended down the ORS from the concentrated LRC zone towards the hair bulb, which contains the highly proliferative, transit-amplifying population of matrix cells responsible for hair production. Intriguingly, some of the cells within this trail displayed decreased nuclear epifluorescence intensity and some were also negative for Ki67, suggestive of a potential precursor-product relation between brighter H2B-GFP LRCs in the upper ORS and dimmer H2B-GFP cells in the lower ORS.

Use of fluorescence activated cell sorting (FACS) to quantify label retention in keratinocytes from fractionated epidermis or HFs (dermis) revealed that unchased HF keratinocytes expressed relatively uniform amounts of label at P0.5, but after 3d of chase,

the spectrum of GFP fluorescence had broadened, indicating that most HF keratinocytes had divided several times (Figure 2.2A). Over 5d of chase, the HF GFP spectrum continued to broaden and diminish in intensity, reflecting rapid cell divisions. That said, a clear tail of GFP-high cells persisted, indicative of a less proliferative subset of HF cells. The variable rates of HF cell division contrasted starkly with the more uniform epidermal cell division rates reflected by symmetric distributions of label retention (Figure 2.2A). Within the GFP spectrum, peaks (denoted by arrows) were often spaced at 2-fold intervals, consistent with cells losing 50% of their H2B-GFP label at each division (Figure 2.2B)

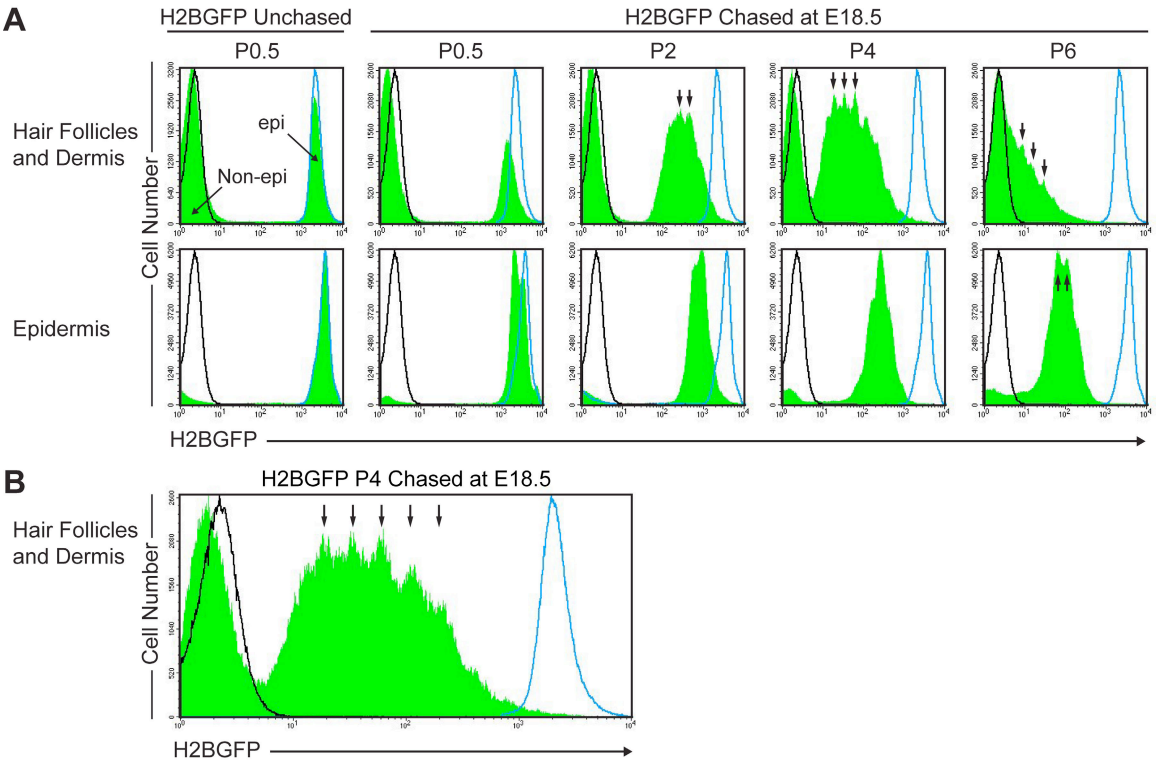

Figure 2.2. FACS quantification of early label retaining cells in the hair follicle. (**A**) FACS analysis of HF/dermis and epidermis from chased P0.5-P6 *H2B-GFP* mice. Within each population, GFP intensity is represented as a green histogram, with overlays from non-GFP mice (black) and unchased *H2B-GFP* mice (blue) representing minimum and maximum endpoints for detecting H2B-GFP fluorescence. Label dilution is detectable 24 hours after the beginning of the chase period (compare chased and unchased P0.5 mice). (**B**) Enlargement of GFP histogram highlighting peaks spaced at 2-fold intensity intervals. Note that the pattern of HF label retention is asymmetric compared to label retention in the epidermis, and that a tail of LRCs is detectable in P4 and P6 HF/dermis histograms. The existence of GFP negative cells (Non-epi) in all HF plots, including unchased mice, is reflective of the non-epithelial cells types (dermal papilla, dermal fibroblasts, melanocytes) that co-purify during HF isolation.

To determine whether early LRCs might be related to adult follicle SCs, I conducted immunofluorescence microscopy with antibodies against a number of adult bulge markers and compared their localization patterns with H2B-GFP (Figure 2.3A). Consistent with prior reports (Nguyen et al., 2006; Vidal et al., 2005), the transcription factors Tcf3 and Sox9 were expressed in P8 ORS. While not restricted to H2B-GFP LRCs, Tcf3 and Sox9 positive cells included the LRC zone (brackets). Notably, Nfatc1 and Lhx2 were also expressed in the LRC zone and displayed even greater restriction than Tcf3 and Sox9 (arrowheads). Whether embryonic or adult, the only other place where Nfatc1, Lhx2 and LRCs are known to co-localize is in adult bulge SCs (Horsley et al., 2008; Rhee et al., 2006; Tumbar et al., 2004).

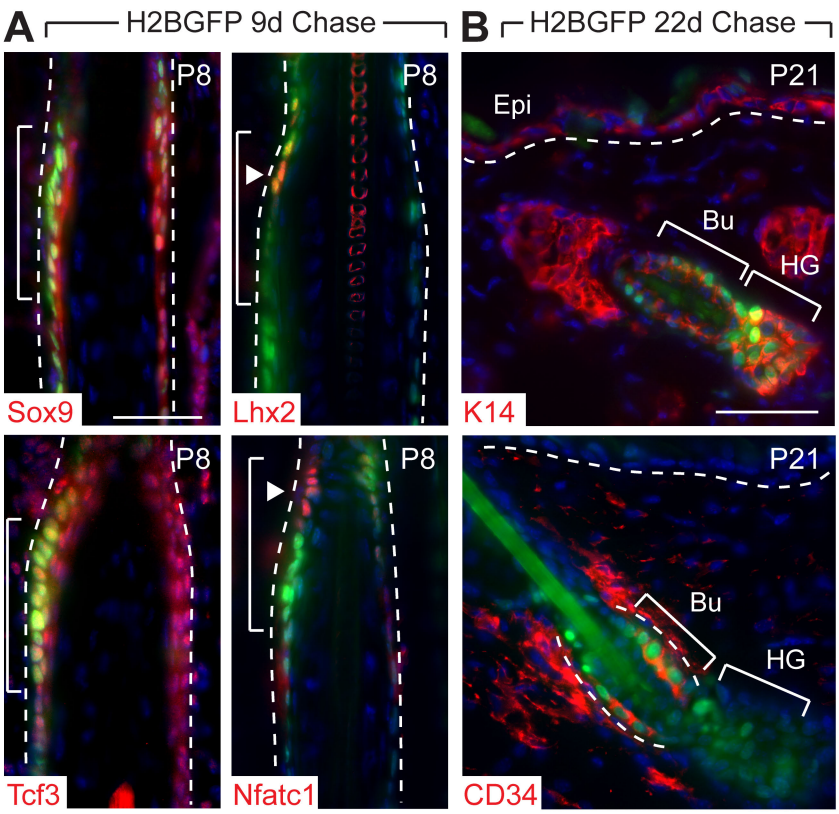

Figure 2.3 Expression of bulge stem cell markers by label retaining cells. **(A)** Immunofluorescence reveals partial co-localization (brackets, arrowheads) of P8 LRCs with antibodies specific for transcription factors expressed preferentially in adult bulge cells. **(B)** Immunofluorescence shows that after 22d of chase, LRCs labeled during embryogenesis are found exclusively in the adult bulge (Bu) niche (CD34-positive) and secondary hair germ (HG), and not in the K5/K14-positive basal layer of the sebaceous gland or interfollicular epidermis (Epi). Scale bars, 50 μm.

To directly evaluate the relation between early follicle LRCs and adult bulge SCs, I labeled mice until E18.5 and then chased until P21, when the first postnatal hair cycle is initiated and the adult bulge niche has appeared (Blanpain et al., 2004). After an entire cycle of hair growth, LRCs marked by H2B-GFP during embryogenesis were still present at P21 where they localized to the CD34-positive adult bulge SC niche and secondary hair germ (HG) (Figure 2.3B). This result, confirmed by FACS analysis on 22d chased

mice (Figure 2.4), established that the early LRC population present in chased P2 and P8 follicles is the major contributor to the adult bulge SC population that appears at P20.

Taken together, these results demonstrate that a quiescent population of cells is specified early in HF development, that LRCs localize to a specific region of the growing HF where they express many SC markers, and that early LRCs persist to form the adult bulge. Notably, all of these quiescent presumptive bulge cells lost some label during the 22d chase period that covered the first complete hair cycle, suggestive of occasional cell divisions. Even when the chase period began at P2, well after all follicles have been specified, the brightest bulge cells still appeared to have divided several times before P21 (Figure 2.4). These results suggested that early LRCs play an active role in HF morphogenesis before being called upon to drive the periodic growth of the adult hair cycle as adult bulge cells.

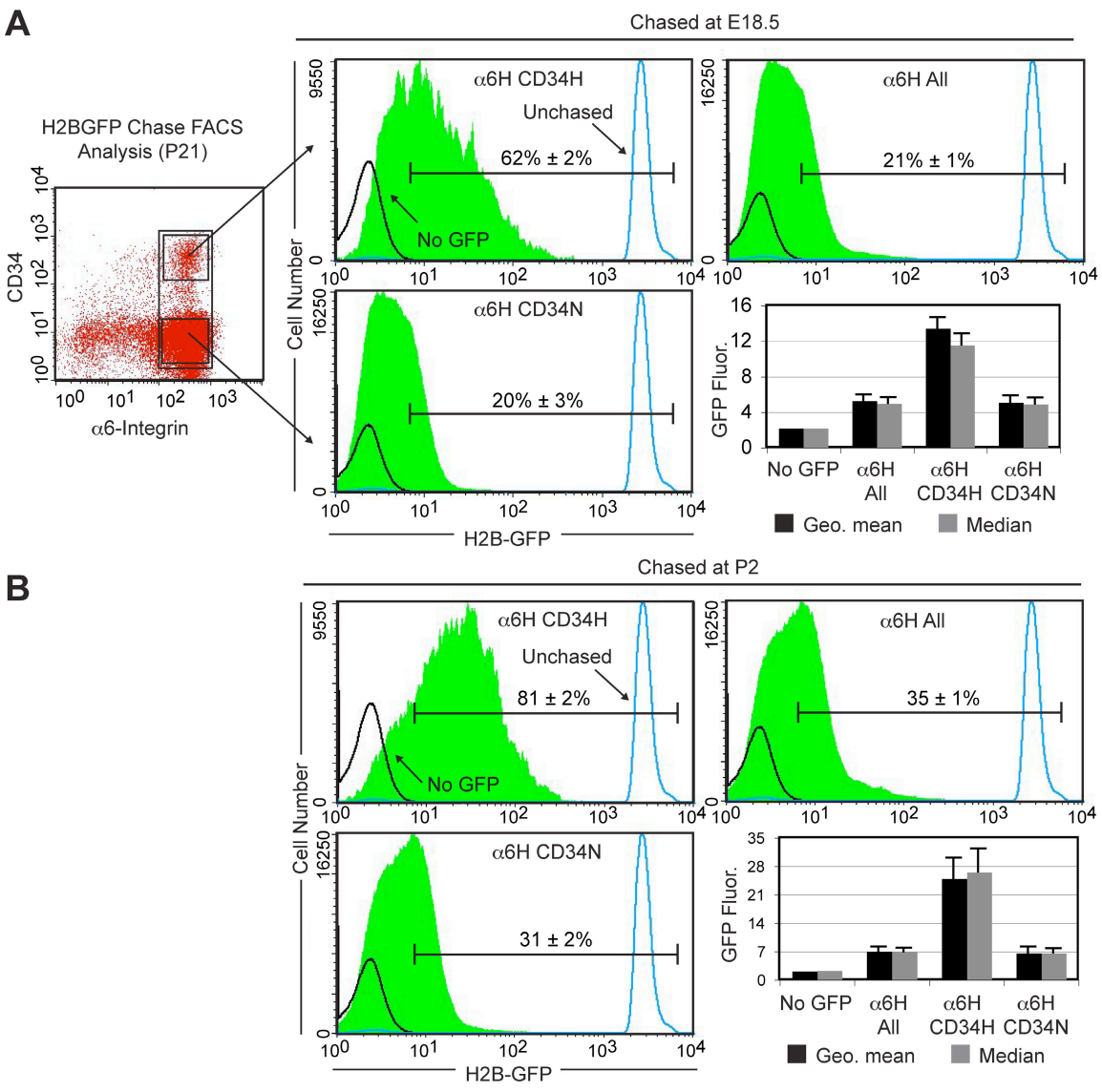

Figure 2.4. Early label retaining cells give rise to adult bulge cells. FACS analysis of skin epithelial cells isolated from P21 mice chased beginning at E18.5 (**A**) or P2 (**B**). Black boxes on dot plot indicate gates for bulge SCs (α6HCD34H), non-bulge basal cells (α6HCD34N) and all basal cells (α6H All) (H, high; N, negative). Horizontal bars indicate percentage of cells (± SD) with detectable fluorescence. Note that the α6HCD34H histogram spans a wider range of fluorescence intensity than α6HCD34N and α6H All histograms and contains more H2B-GFP-positive cells. Graph displays quantification of GFP fluorescence levels in all three populations. GFP negative mice are shown as a control. Note higher geometric mean and median fluorescence levels in the α6HCD34H population. Errors bars represent one standard deviation.

Label retaining cells in the adult hair cycle

The embryonic pulse-chase data suggested that all early LRCs divide multiple times during the first anagen to fuel production of the initial hair coat. To determine whether adult bulge stem cells also operated in a similar manner, I conducted an analogous H2B-GFP pulse chase experiment spanning the entire first postnatal hair cycle. By employing CD34 and α6-Integrin to specifically identify bulge cells by FACS, I was able to quantify label retention in both bulge and the non-bulge epithelial cells throughout the hair cycle (Figure 2.5A).

Beyond measuring average fluorescence in entire populations, it was possible to use GFP fluorescence intensity values to calculate the number of cell divisions that had occurred in any given population. This analysis was made possible by the very uniform level of label in unchased adult bulge cells as well as the fact that H2A-H2B dimers dynamically exchange between nucleosomes during interphase, allowing H2B-GFP label to be distributed evenly among daughter cells after a cell division (Kanda et al., 1998; Luger and Hansen, 2005). While division-independent degradation of H2B-GFP label might be expected to bias these calculations towards over-estimating the number of divisions, the measured half-life of H2B-GFP label in adult skin epithelial cells is ~24 days, suggesting that for chase periods of one month or less, estimates of cell division based strictly on two-fold dilution of H2B-GFP label should be correct to within one cell division (Waghmare et al., 2008). Notably, since H2B-GFP turnover would be expected

to affect all cells equally, comparisons between bulge and non-bulge cells should be equally accurate at all time points, regardless of degradation artifacts.

Similar to the embryonic pulse-chase series, unchased H2B-GFP showed uniform levels of label throughout the epidermis, hair follicle and bulge (Figure 2.5B,C). Remarkably, after three days of chase, some cells in the bulge population had divided up to 5 times, but many had not divided at all, while most non-bulge cells had divided at least once (Figure 2.5; Table 2.1). Notably, the range of GFP fluorescence extended to a lower value in the bulge compared to the non-bulge population at this timepoint, demonstrating that some bulge cells have transiently proliferated faster than all other epithelial cells between P21-P24. After one week of chase, at P28, it was clear that most bulge cells had divided at least once, and some had divided up to 6 times. Virtually all non-bulge cells had divided at least several times by this point. This pattern became more distinct at P35 and P42, and while the bulge population still continued to divide, the geometric mean fluorescent intensity of the bulge population remained almost ten times higher than that of the non-bulge population, consistent with slow-cycling behavior.

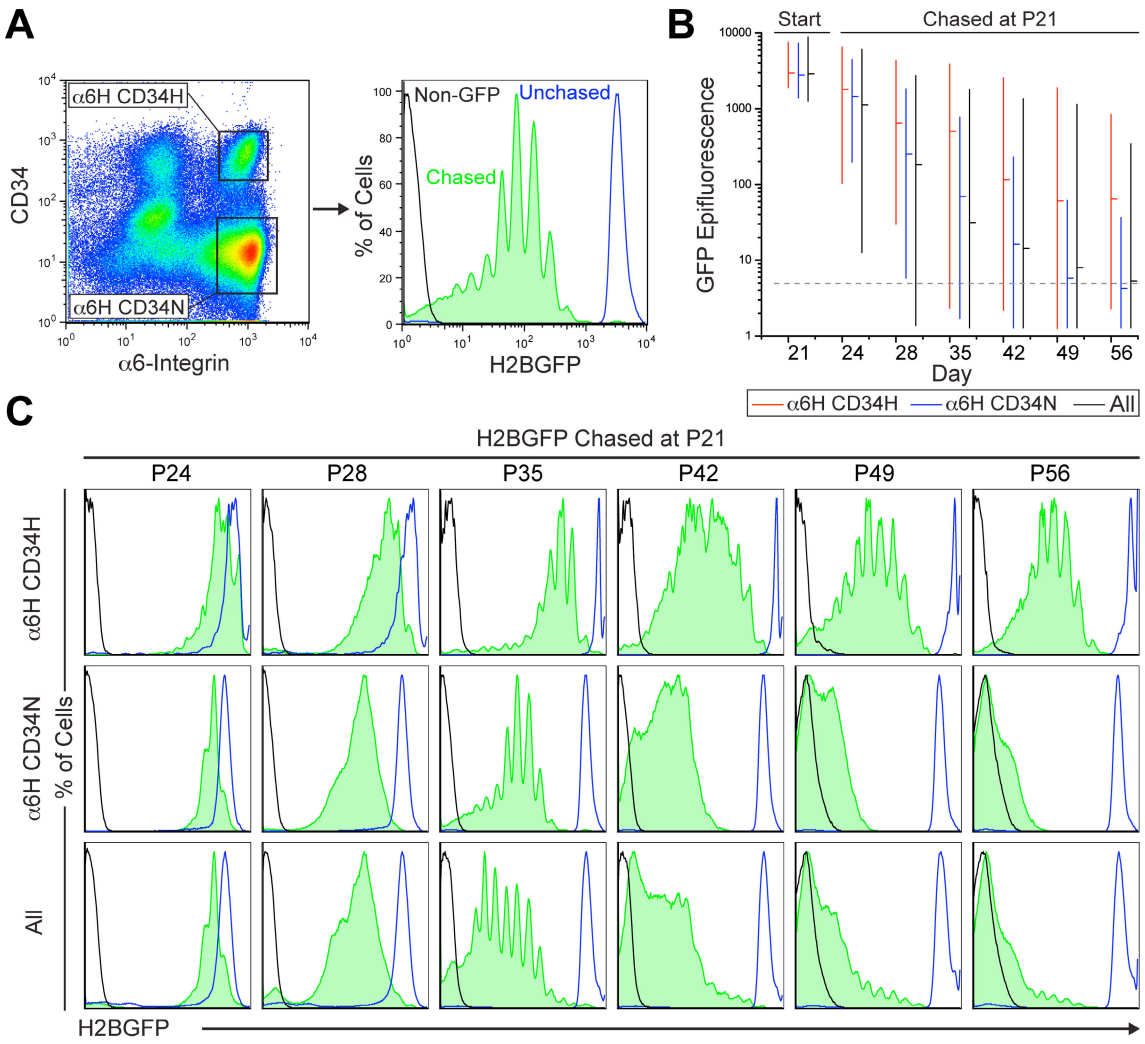

Figure 2.5 FACS quantification of label retention in the adult hair cycle. FACS analysis of skin epithelial cells from *H2B-GFP* mice chased for indicated periods of time beginning at P21. (**A**) A representative FACS plot depicting gates for bulge (α6HCD34H) and non-bulge basal layer epithelial cells (α6HCD34N). Within each population, GFP intensity is represented as a green histogram, with overlays from non-GFP mice (black) and unchased *H2B-GFP* mice (blue) representing minimum and maximum endpoints for detecting H2B-GFP epifluorescence. (**B**) Quantification of GFP label retention within bulge, non-bulge and ungated parent populations (All). Endpoints of each line indicate 1st and 99th percentile for GFP epifluorescence range, and tick marks indicate geometric mean GFP epifluorescence. Dotted line indicates threshold for positive detection of H2B-GFP label. (**C**) Individual histograms of GFP fluorescence for data summarized in (B). Note the wide distribution of label in bulge compared to non-bulge cells, and the progressive reduction of label in bulge cells from P24 to P42.

Notably, at P42 and later time points, the range of bulge GFP epifluorescence was very large, reflecting the fact that some bulge cells had divided up to 10 times, which others had divided only once (Figure 2.5B,C; Table 2.1). Once follicles were in the resting telogen stage of the hair cycle at P42, dilution of H2B-GFP label in the bulge population slowed dramatically, reflecting the quiescent nature of hair follicles in this stage. In contrast, non-bulge cells continued to steadily lose label, consistent with this population being comprised primarily of cells from the interfollicular epidermis, which undergoes continuous self-renewal.

Table 2.1 Cell divisions in bulge and non-bulge cells in the adult hair cycle. Geometric mean, 1st and 99th percentile values for the GFP fluorescence range of bulge (α6HCD34H), non-bulge (α6HCD34N) and ungated cells (All) at the listed time points were used to calculate a mean (bold) and range (parenthesis) for the number of divisions that cells in each population had undergone during the chase period which began at P21. Ten divisions is the maximum number that can be definitively counted based on the difference in signal intensity between unchased *H2B-GFP* mice and *H2B-GFP* negative mice. Plus sign indicates greater than 10 divisions. Note that some bulge cells have divided only twice during the entire chase, while all non-bulge cells have divided at least six times.

Chase End	Divisions in bulge	Divisions in non-bulge	Divisions in All
P24	**0.7** (0-5)	**1.4** (0-4)	**1.7** (0-8)
P28	**2.2** (0-6)	**3.9** (0-9)	**4.4** (0-10$^+$)
P35	**2.6** (0-10)	**5.8** (2-10$^+$)	**6.9** (0-10$^+$)
P42	**4.7** (1-10$^+$)	**7.8** (3-10$^+$)	**8.0** (1-10$^+$)
P49	**5.5** (1-10$^+$)	**9.3** (5-10$^+$)	**8.9** (1-10$^+$)
P56	**5.6** (2-10$^+$)	**9.8** (6-10$^+$)	**9.5** (2-10$^+$)

Histological analysis of skin from *H2B-GFP* mice confirmed and extended the data acquired by FACS analysis. As expected, H2B-GFP bright cells persisted in the both

the basal (α6H) and suprabasal (α6L) bulge niches during the entire chase period, which extended into the anagen phase of the second postnatal hair cycle (Figure 2.6). At all times, the matrix of growing follicles was essentially free of H2B-GFP label, consistent with its highly proliferative nature. As in the embryonic pulse-chase, some H2B-GFP bright cells were detectable in the secondary hair germ during telogen at later timepoints, underscoring a possible similarity between the bulge and secondary hair germ.

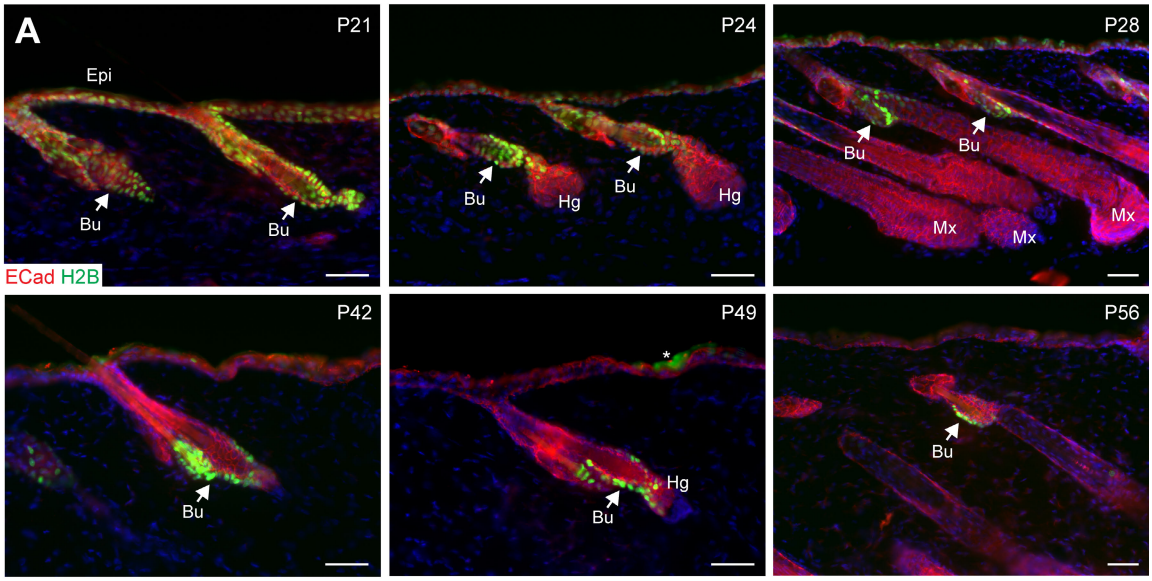

Figure 2.6 Label retaining cells persist throughout the hair cycle. (A) Immunofluorescent analysis of back skin from *H2B-GFP* mice chased for indicated periods of time beginning at P21. E-cadherin marking epithelial cells is stained in red. Unchased skin shows uniform expression of H2B-GFP at P21. Note that bright cells persist in the bulge (Bu) across the entire hair cycle, while hair germ (Hg) and matrix (Mx), derived from bulge cells, are essentially free of label. H2B-GFP label in the interfollicular epidermis progressively declines over time. Asterisk indicates autofluorescence from the stratum corneum. Epi, epidermis. Scale bars, 50 μm.

In summary, these results show that adult bulge cells enter a sustained period of proliferation during the anagen phase of the hair cycle and that virtually all bulge cells

divide at least once during anagen, with some bulge cells dividing up to 10 times. While bulge cells appear to proliferate more rapidly at the beginning of anagen, they cumulatively accomplish at least half of their total divisions after the first three days of anagen initiation. Once hair follicles enter telogen, bulge cells become profoundly quiescent, with little detectable division, but continue to display a wide range of label retention reflective of substantial heterogeneity within their division history.

Discussion

Since quiescence is a hallmark of cells residing in the adult bulge SC niche (Cotsarelis et al., 1990; Morris and Potten, 1999; Taylor et al., 2000), I reasoned that by determining when and where quiescence is established, I might use this property to identify and characterize a putative early SC population within HFs and thereby trace the developmental origins of adult SCs. Embryonic H2B-GFP pulse-chase studies demonstrated that HF LRCs are specified early in morphogenesis, and begin to accumulate in a specific region of the HF where they express bulge-preferred transcription factors. Despite being relatively slow-cycling, all of these early LRCs divided at least several times during the initial wave of hair production, suggesting that they may participate actively in initial follicle growth and do not simply function as a quiescent reserve for postnatal hair cycles. Although early expression of several bulge-preferred transcription factors has been previously noted in hair follicles, it was not known that this expression correlated with the emergence of a developing niche of LRCs. My studies

placed these earlier clues in perspective and suggested the existence of a functional niche of slow-cycling SCs within early developing HFs.

Importantly, by extending the chase after embryonic labeling, I demonstrated that early LRCs are the direct precursors of the LRCs that reside in the adult bulge niche. Interestingly, while early LRCs express many of the same transcription factors that adult bulge cells do, they do not express CD34, which has been widely used as a key SC marker (Trempus et al., 2003; Morris et al., 2004; Blanpain et al., 2004). This result highlighted the possibility that key regulators of stem cell identity are more likely to be genes expressed beginning at the earliest stages of stem cell specification rather than markers gradually acquired as stem cells mature.

By also performing an H2B-GFP pulse-chase experiment covering the complete first postnatal hair cycle, I was able to compare the kinetics of embryonic hair follicle label retention with adult bulge cell label retention kinetics. While cell isolation methods for embryonic and adult FACS analysis yield slightly different populations, and while it was not possible to prospectively identify an early hair follicle stem cell population using a specific marker analogous to CD34 for adult bulge cells, several common principles appear to apply to the behavior of early hair follicle LRCs and adult bulge LRCs. The first is that all LRCs, whether embryonic or adult, divide at least once during a cycle of hair growth. This widespread participation of adult bulge cells in hair follicle growth was especially unexpected and could not have been predicted by previous studies which lacked the ability

to cumulatively tally bulge cell divisions, and which proposed that as few as four multipotent progenitors might divide within each adult bulge niche to fuel an entire cycle of hair growth (Kopan et al., 2002). This division data is also consistent with a recent paper which similarly used the inducible H2B-GFP system to analyze bulge cell division after one cycle of hair growth and concluded that virtually all bulge cells divide during the hair cycle, most at least 3-5 times (Waghmare et al., 2008).

The second principle which appears to be shared between embryonic and adult hair follicle LRCs is a large heterogeneity in the accumulated number of cell divisions. Both LRC populations contained cells which had divided only 1-2 times in the course of a hair cycle, as well as other cells which had divided at least 10 times. While the significance of this heterogeneity is not yet clear, it suggests that all bulge cells may be not be functionally equivalent or that cells in spatially distinct regions of the bulge niche are differentially activated to proliferate. Notably, heterogeneity of label retention is the only property currently known to subdivide the two basal and suprabasal CD34-positive adult bulge populations into smaller subpopulations.

A final principle which appears to be shared between embryonic and adult LRCs is a state of slow but continuous proliferation throughout the entire anagen phase of hair growth. While there is an apparent burst of accelerated proliferation which initiates anagen, FACS analysis shows that adult follicle bulge cells lose a substantial amount of their label in the time period after the first three days of anagen. This result is

qualitatively similar to the label dilution pattern displayed by P21 adult bulge cells from mice chased beginning at P2, after all follicles have been specified and initial matrix populations have formed.

This result is in direct contrast to previous histological studies which suggested that bulge cells proliferate in a transient burst during the first several days of anagen and then quicky regain their quiescence (Ito et al., 2004; Wilson et al., 1994). This difference may have arisen from the difficulty in accurately counting cell divisions by histology and highlights the advantages of the H2B-GFP flow cytometry approach for rapid, precise quantification of cumulative cell divisions in large cell populations. Notably, the concept of sustained, slow proliferation within the bulge throughout anagen is consistent with lineage tracing studies which demonstrate a continual flux of cells from the bulge down the outer root sheath towards the matrix throughout anagen in whisker follicles (Oshima et al., 2001). It is also supported by a previous study which showed that many cells in the bulge could be labeled by a three day BrdU bulse administered beginning at P28 when follicles are in mid-anagen (Lowry et al., 2005).

Taken together, these results reveal the unexpected existence of a population of label retaining cells that appears at the earliest stages of hair follicle morphogenesis and expresses multiple bulge-preferred transcription factors before giving rise to the adult bulge stem cell population. Analogous to the behavior of adult bulge stem cells during anagen in postnatal hair cycles, these early LRCs nevertheless all divide at least several times

during the initial wave of hair production, and display a large heterogeneity in their division history. Unexpectedly, both early LRCs and adult bulge SCs appear to proliferate slowly but continuously throughout the entire anagen phase of the hair cycle. These results suggest that a slow-cycling stem cell population might be specified early in follicle morphogenesis and may play an active role in follicle development before the appearance of the adult bulge stem cell population.

Materials and Methods

Mice and labeling experiments

pTRE-H2BGFP/K5-tetVP16 (Tumbar et al., 2004) mice have been described. For embryonic H2B-GFP pulse-chase experiments, pregnant *pTRE-H2BGFP/K5-tetVP16* females with known plug or delivery dates were fed continuously with doxycycline chow beginning at E18.5 or P2. For adult H2B-GFP pulse-chase experiments, animals were placed on a doxycycline chow diet on the evening of P21, and sacrificed on the evening of the required time point.

Histological Analysis

Midline samples of backskin from a consistent rostrocaudal location were embedded in O.C.T. compound (Sakura), frozen on dry ice and stored at -80°C. Frozen sections were obtained by cryostat sectioning at a thickness of 10 μm and collected on glass microscopy slides (Superfrost, VWR).

For staining, slides were fixed for 10 minutes in 4% paraformaldehyde in PBS, rinsed three times in PBS and blocked for one hour in gelatin block (PBS containing 2.5% normal goat serum, 2.5% normal donkey serum, 1% BSA, 2% fish gelatin, and 0.1% Triton X-100). Primary antibodies were diluted in gelatin block and incubated on slides overnight at 4°C. After rinsing three times with PBS, fluorescently-labeled secondary antibodies diluted in gelatin block were incubated on slides for one hour at room temperature. Hoechst 33342 was included in the secondary antibody incubation to permit visualization of nuclear DNA. After washing three times in PBS, slides were mounted with glass coverslips using a glycerol-based antifade reagent. When applicable, staining using mouse primary antibodies was conducted using the Basic Vector Mouse on Mouse Immunostaining Kit (Vector Laboratories) in place of gelatin block.

Primary antibodies and dilutions used were: E-Cadherin (rat, 1:200, M. Takeichi, RIKEN, Kobe), K14 (rabbit, 1:500, Fuchs Lab), Lhx2 (rabbit, 1:2000, T. Jessell, Columbia, New York), Nfatc1 (mouse, 1:100, Santa Cruz), Sox9 (rabbit, 1:200, Santa Cruz), and Tcf3 (guinea pig, 1:200, Fuchs Lab). Secondary antibodies coupled to FITC (1:250) or Rhodamine Red-X (1:500) were from Jackson Laboratories. Imaging was performed using Zeiss Axioskop and Axiophot microscopes equipped with Spot RT (Diagnostic Instruments) and Axiocam (Zeiss) digital cameras, respectively.

Isolation of hair follicle and interfollicular epithelial cells from young mice

Isolation of separate populations of hair follicle and interfollicular epithelial cells (epidermis) was performed as previously described (Rendl et al., 2005). Backskin from young postnatal mice was dissected away from loosely adherent fat and floated dermis down in dispase (Gibco, 0.4mg/ml) dissolved in PBS overnight at 4°C. The next morning, the epidermis was removed as a single sheet from the dermal portion of the tissue where hair follicles remained embedded.

The epidermal sheet was incubated basal layer down in pre-warmed 0.25% trypsin/EDTA (Gibco) for 10 minutes at 37°C, and then briefly dissected with a scalpel to generate pieces that could be suspended in solution. After the addition of 5 mls of PBS, the suspension was extensively triturated with a 10ml pipette and passed over a 40 μm cell strainer. The final volume was brought up to 30 mls in a Falcon tube using PBS and was then centrifuged for 10 minutes at 300g at 4°C to pellet cells.

The dermal portion of the tissue remaining after dispase separation was extensively minced with a scalpel and resuspended in a 6 cm tissue culture dish containing 4 mls of HBSS (HyClone) and 0.25% collagenase (Sigma). After incubation at 37°C for 45 minutes with moderate shaking, 11 mls of PBS were added to each dish and the suspension was repeatedly triturated with a 25 ml pipette. Afterwards, suspensions were brought up to 40 mls with PBS in a 50 ml Falcon tube and centrifuged for 10 minutes at 300g at 4°C to pellet cells. After aspiration of the supernatant, pellets were resuspended

in 30 mls of PBS in a new 50 ml Falcon tube using a 25 ml pipette. After centrifugation for 6 minutes at 20g at 4°C to pellet hair follicles but leave dermal cells in suspension, supernatants were removed by pipette and the loose hair follicle pellet was resuspended in pre-warmed 0.25% trypsin/EDTA and transferred to a 6 cm tissue culture dish. After incubation at 37°C for 10 minutes with moderate shaking, 5 mls of PBS were added to each sample, which was then passed over a 40 μm cell strainer. Strained suspensions were brought up to 40 mls with PBS and then centrifuged for 10 minutes at 300g at 4°C to pellet cells.

Isolation of epithelial cells from adult mice

Epithelial cell isolation from P21 and older mice was performed as previously described (Blanpain et al., 2004). After sacrifice, mice were shaved and trunk skin was removed as a single sheet. Dermal fat was scraped away with a scalpel and skin was floated dermis down in 0.25% trypsin/EDTA overnight at 4°C. The next morning, epithelial cells were gently scraped into the trypsin solution and the remaining dermal tissue was removed from the suspension. After neutralization with E medium (Rheinwald and Green, 1977), cell suspensions were sequentially passed over 70 μm and then 40 μm cell strainers. After bringing the final volume up to 25 mls with E medium in a 50 ml Falcon tube, cells were centrifuged for 10 minutes at 300g at 4°C. Pellets were then resuspended with PBS containing 2% chelexed FBS and centrifuged as above to remove residual trypsin and media.

FACS Analysis of H2B-GFP label retention

All cell staining and analyses were performed on cells suspended in PBS with 2% chelexed FBS containing no calcium. For analysis of hair follicle and interfollicular epidermal cells from young mice, freshly isolated cell suspensions were incubated with propidium iodide for live/dead cell discrimination and directly analyzed by flow cytometry. For analysis of adult epithelial cells, suspensions were first stained on ice with fluorescently conjugated antibodies against α6-integrin (rat PE-conjugated, 1:30, BD-Pharmingen) and CD34 (rat biotin-conjugated, 1:50, eBioscience; streptavidin-APC, 1:300, BD-Pharmingen). Propidium iodide was added after antibody staining. Cells from *H2B-GFP* negative mice and unchased *H2B-GFP* mice were included in all acquisition sessions as negative and positive controls from the range of detectable GFP epifluorescence. In all cases, cell populations were initially gated for viability and forward and side scatter before GFP or antibody analysis. FACS data acquisition was performed on a FACSCalibur flow cytometer (BD Biosciences) using CellQuest Pro software. In some cases, data was additionally analyzed using the FlowJo software package (Treestar). GFP fluorescence intensity was used to calculate the number of division a cell had undergone by the following formula: # divisions = $\log_2$ [(Unchased GFP intensity) / (chased GFP intensity)].

CHAPTER 3
THE ROLE OF SOX9 IN SPECIFICATION OF HAIR FOLLICLE EPITHELIAL STEM CELLS

Adult bulge stem cells play a well defined in role in skin function, and many genes and signaling pathways are known to specifically regulate adult bulge cell activity. However, little is known about the developmental origins of adult bulge cells and whether a stem cell population might exist in the hair follicle before the adult bulge appears at the commencement of postnatal hair cycling. Based on results from embryonic pulse-chase experiments (Chapter 2), a label retaining cell population, which appears early in hair follicle morphogenesis, displays numerous features that suggest it may function as an early stem cell population in the hair follicle. Most notably, these early hair follicle LRCs express several biochemical markers characteristic of adult bulge cells, and they also appear to directly give rise the adult bulge cell population.

To determine whether early LRCs might be important for HF morphogenesis, I focused on the known SC markers that I found to co-localize with these cells as potential regulators of the early label retaining cell population. Of the four bulge transcription factors, only Lhx2 and Sox9 were known to be expressed in the early hair placodes (Rhee et al., 2006; Vidal et al., 2005). Although Lhx2 is a known regulator of placode formation and adult bulge quiescence, it does not appear to be necessary for specification of the bulge population (Rhee et al., 2006). I therefore focused on Sox9 as a particularly good

candidate for regulating LRC establishment during embryogenesis. It was first identified in 2001 in the Fuchs' laboratory as a transcription factor whose expression was upregulated by microarray analysis during skin development, concomitant with HF morphogenesis (C. Kaufman and D. Bolotin, Ph.D. thesis research; Kaufman et al., 2003). Interestingly, fortuitous postnatal HF targeting of *Sox9* with a human WT1 YAC construct driving Cre expression had resulted in adult backskin HFs that lacked CD34 and which could not be maintained (Vidal et al., 2005).

Sox9 is a member of the SOX (*Sry*-like) group of transcription factors which are present throughout the animal kingdom and function as key regulators for a wide variety of developmental processes (Busslinger, 2004; Hong and Saint-Jeannet, 2005; Ikeda et al., 2005; Wegner, 1999). Mammals contain 20 SOX proteins, all of which contain an HMG (high mobility group) DNA binding domain, whose sequence conservation with that of the mammalian testes determining factor *Sry* dictates their inclusion in the SOX group, as well as a single transactivation domain (Bowles et al., 2000). Notably, while *SOX* genes are often expressed in overlapping patterns, SOX proteins are generally not functionally redundant, and loss of even a single family member frequently leads to a severe phenotype (Hong and Saint-Jeannet, 2005; Wegner and Stolt, 2005). While Sox9 is an important developmental regulator in many tissues, it is best understood for its role as a master regulator of chondrogenic differentiation and in specification of the male gonad (Akiyama et al., 2002; Bi et al., 1999; Chaboissier et al., 2004; Foster et al., 1994).

Mutations affecting Sox9 function in humans underlie the skeletal malformation syndrome campomelic dysplasia, which is frequently associated with autosomal sex reversal (Foster et al., 1994).

By documenting Sox9-expressing cells and their progeny in the skin, I found that in early morphogenesis, hair follicles are initially composed of two distinct cell populations—one which is Sox9 positive and one which never expresses Sox9. However, as follicle morphogenesis reaches completion, the entire follicle becomes derived from the Sox9-expressing cell population. Conditional ablation of *Sox9* in the skin epithelium by *K14-Cre* prior to follicle morphogenesis resulted in a specific failure to form an early label retaining stem cell population in hair follicles. By using *Sox9* conditional knockout mice as a tool to address the functional importance of the early stem cell population, I demonstrated that all three epithelial lineages of the skin are dependent upon these early stem cells for either proper completion of morphogenesis or wound repair.

Results

Expression of Sox9 in hair follicle development

To begin addressing the possible role of Sox9 in hair follicle morphogenesis, I first documented its expression at different stages of skin development. In WT E14.5 embryos, the skin was marked by uniform E-cadherin expression and Sox9 protein was not present (Figure 3.1A). As predicted from the pattern of Sox9 *in situ* hybridization which showed general expression throughout the placode (Vidal et al., 2005), Sox9

protein marked developing placodes as soon as they could be architecturally discerned in the main waves of HF specification (E15.5-P0). Interestingly and unexpectedly, however, nuclear Sox9 protein expression was not uniform throughout the placode, but rather resided in the suprabasal cells of the placode and not the P-cadherin and Lhx2 positive basal layer (Figure 3.1B). No previous studies on genes or signaling pathways have uncovered the existence of this discrete Sox9-positive cell population within the placode.

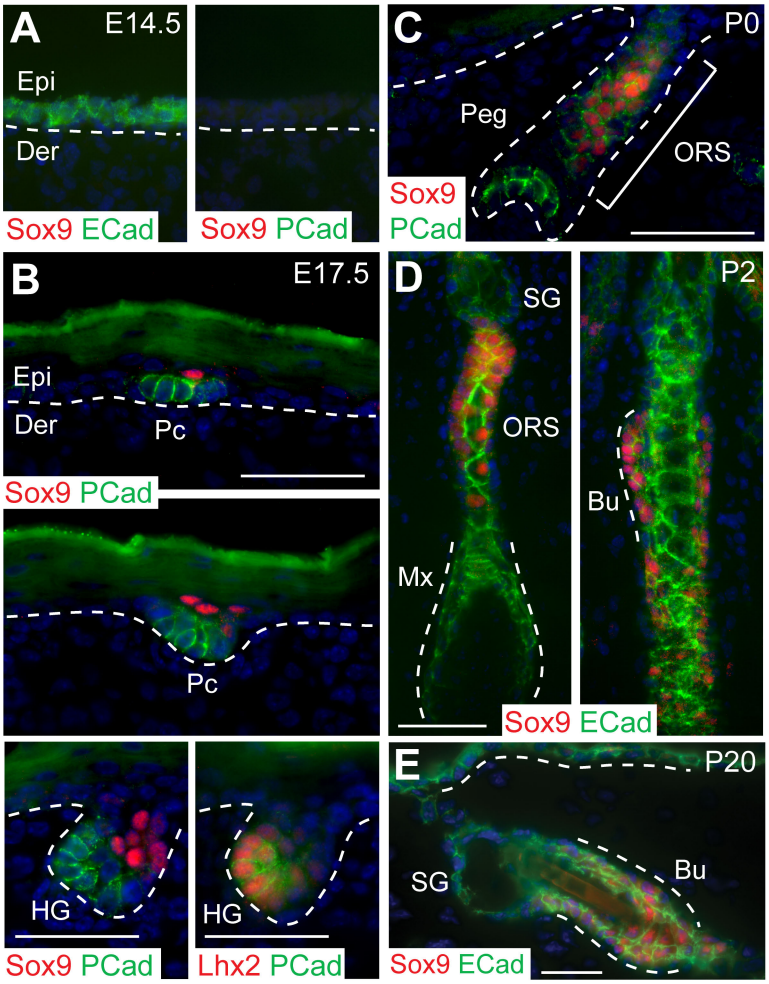

Figure 3.1. Sox9 expression in hair follicle morphogenesis and adult hair follicles. (**A-E**) Immunofluorescence microscopy with indicated antibodies (color coded). Sox9 is first expressed in a few suprabasal cells of the hair placode (Pc), while P-cadherin (Pcad) and Lhx2 mark basal Pc cells. As morphogenesis proceeds, Sox9 continues to mark a zone of cells within the upper ORS, a region that becomes the bulge of the adult follicle. Note that during the rapid anagen growth phase at P2, Sox9 expression is absent from the transit-amplifying matrix. Dotted lines indicate epidermal-dermal border. ECad, E-cadherin. Scale bar, 50 μm.

By the peg stage, Sox9-expressing cells concentrated in a region in the upper ORS with moderate P-cadherin expression, while the brightest P-cad-positive cells localized to the leading edge of developing follicles (Figure 3.1C). Once sebaceous glands (SG)

emerged, it was clear that this Sox9-expressing ORS zone encompassed the presumptive bulge region (Figure 3.1D). By P2, a trail of Sox9-positive cells extended down the ORS, diminishing towards the matrix which was negative for Sox9. As previously reported (Vidal et al., 2005), the bulge SCs of adult HFs were positive for Sox9 (Figure 3.1E). Real time PCR on FACS-purified skin cells revealed background levels of Sox9 mRNA expression in all populations besides ORS, validating the accuracy of Sox9 immunofluorescence results (Figure 3.2).

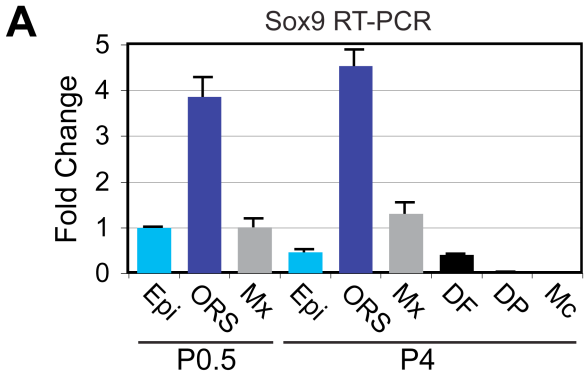

Figure 3.2. Expression of Sox9 mRNA in FACS-purified skin populations. (A) Real time PCR of FACS-purified populations from the skin (Rendl et al., 2005) reveals the specificity of Sox9 mRNA expression in the ORS. DF, dermal fibroblasts; Mc, melanocytes.

Expression of Sox9 in hair follicle genetic mutants

To gain further insights into how Sox9 function might be regulated early in follicle development, I examined Sox9 expression in skin from mice that harbor different gene mutations that disrupt HF morphogenesis (Figure 3.3). Consistent with prior reports, Sox9 was not expressed in *Shh* null skin (Vidal et al., 2005), whose follicles arrest at the placode/hair germ stage (Chiang et al., 1999; St-Jacques et al., 1998). Sox9 was also

not expressed in *β-catenin (fl/fl)/K14-Cre* skin (Huelsken et al., 2001), which lacks all signs of placode formation. Sox9 was present in the few placodes that develop in skins null for either *Lef1* or the BMP inhibitor *Noggin* (required for Lef1 expression in placodes), indicating that, like placode formation, the β-catenin signal essential for Sox9 expression can be mediated by factors besides Lef1 (Botchkarev et al., 1999; Jamora et al., 2003; van Genderen et al., 1994). Additionally, Sox9 was expressed normally in placode and hair germ stages of follicles lacking BMP receptor signaling needed for matrix specification (Andl et al., 2004; Kobielak et al., 2003; Kobielak et al., 2007; Ming Kwan et al., 2004; Yuhki et al., 2004). However, in postnatal *BMPr1a*-null follicles, the population of Sox9 expressing cells had dramatically expanded into the matrix region, indicating a block in complete differentiation along the matrix lineage. Finally, Sox9 was appropriately expressed in adult HFs in skin grafted from *Lhx2*-null mice, which display sparse HFs and a reduction in adult SC quiescence (Rhee et al., 2006). Together, these findings place Sox9 downstream from Wnt and Shh signaling in follicle morphogenesis, but upstream from Lhx2 and the initial dampening of BMP receptor signaling that is required for Lef1 and early hair follicle specification.

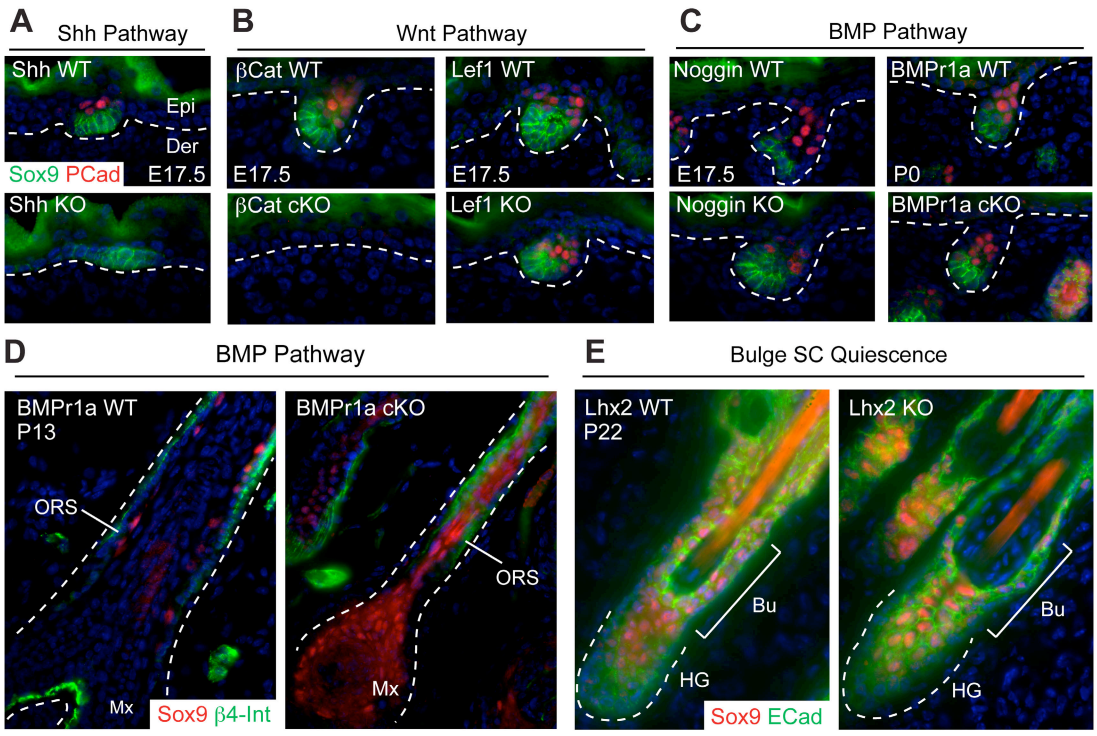

Figure 3.3. Sox9 expression in hair follicle genetic mutants. (**A-C**) Double immunofluorescence microscopy analyzing Sox9 expression in P-cadherin marked placodes and hair germs from mice defective in Shh, Wnt and BMP signaling. Sox9 expression in absent from placodes formed in *Shh* KO mice. *β-Catenin* cKO skin lacks placode formation and does not express Sox9, while *Lef1* KO mice still express Sox9 in hair germs. *Noggin* KO mice display Sox9, but at a reduced level, while Sox9 is normally expressed in hair germs from *BMPr1a* cKO skin. (**D**) HFs from grafted *BMPr1a* P13 cKO skin display an expansion of Sox9 positive cells extending down the ORS and into the matrix region, where Sox9 is normally absent. (**E**) HFs from grafted P21 *Lhx2*-null skin display normal Sox9 expression. β4-Int, β4-Integrin; ECad; E-cadherin.

Contribution of genetically marked Sox9 cells to skin epithelial lineages

Given the similarity between Sox9 expression and LRC location in developing HFs, I wondered whether Sox9-expressing cells in embryonic skin might actively contribute to HF morphogenesis. To test this possibility, I conducted a genetic marking analysis using *Sox9-Cre/R26R* skin. In this assay, *Sox9-Cre* expressing cells become

permanently marked for LacZ expression, and all progeny of *Sox9-Cre* expressing cells can then be readily monitored over time by β-galactosidase cleavage of XGal to generate a blue dye.

Although some portions of backskin express *Sox9-Cre* as early as E10.5 (Akiyama et al., 2005), tailskin, which is similar to backskin (Braun et al., 2003), was free of *Sox9-Cre* activity prior to HF development. At E18.5, tailskin XGal reactivity paralleled Sox9 immunolabeling, specifically marking cells in the upper portion of developing HFs, but remaining absent from the leading edge of HFs and the IFE (Figure 3.4). By P8, however, HFs were almost entirely blue, demonstrating that the population of Sox9-expressing cells in the upper ORS had contributed not only to all differentiated layers of the growing HF but also the sebaceous gland. By the first telogen (P21), Sox9-derived progeny encompassed most if not all cells of the HF, including those of the infundibulum, sebaceous gland, bulge and secondary hair germ, but were absent from IFE (Figure 3.4).

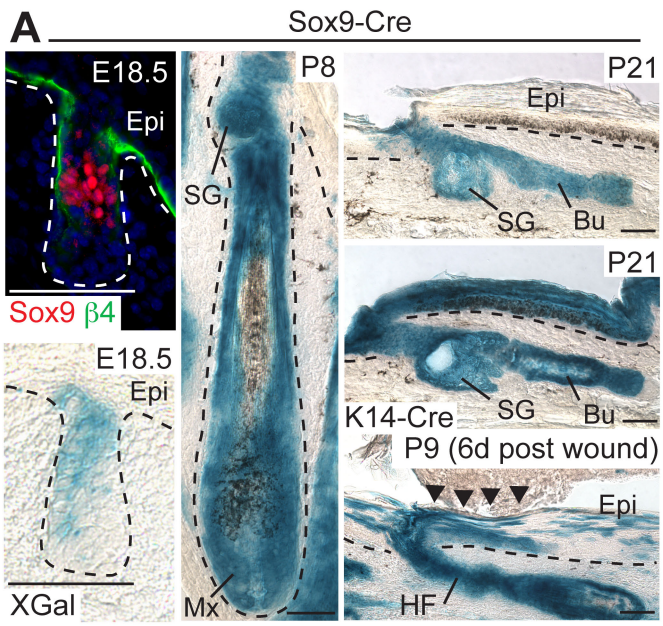

Figure 3.4. Sox9-derived progeny can contribute to all skin epithelial lineages. (**A**) Genetic marking studies with *Sox9-Cre/R26R* reporter mice. Blue XGal staining marks β-galactosidase activity, reflective of Sox9-expressing cells and their progeny in tail skin HFs. At E18.5, XGal staining is similar to Sox9 protein expression. By P8 and thereafter, the entire HF and SGs are nearly completely comprised of blue cells, indicating derivation exclusively from Sox9-expressing cells. *K14-Cre/R26R* skin provides a positive control for XGal reactivity in the IFE. Scratch wounding of *Sox9-Cre/R26R* P3 mice demonstrates the contribution of Sox9-derived HF cells to the IFE lineage. Scale bars, 50 μm.

In normal homeostasis, a resident unipotent progenitor population within the IFE maintains skin turnover. In response to wounding, however, adult bulge SCs can be recruited to the IFE to assist in repair (Ito et al., 2005; Claudinot et al., 2005; Levy et al., 2007). Interestingly, in P3 *Sox9-Cre/R26R* mice, scratch wounding resulted in a robust contribution of *Sox9-Cre* marked HF cells into the regenerating IFE (Figure 3.4). Taken together, these studies revealed that Sox9-expressing cells within developing skin display

key properties of adult HF stem cells in that they contribute to HF and SG morphogenesis and can repair an injured IFE.

Sox9 is required for early bulge cell specification

In conditionally targeted *Y10:Cre/Sox9(fl/fl)* mice, HFs produced an atrophic hair coat that was retained into adulthood, thereby directing that study to a role for Sox9 in the adult hair cycle (Vidal et al., 2005). In light of my finding that a Sox9-marked stem cell population may form during skin embryogenesis, however, I was intrigued that hair defects had been noted in *Y10:Cre/Sox9(fl/fl)* mice as early as P8 (Vidal et al., 2005). To directly test whether Sox9 is functionally required for skin morphogenesis, I targeted Sox9 ablation using *K14-Cre*, active in skin by E13.5. At E16.5, when many follicles are present only as placodes, the *Sox9* locus had been efficiently targeted (Figure 3.5).

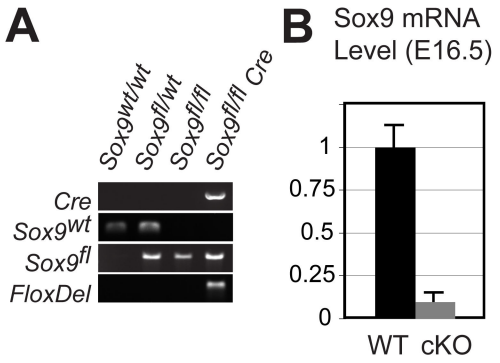

Figure 3.5. Embryonic ablation of *Sox9* by *K14-Cre*. (**A**) Representative genotyping results from E16.5 skin show specific detection of $Sox9^{WT}$, $Sox9^{Flox}$,and $Sox9^{FloxDel}$ alleles and demonstrate deletion of floxed *Sox9* alleles by *K14-Cre*. (**B**) RT-PCR analysis of Sox9 mRNA levels in E16.5 epidermis shows a greater than 10-fold decrease in Sox9 expression in cKO compared to WT. Error bars represent one standard deviation.

At birth, *K14-Cre/Sox9(fl/fl)* (cKO) mice were phenotypically distinguished from WT by an 80% reduction in whisker number, and at P6, when the hair coat first appears, cKO mice displayed a smooth epidermal surface with no sign of protruding hairs (Figure 3.6A,B). As cKO mice aged, they remained completely devoid of a hair coat (Figure 3.6C,D). These findings strongly supported an early role for Sox9 in proper hair follicle function.

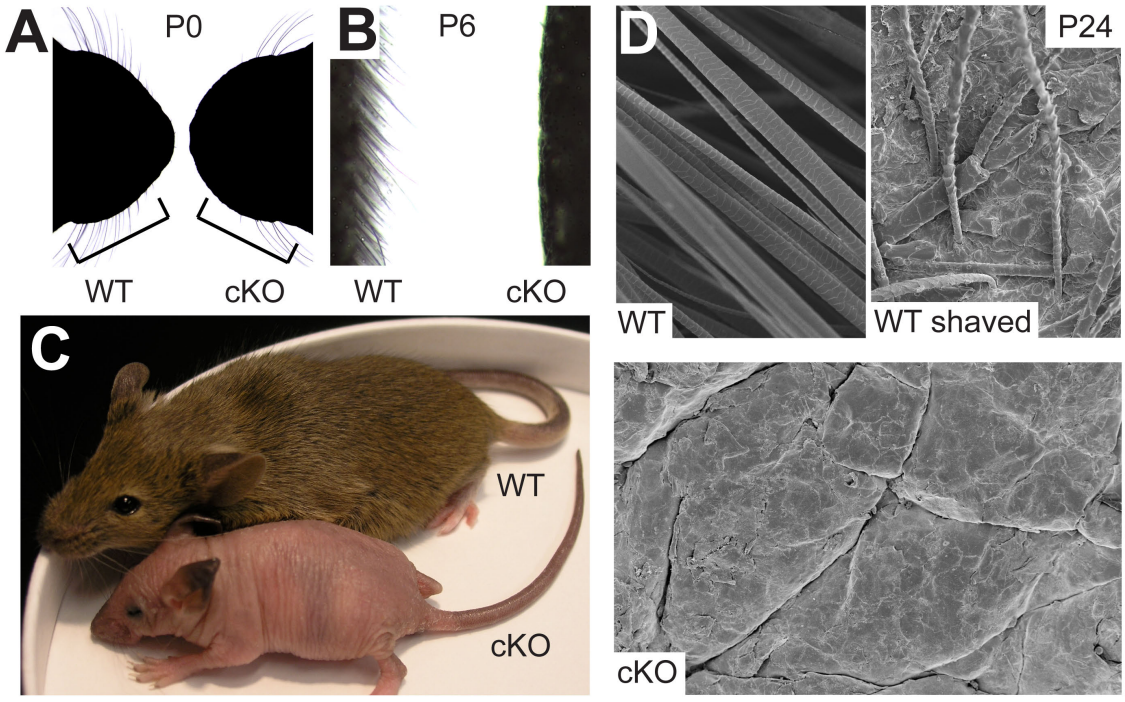

Figure 3.6. Embryonic ablation of *Sox9* results in failure to form a hair coat. (**A**) *Sox9* cKO P0 mice display an 80% reduction in whisker number compared to WT mice. (**B**) Analysis of P6 backskin shows *Sox9* cKO mice fail to form a visible pelage hair coat. (**C**) Gross appearance of adult WT and cKO mice showing profound lack of hair on cKO. Adult cKO mice were consistently smaller than WT mice, and the abundant expression of Sox9 in the K14-positive epithelial portion of salivary glands suggests that impaired feeding is a possible cause of smaller size. (**D**) Scanning electron microscopy of adult backskin demonstrates a total absence of hair on cKO backskin. Shaving the hair coat of WT mice reveals the surface of the epidermis and the insertion points of hair shafts. Scanning electron microscopy images courtesy of H.A. Pasolli.

The effects of Sox9 ablation during embryogenesis appeared to be specific for the early SC population in the presumptive bulge. Immunofluorescence for Sox9 protein demonstrated that, even though *Sox9* had clearly been targeted before E16.5, placodes and germs had formed normally in the cKO at this timepoint (Figure 3.7A). And later at P2, cKO follicles had matured and displayed a morphologically intact, keratin 17-positive ORS (Figure 3.8A). However, the thickening that normally marks the location of early Sox9-positive bulge cells was missing in cKO follicles (Figure 3.7B). Moreover, in contrast to WT HFs, where nuclear Nfatc1 marked a few cells within the presumptive bulge, Nfatc1 was never detected in developing cKO skin (Figure 3.7C, 3.8B). Additionally, even though Sox9 was absent in cKO hair germs, Lhx2 was still expressed in its normal location at the leading edge. However, in more developed follicles, Lhx2 failed to subsequently appear in the presumptive bulge (Figure 3.7D). Finally, although Tcf3 was detected initially in the ORS of developing cKO follicles, it was progressively lost during the first week after birth (Figure 3.7E). Notably, the earliest disappearance of Tcf3 occurred within the presumptive bulge region, and then proceeded unidirectionally towards the follicle base (Figure 3.7E).

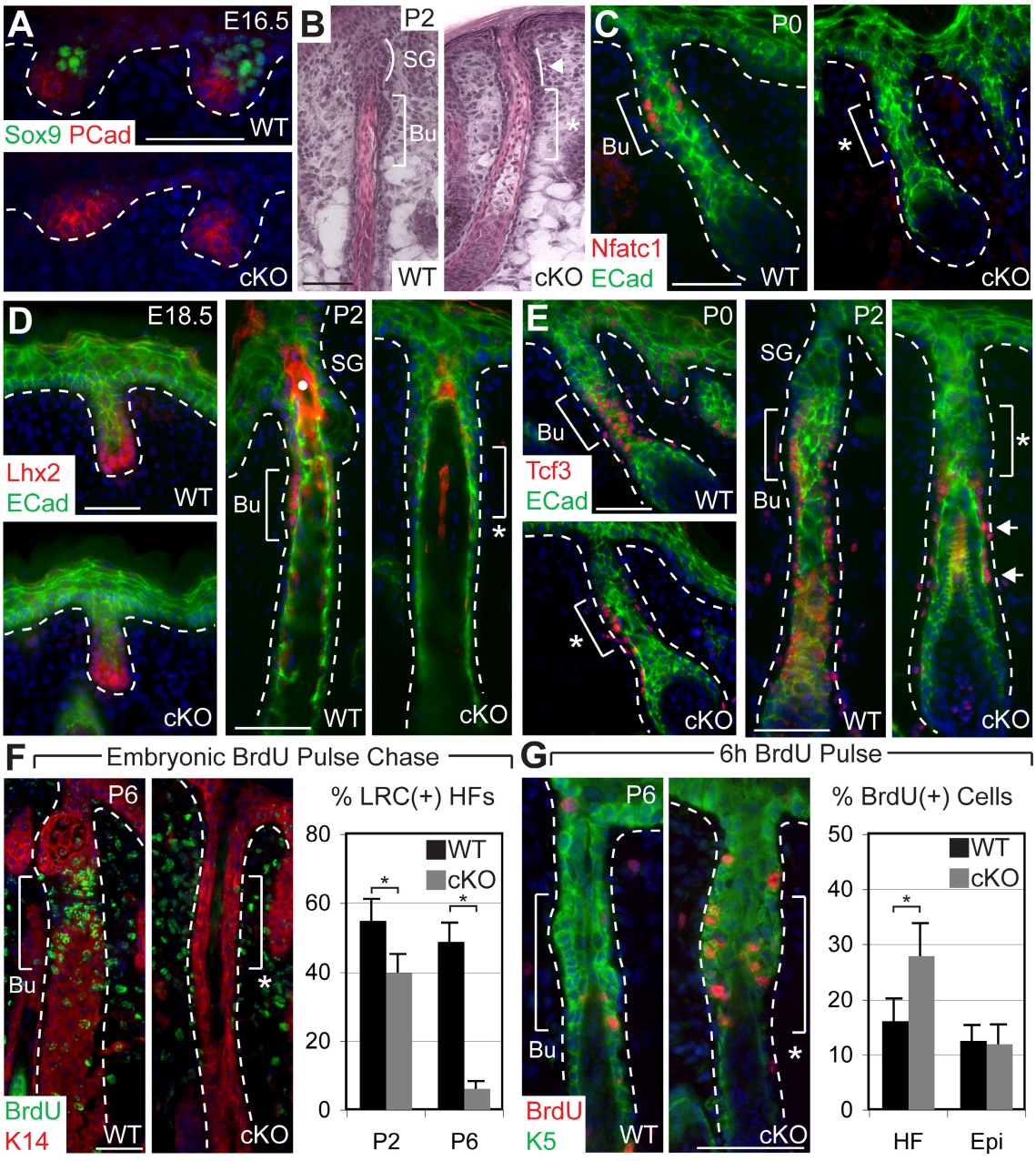
A
E16.5
Sox9 PCad
WT
cKO
B
P2
SG
Bu
WT
cKO
C
P0
Bu
Nfatc1
ECad
WT
cKO
D
E18.5
Lhx2
ECad
WT
cKO
P2
SG
Bu
WT
cKO
E
P0
Bu
Tcf3
ECad
WT
cKO
P2
SG
Bu
WT
cKO
F
Embryonic BrdU Pulse Chase
P6
Bu
BrdU
K14
WT
cKO
% LRC(+) HFs
80
60
40
20
0
WT
cKO
P2
P6
G
6h BrdU Pulse
P6
Bu
BrdU
K5
WT
cKO
% BrdU(+) Cells
50
40
30
20
10
0
WT
cKO
HF
Epi

Figure 3.7. Failure of early bulge stem cells to form in the absence of *Sox9*. WT early bulge region (Bu) and approximate cKO bulge region (asterisk) are indicated by brackets. White dotted lines denote epidermal-dermal border. (**A**) E16.5 backskin shows absence of Sox9 in P-cadherin (Pcad) marked cKO placodes and hair germs. (**B**) H&E stained P2 backskin reveals that the thickened zone of ORS which normally develops just below the SG (curved line) is absent in cKO HFs. (**C-E**) Nfatc1, marking developing bulge cells, never appears in cKO follicles. In contrast, Lhx2 is appropriately expressed at the leading edge of cKO follicles but is completely lost by P2. Tcf3 is initially present in P0 cKO follicles, but is progressively lost. White dot in (D) marks autofluorescent hair shaft. (**F**) Embryonic BrdU pulse-chase demonstrates that early LRCs do not form in *Sox9* cKO HFs. (**G**) A 6h BrdU pulse at P6 shows enhanced proliferation in the cKO approximate bulge region. Asterisk indicates p-value < 0.05. Scale bars, 50 μm.

Although establishment of early bulge architecture and gene expression was clearly impaired in developing *Sox9*-deficient HFs, it remained possible that early bulge cells were still present within the ORS but could no longer be identified by these criteria. Since my studies had shown that early bulge cells reduce their cycling rate as they develop, I conducted an embryonic BrdU pulse-chase to see if early LRCs were also lost when *Sox9* was absent. Consistent with the H2B-GFP embryonic pulse-chase, a discrete population of BrdU-positive cells accumulated in the ORS of most follicles just below the sebaceous gland and later localized exclusively to the adult bulge stem cell niche (Figures 3.7F, 3.8C). Strikingly, significant differences in the numbers of cKO follicles with LRCs were already evident by P2 and by P6, LRC-containing HFs were diminished by ~8-fold (Figures 3.7F, 3.8C). The dramatic reduction in LRCs in the presumptive bulge of *Sox9*-deficient neonatal HFs was accompanied by a substantial increase in proliferation in this zone. A 6 hr pulse of BrdU at P6 revealed an increase of ~40% in BrdU-labeled cells

within the total Sox9 cKO upper ORS population, mostly concentrated in the region of the presumptive bulge (Figure 3.7G). Similar differences were observed with proliferation marker Ki67 (Figure 3.8D). Importantly, proliferative differences were not observed in the interfollicular epidermis of WT and cKO mice, where Sox9 is not expressed, underscoring the specific nature of the *Sox9* cKO phenotype on hair follicles (Figure 3.7G, 3.8D). Notably, the kinase Cdk4, whose expression is required for progression through the G1/S cell cycle checkpoint, was markedly upregulated in cKO HFs (Figure 3.8E). Given that *Cdk4* is known to be transcriptionally repressed by Nfatc1 in adult bulge cells, this finding is consistent with the failure of cKO HFs to properly express Nfatc1 in the presumptive bulge region (Horsley et al., 2008).

These findings unveiled new requirements for Sox9, namely in the early expression and maintenance of transcription factors and slow-cycling bulge SC features which were found to be established during embryogenesis, long before other bulge markers, such as CD34, appear. When taken together with my earlier label retention and genetic marking studies, these additional data provided compelling evidence that not only does a population of early bulge stem cells form during skin development, but that its features critically rely upon one of the transcription factors that marks it.

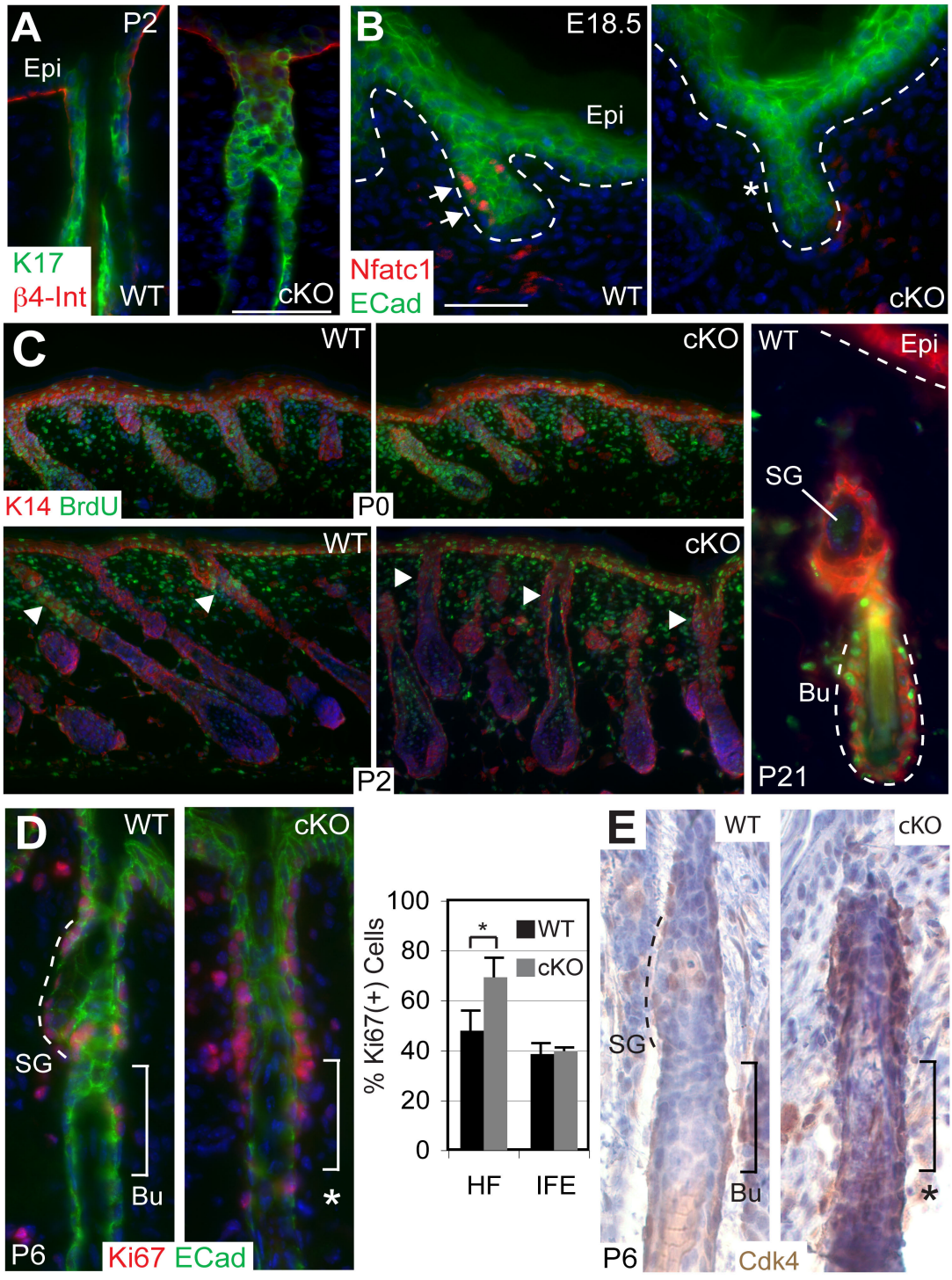
A
P2
Epi
K17
β4-Int
WT
cKO
B
E18.5
Epi
Nfatc1
ECad
WT
cKO
C
WT
cKO
K14 BrdU
P0
WT
cKO
P2
WT
Epi
SG
Bu
P21
D
WT
cKO
SG
Bu
P6
Ki67 ECad
% Ki67(+) Cells
100
80
60
40
20
0
*
WT
cKO
HF
IFE
E
WT
cKO
SG
Bu
P6
Cdk4

Figure 3.8. Specific loss of early bulge quiescence in the absence of Sox9. (**A**) General ORS marker keratin 17 (K17) remains properly expressed in cKO HFs. β4-Int, β4-Integrin. (**B**) Nfatc1, marking developing early bulge cells (arrows) is absent at E18.5 in cKO HFs (asterisk). Dotted lines indicate epidermal-dermal border. ECad, E-cadherin. (**C**) An embryonic BrdU pulse-chase completely labels keratin 14 (K14) positive epithelial cells in WT and cKO skin. As early as P2, clusters of BrdU positive LRCs (arrowheads) begin to appear in the upper portions of WT follicles, but are less apparent in cKO follicles. Bu, bulge. SG, sebaceous gland. (**D**) Ki67, a marker of proliferative cells, is more widely expressed in the upper ORS of cKO HFs (69%) compared to WT (48%). IFE, interfollicular epidermis. Graph shows average data (± SEM). (**E**) Cdk4 expression is increased in the entire ORS of cKO mice compared to WT.

Early bulge cells are required to complete hair follicle morphogenesis

I next addressed my finding that Sox9-dependent early bulge SCs form during HF morphogenesis in the context of the absent hair coat phenotype of *Sox9* cKO mice. Histological analysis of skin from P0 cKO mice revealed no significant differences in overall HF density or developmental stage (Figure 3.9A). By contrast, differences in HF length were already evident at P0 and by P6, cKO follicles averaged ~60% the length of WT follicles (Figure 3.9B). Despite gross perturbations in HF length, overall morphology and biochemical features of HF differentiation were relatively normal, and the ORS, IRS and hair shaft all appeared to be present and correctly organized (Figure 3.10). Importantly, *K14-Cre* targeted *Sox9* ablation efficiently prior to the main waves of HF specification and well before differentiated HF lineages developed. Thus, rather than specifying HFs or governing their differentiation, Sox9 appeared to function in maintaining the growth of HFs once morphogenesis was initiated.

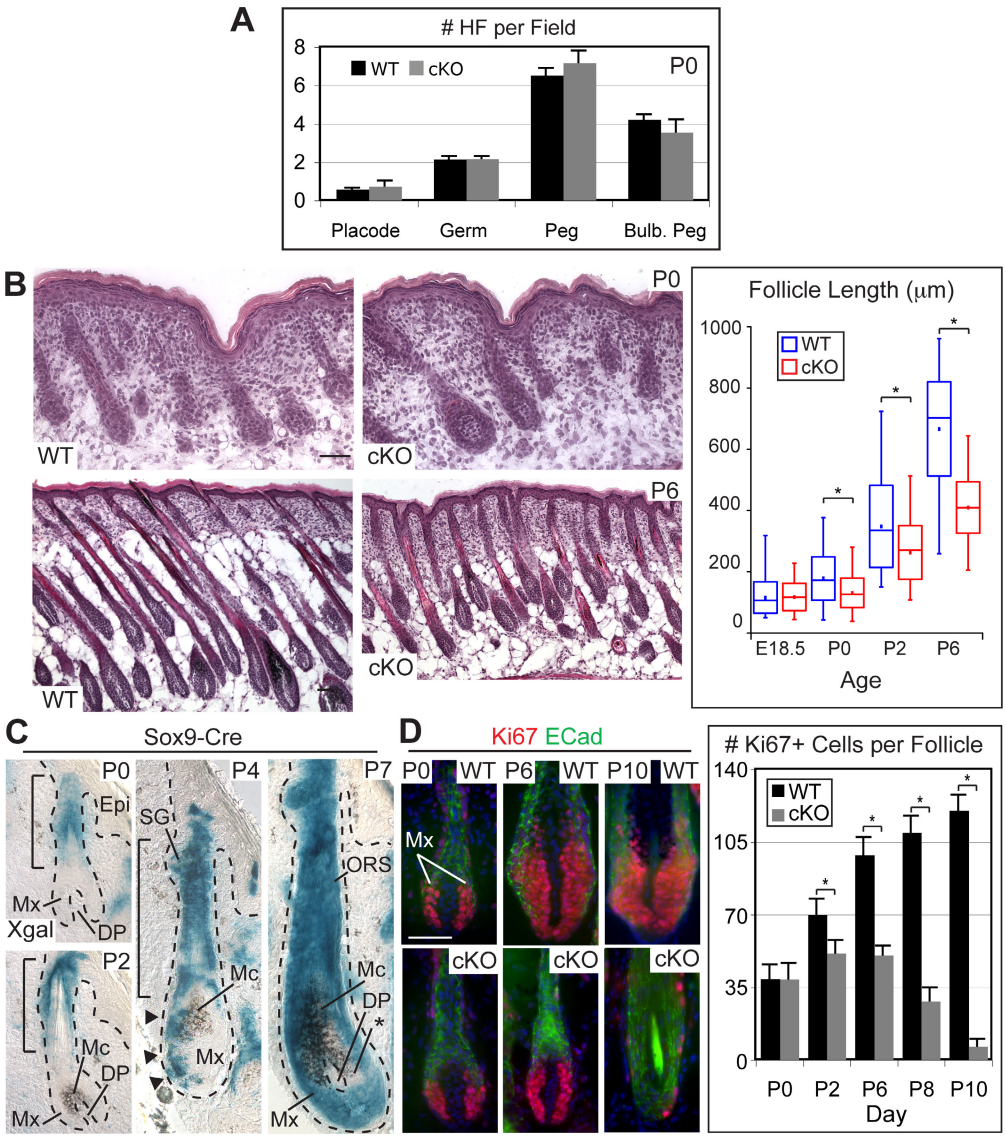

Figure 3.9. Early bulge SCs are required to maintain the transit-amplifying matrix. (**A**) Quantification of HF number and development stage at P0 reveals no defects in initial cKO follicle specification or developmental progression. (**B**) H&E stained backskin reveals normal HF density but impaired HF growth. Box and whisker plots quantify HF length: min. and max. length are marked by whiskers; upper and lower box boundaries indicate quartile divisions; central line indicates median; square dot indicates mean length. (**C**) Genetic marking studies with *Sox9-Cre/R26R* reporter mice demonstrate a temporal progression of blue ORS cells that move to and enter the matrix (Mx), eventually replacing all prior Mx cells during HF morphogenesis. Asterisk indicates XGal negative Mx cells. Mc, melanocytes. (**D**) Tracking of Ki67-positive Mx cells over time. The cKO Mx expands only transiently before reaching an abnormally small maximal size and then shrinking. ECad, E-cadherin. Graph displays the average number of Ki67 positive cells in the Mx. Asterisk indicates p-value < 0.05. Scale bars, 50 μm.

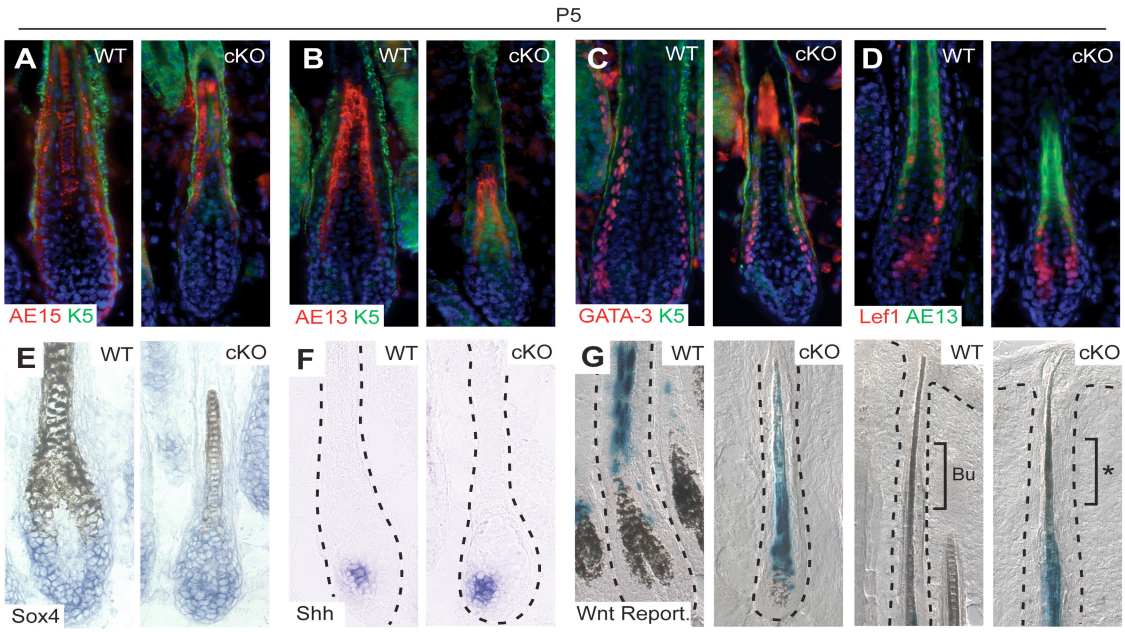

Figure 3.10. Hair follicle differentiation is unimpaired in the absence of early SCs. **(A-D)** Immunofluorescence microscopy on P5 HFs demonstrates that structural proteins such as trichohyalin (AE15), an inner root sheath (IRS) marker, and hair keratin (AE13), a hair shaft marker of the cortex and medulla, were correctly expressed in the appropriate subrabasal layers of Sox9-deficient HFs. Transcription factors such as GATA-3 and Lef1, which are key regulators of differentiating IRS and pre-cortical cells, respectively, were also expressed correctly. **(E-F)** *In situ* hybridization demonstrates no abnormalities in Sox4 or Shh mRNA expression, which in anagen-phase postnatal HFs, precede GATA-3 and Lef1, but are downstream of Sox9. Black dotted lines indicate the dermis/HF border. **(G)** XGal staining on skin sections obtained by breeding to the *BATGAL* Wnt reporter mouse revealed that Sox9-deficiency did not appear to perturb Wnt signaling within the precursor cells that generate the hair shaft of cKO follicles. Notably, although Sox9 has been implicated as a repressor of Wnt/β-catenin signaling (Akiyama et al., 2004), *BATGAL* expression did not appear to be activated in the cKO ORS.

To investigate this fascinating possibility further, I returned to *Sox9-Cre/R26R* mice, this time focusing on the developmental activity of Sox9-expressing cells at the same time points when defects became apparent in *Sox9* cKO mice. At P0 and P2, blue cells were detected in the upper ORS (bracketed) (Figure 3.9C). Notably, the initial matrix was negative for XGal reactivity. By P4 however, a trail of blue cells extended

from the ORS into the matrix (Figure 3.9C). By P7, most matrix cells were blue, and only small patches of negative cells could be detected within the hair bulb (asterisk). While the mesenchymal DP cells encapsulated by the Mx and follicle melanocyte population were not affected, melanocytes provide brown pigment to differentiating hair shaft cells, giving some intermingled blue and brown cells. Since the matrix was negative for Sox9 mRNA and protein, the progressive expansion of XGal reactivity into these compartments at the expense of unmarked cells implies that during early HF development, Sox9-expressing cells provide an active input to the newly formed matrix, whose initial residents are transient.

To test whether the loss of early bulge SCs in *Sox9* cKO mice might result in an early failure to maintain the transit-amplifying matrix population, I next analyzed matrix size over time. No differences were noted at P0, suggesting that initial specification of matrix was unimpaired in the absence of early SCs (Figure 3.9D). However, in contrast to WT matrix, which gradually expanded from P0 to P10, *Sox9* cKO matrix only transiently expanded until P2 before it began to shrink and nearly disappear by P10 (Figure 3.9D). Concomitant with the loss of Ki67-positive matrix cells at P10 was an abrupt change in dermal papilla morphology (Figure 3.11), commensurate with that known to occur upon exit of HFs from the growth phase of the hair cycle (Stenn and Paus, 2001). This change in DP morphology was accompanied by a rapid degeneration of cKO follicles, many of which regressed upwards and merged into the interfollicular

epidermis, often leaving a DP completely isolated in the dermis (Figure 3.11). This result demonstrated that proper anagen follicle morphology is critically dependent upon the maintenance of a proliferative matrix population.

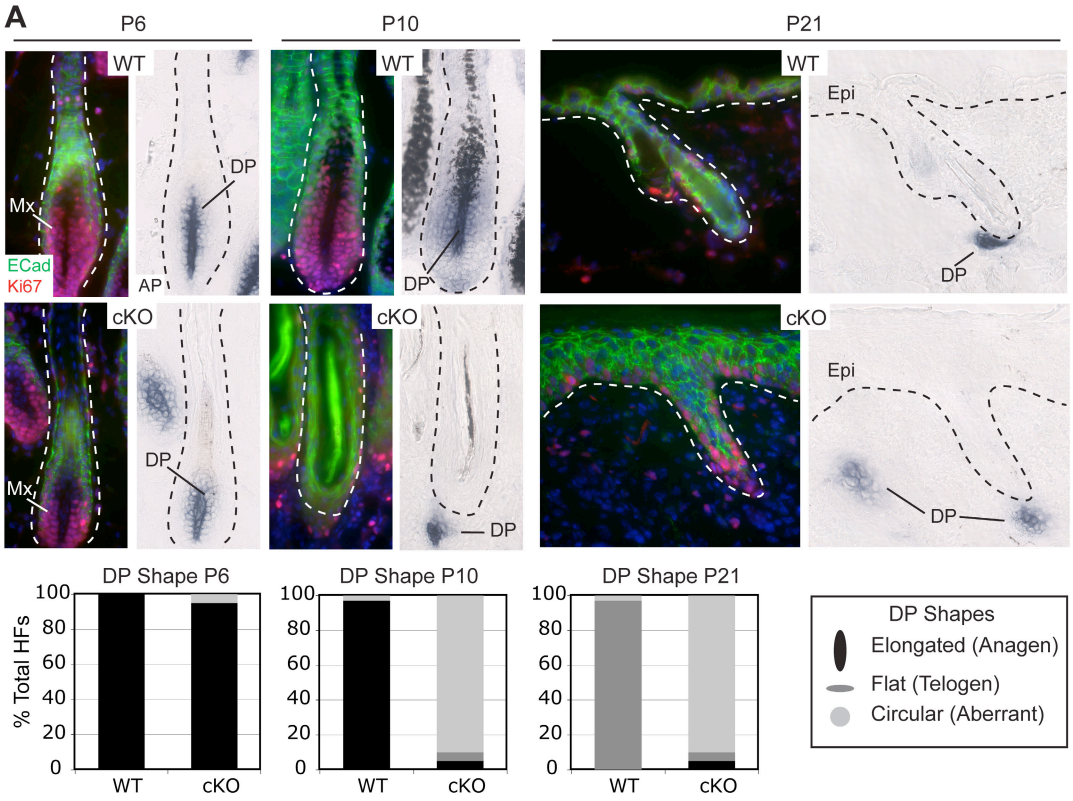

Figure 3.11. Loss of matrix in the *Sox9* cKO causes premature exit from the hair cycle. (**A**) HFs from WT and cKO mice were stained with antibodies against E-cadherin (ECad) and Ki67 to detect follicle morphology and subsequently stained for alkaline phosphatase (AP) activity to detect dermal papilla cells. Note that the WT DP retains a vertically elongated shape characteristic of anagen between P6 and P10, while the cKO DP switches from an elongated anagen shape at P6 to an abnormally round shape at P10. At P21, WT DPs display a flattened shape characteristic of telogen stage follicles, while cKO DPs are circular, amorphous and frequently found isolated in the dermis without adjacent epithelial cells. Graphs quantify the percentage of DPs with each shape at each time point. Fifty HFs were examined for both WT and cKO at each time point.

Direct evidence for a decreased input of SCs to the matrix in *Sox9* cKO HFs was provided by a series of short BrdU pulse chase experiments which allowed me to distinguish possible causes of a smaller matrix population, including precocious differentiation, decreased proliferation or impaired input of SCs to the matrix (Alonso et al., 2005). At all times, the percentage of BrdU-positive cells per bulb was similar, suggesting that cKO cells proliferate at the same rate as WT cells (Figure 3.12). Additionally, only minor differences in differentiation rate were detected, suggesting that the relative balance of proliferation and differentiation was largely unimpaired (Figure 3.12). The cKO HFs were also generally free of apoptotic cells, suggesting that cell death was not a major cause of smaller matrix size (Figure 3.13). Strikingly, however, cKO HFs displayed a marked decline in ORS input to the matrix, with an ~33% reduction in the percentage of BrdU-positive cells in the lower ORS at 12h and an ~50% reduction at 20h (Figure 3.12).

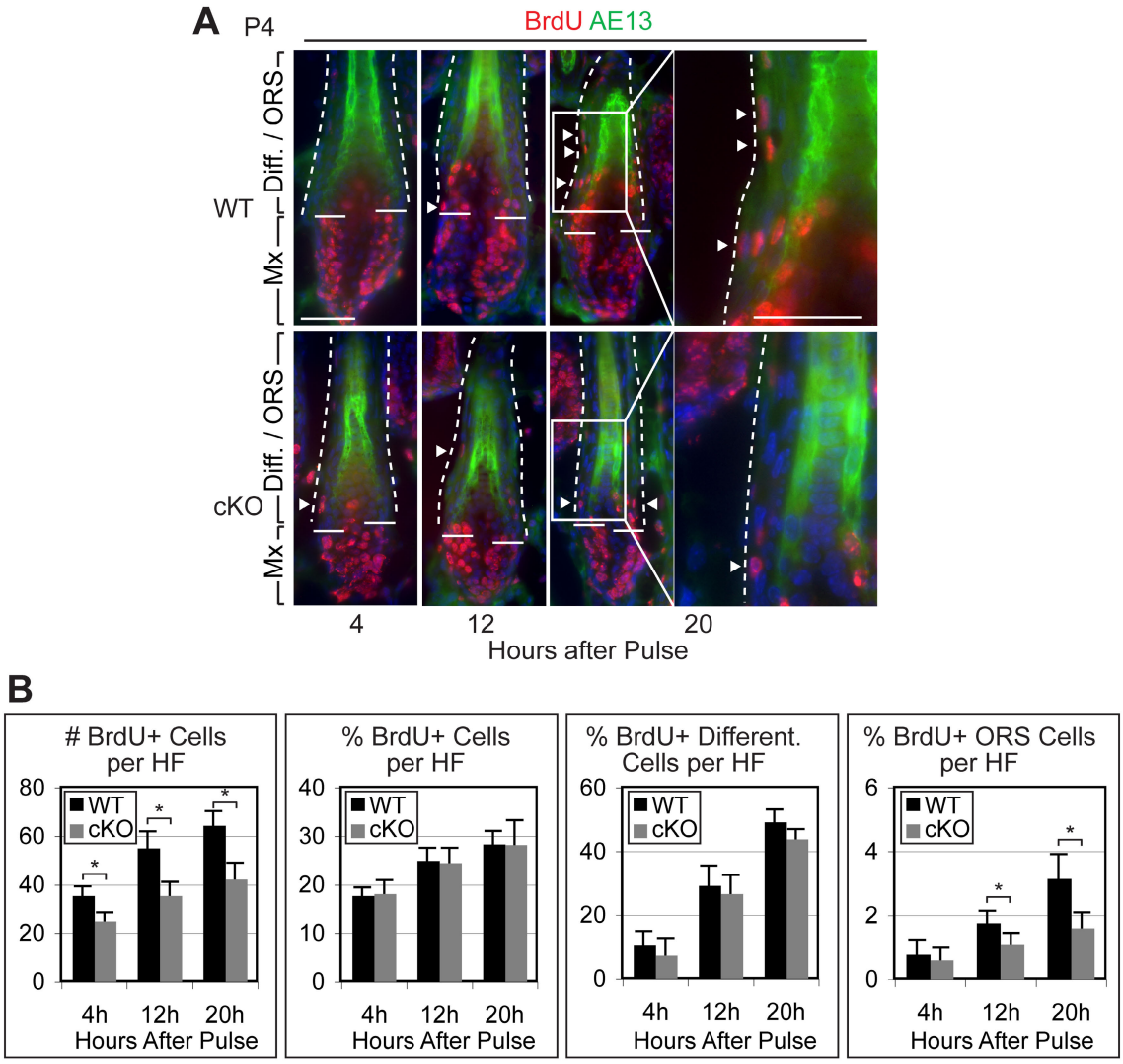

Figure 3.12. ORS input to the matrix is impaired in *Sox9* cKO hair follicles. (**A**) Immunofluorescence microscopy for BrdU and hair keratin (AE13) in representative HFs at indicated time points after a single BrdU pulse at P4. White dotted lines indicate the outside border of the ORS and solid horizontal lines indicate the border between the Mx and the zone of differentiation, demarcated by the lowest AE13 positive cells. Arrowheads indicate examples of BrdU labeled cells in the ORS, which are readily apparent in higher magnification views of HFs at the 20h time point. (**B**) Mx proliferation and differentiation kinetics were analyzed by short BrdU pulse-chases at P4. Note that the percentage of BrdU positive cells in the lower ORS was lower in cKO HFs compared to WT at both the 12h and 20h timepoints, whereas the percentage of total BrdU positive cells and BrdU/AE13 double positive, differentiated cells was largely unchanged. Asterisk indicates p-value < 0.05. Scale bars, 50 μm.

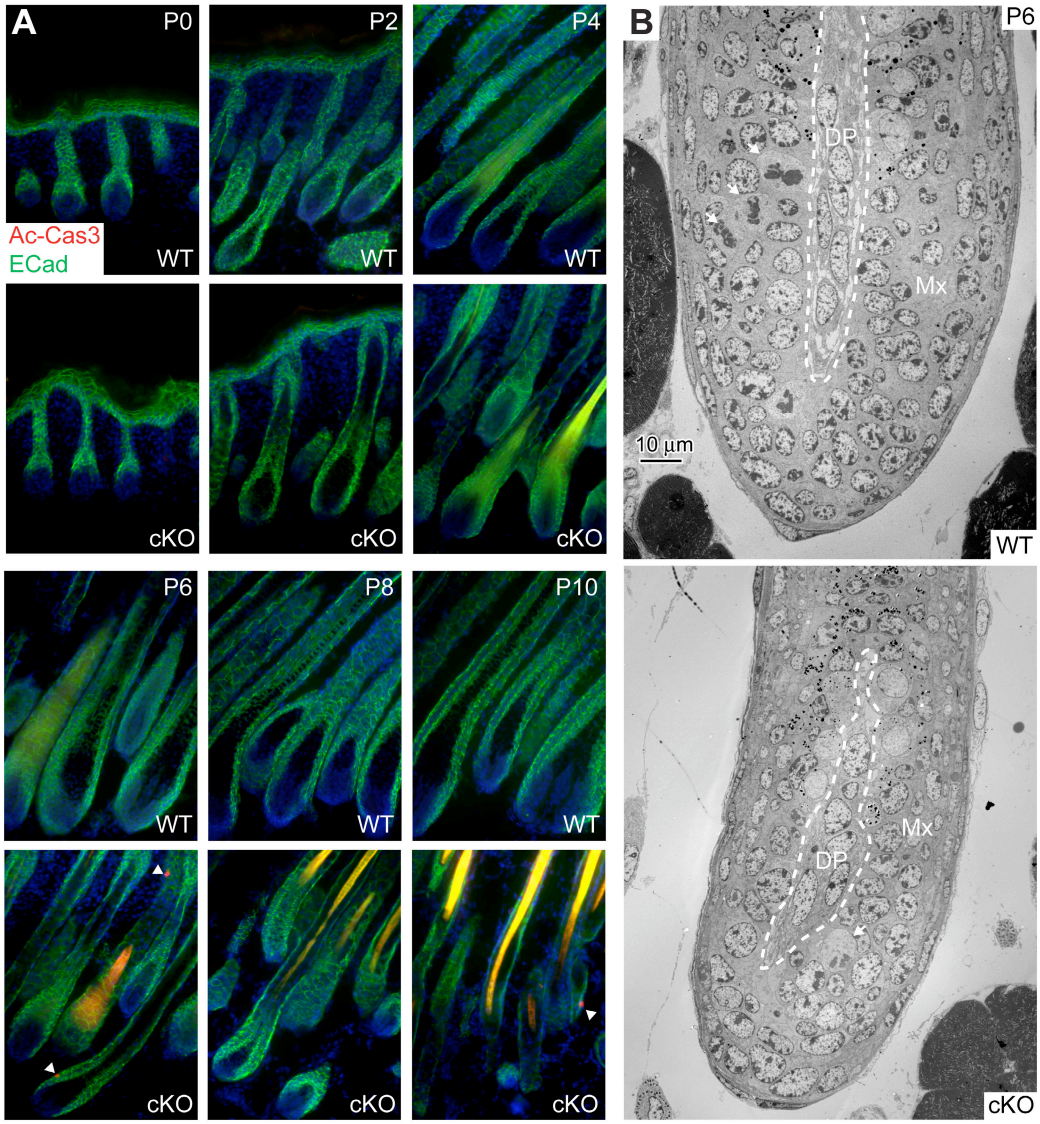

Figure 3.13. The reduction in *Sox9* cKO matrix size is not due to apoptosis. (**A**) HFs from WT and cKO mice at indicated time points were stained with antibodies against activated Caspase-3 (Ac-Cas3), a specific marker of apoptotic cells, and E-cadherin (ECad). Prior to P6, no apoptotic cells were observed in any compartment of the cKO skin, including the matrix, ORS, interfollicular epidermis and dermis. Beginning at P6 and continuing to P10, rare activated Caspase-3 positive cells could be detected in the skin, but were randomly distributed and not confined to the matrix or ORS. Notably, more than 95% of all cKO follicles remained completely free of activated Caspase-3 staining from P6 to P10. Examples of rare activated Caspase-3 positive cells (arrowheads) are shown in the cKO at P6 and P10 to illustrate their isolated nature and positive antibody reactivity. (**B**) EM analysis of the matrix from P6 WT and cKO mice reveals the presence of multiple mitotic figures (arrows) and the absence of pyknotic nuclei, indicating a lack of apoptotic cells. DP, dermal papilla; Mx, matrix.

Based upon these results, the initial cells that formed the matrix and differentiated HF lineages appeared to be transient and not dependent upon Sox9 for their specification. However, without input from Sox9-positive early bulge SCs, this pool of transit amplifying matrix cells was not maintained and as a direct consequence, HFs did not fully progress through the growth phase of the hair cycle.

Early bulge cells are required for formation of the sebaceous lineage

Although SGs possess their own resident unipotent progenitors marked by Blimp1, adult bulge SCs can differentiate along a sebaceous lineage in a wound environment or when SG progenitors are defective (Blanpain et al., 2004; Horsley et al., 2006; Morris et al., 2004). Based upon my *Sox9-Cre* marking results and the temporal appearance of early bulge SCs prior to development of SGs, I wondered whether early bulge SCs might be essential for this lineage. Indeed, Blimp1-positive SG progenitors, which mark the site where the sebaceous gland will develop, were completely absent in cKO follicles (Figure 3.14A). Also missing was PPARγ, a key sebocyte differentiation marker (Figure 3.14B). Lipid dye (Oil-red O), which normally permits visualization of SG morphology by P6, only stained the subcutaneous adipocytes and revealed no morphological signs of SGs in cKO follicles (Figure 3.14C).

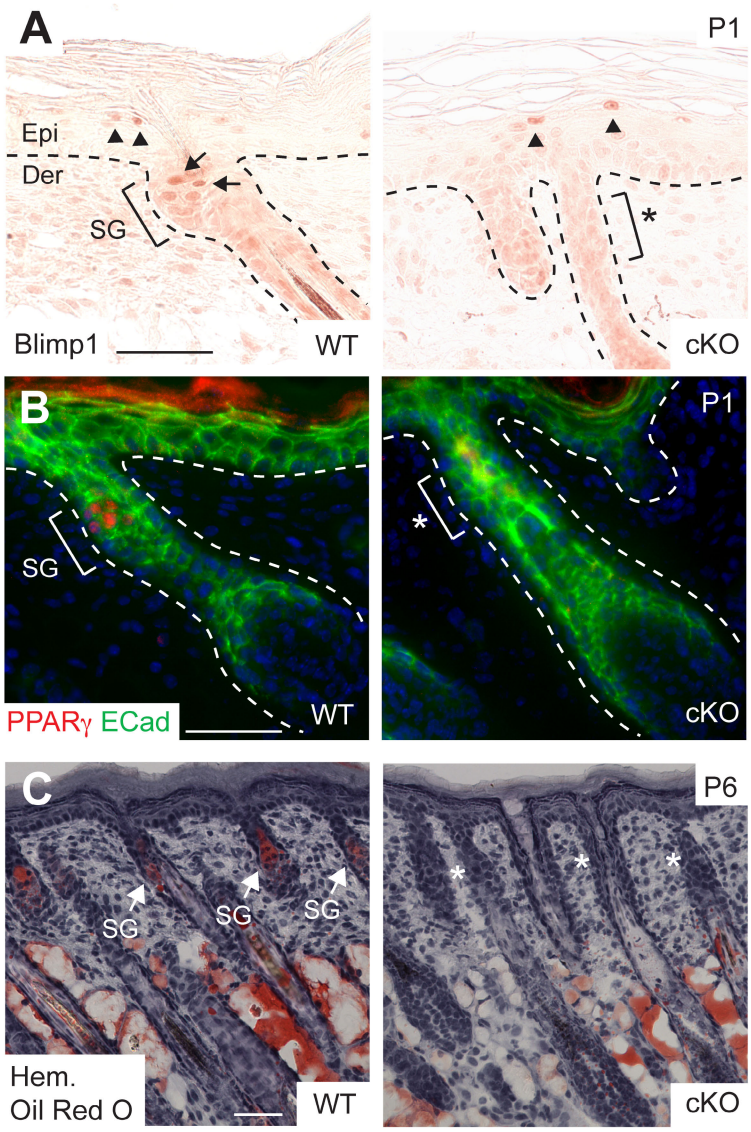

Figure 3.14. Early bulge SCs are required to form the sebaceous lineage. (**A**) Immunohistochemical analysis of Blimp1 expression shows an absence of unipotent SG progenitors in the upper ORS of *Sox9* cKO HFs where the SG should normally form. Arrows indicate Blimp1-positive cells in the early SG of a WT HF. Note that Blimp1 is still appropriately expressed in suprabasal cells of cKO epidermis (arrowheads). (**B**) Immunofluorescence reveals that PPARγ, a sebocyte differentiation marker (bracket, SG), is absent in cKO follicles (bracket, asterisk). (**C**) Detection of lipids by Oil-red O staining reveals no evidence of lipid-accumulating SGs (arrows) associated with cKO follicles (asterisks). By contrast, the formation of subcutaneous fat is not affected when *Sox9* is conditionally targeted by *K14-Cre*. Hem, hematoxylin. Other abbreviations are as in the legend for previous figures. Scale bars, 50 μm.

Early bulge cells are required for follicle-mediated wound healing

My genetic marking experiments using *Sox9-Cre* mice also provided evidence that HF cells derived from a Sox9-expressing population can contribute to repair of wounded IFE. To test whether Sox9-expressing early bulge SCs might be essential for efficient HF contribution to IFE repair, I conducted engraftment experiments on *Nude* mouse recipients with split-thickness P0.5 dermis/HF tissue (Figure 3.15A). This approach leaves hair follicles, including the early bulge region, almost completely intact and embedded in the dermis at the proper orientation while completely removing the overlying interfolicullar epidermis. Pilot experiments with *K14-H2BGFP* mice validated the split thickness grafting technique and remarkably, two weeks after placement of dermis/HF grafts, cells from GFP-marked hair follicles had generated a well-healed epidermis that covered almost the entire area above the grafted tissue (Figure 3.15B). The specific presence of hair in this area demarcated the borders of the graft. Histological analysis confirmed the gross findings and showed greater than 90% GFP-positive donor cell IFE reconstitution (Figure 3.15C). Importantly, despite the substantial amount of additional proliferation that cells from the hair follicle would have to undergo to regenerate the entire epidermis, hair follicles appeared morphologically normal in the graft, suggesting that the epidermis had not be rebuilt at the expense of other epithelial lineages.

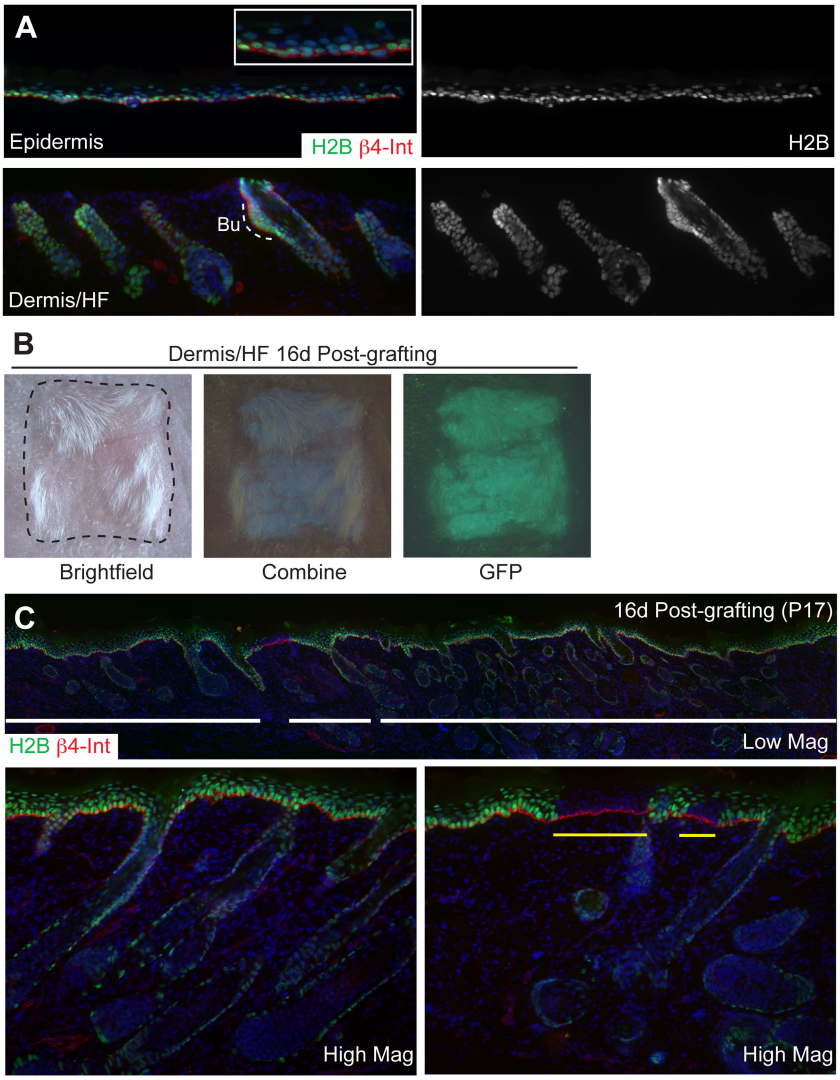

Figure 3.15. A grafting assay for measuring follicle-mediated epidermal repair. (**A**) Backskin from P0.5 *K14-H2BGFP* mice was chemically treated and physically separated into epidermis and dermis/HF components. Immunofluoresence analysis shows that the epidermis is removed in a single, complete sheet from the underlying dermis, where HFs remain properly oriented. Inset shows β4-Integrin (β4-Int), marking the basement membrane, retained in the isolated epidermis. (**B**) Brightfield and GFP epifluoresence pictures of a P0.5 *K14-H2BGFP* split thickness graft 16 days after grafting. (**C**) Immunofluorescence analysis of grafted split thickness skin shows robust regeneration of the interfollicular epidermis by H2BGFP positive donor cells. White horizontal bars mark the extent of H2BGFP positive cells in the IFE at low magnification. High magnification shows one example of a skin region with complete IFE reconstitution and one example of incomplete IFE reconstitution where *K14-H2BGFP* negative *Nude* cells are present in the IFE (region marked by yellow bars). Bu, bulge.

To distinguish donor from host cell contributions in *Sox9* cKO test grafts, male skins were grafted onto female *Nude* recipients, and fluorescence *in situ* hybridizations were performed with a Y chromosome specific probe (Y-FISH). As controls, full thickness skin from both WT and cKO mice was also grafted to ensure efficacy of the grafting procedure and to demonstrate that cKO interfollicular epidermis can be maintained for long periods of time in the absence of injury by its own unipotent progenitor population. The data from the engraftments of *Sox9* cKO and WT skins are summarized in Figure 3.16. Full and split thickness grafts from WT mice displayed comparably thick, uniform hair coats, and quantification of skin surface areas revealed no significant differences. Similarly, although full thickness grafts from *Sox9* cKO skin lacked hair and showed a slightly scaly epidermis, the average graft areas were similar to WT. All of these grafts expanded in size over time, indicating their robust nature in growth and ability to repair wounds. Y-FISH revealed that the IFE of all of these grafts was almost completely donor-derived and was stably maintained over a four month period.

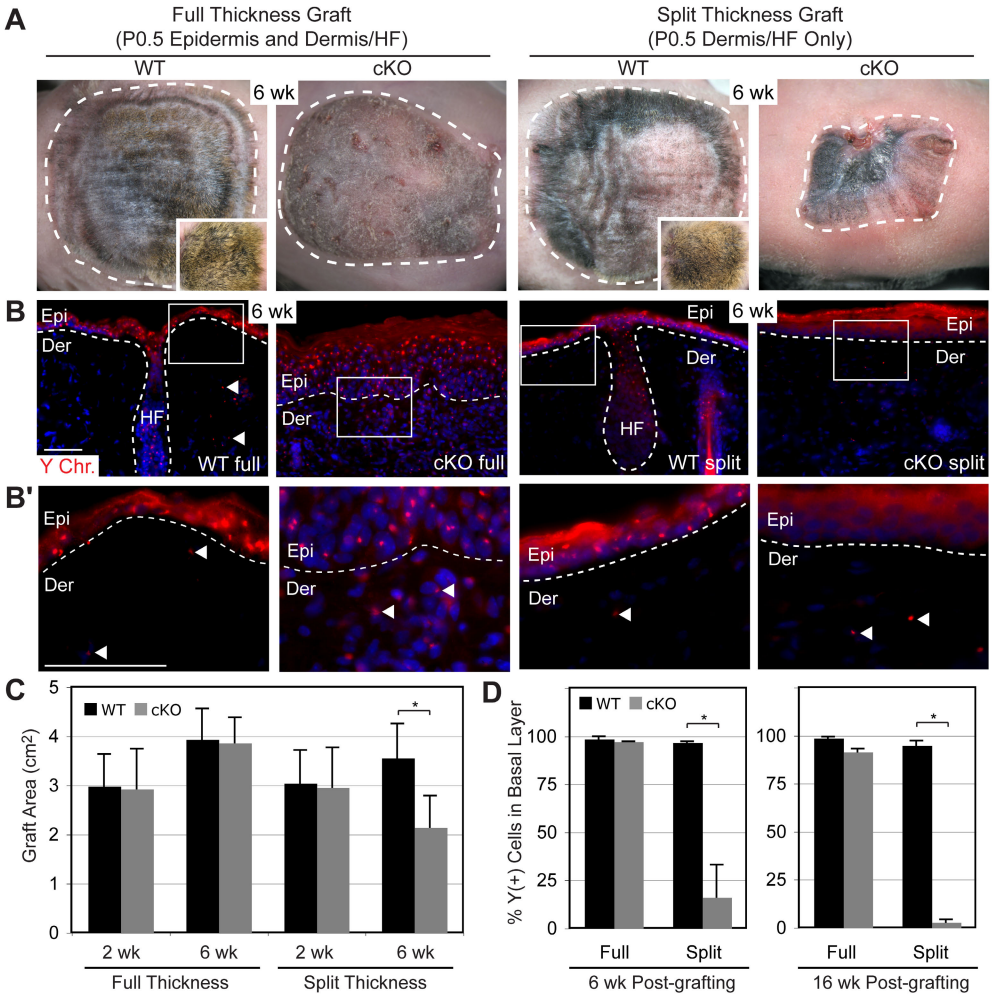

Figure 3.16. Early bulge SCs are required for follicle-mediated epidermal repair. Full thickness (epidermis and dermis/HFs) and split thickness (dermis/HFs) skins from newborn male WT and *Sox9* cKO mice were grafted onto female *Nude* recipients and analyzed for their gross appearance 6 wks after placement (**A**) and contribution of engrafted cells to the repaired epithelium, as judged by Y-chromosome *in situ* hybridization (Y-FISH) (**B,B′**). Quantifications of these data are presented in (**C**) and (**D**), respectively. Notes: 1) WT grafts were shaved to expose skin surface. Insets in (A) show unshaved hair coat. 2) Quantifications in (C) are of average graft areas (± SD) from 10 experiments. 3) Y-FISH reveals that *Sox9* cKO HFs are impaired in contributing to the epidermis (Epi). 4) Full thickness grafts show abundant Y-chromosome labeling, indicating donor origin and efficacy of the engraftments, while split thickness grafts show a striking absence of Y-positive cells in cKO vs WT epidermis. Panels in (B′) represent enlargements of boxed areas in (B) and illustrate Y-positive cells (arrowheads) in the dermis of all grafts. Dotted white lines indicate epidermal-dermal border. Asterisk indicates statistical significance of $p < 0.01$. Scale bars, 50 μm.

While split thickness grafts from cKO skin were initially the same size as the other grafts, they always shrank substantially within a 6 week period and displayed markedly reduced numbers (typically ~15%) of Y-positive IFE cells (Figure 3.16C,D). The presence of Y-positive dermal cells underlying the Y-negative IFE confirmed the efficacy of the initial grafting procedure, and a delay in IFE regeneration was ruled out by monitoring grafts for up to 16 wk after engraftment, at which time the percentage of Y-positive IFE cells had further decreased (Figure 3.16D). Importantly, Sox9 expression was never detected in the interfollicular epidermal cells undergoing wound healing in WT mice, suggesting that it is not directly involved in the wound healing process *per se*. Together, these experiments revealed that neonatal *Sox9* cKO HFs lacking early SCs are severely impaired in their ability to repair damaged IFE.

Surprisingly, however, *Sox9* cKO hair follicles adopted multiple markers and a stratified morphology characteristic of the interfollicular epidermis after hair shaft production had ceased at P10 (Figure 3.17). Given this apparent conversion of a hair follicle fate to an interfollicular epidermal fate, it might have been reasonable to expect that cKO follicles could contribute readily to interfollicular epidermal repair. Instead, the severe impairment in interfollicular epidermal repair by *Sox9* cKO hair follicles is especially remarkable and suggests that mere adoption of interfollicular markers and morphology is insufficient for a hair follicle cell to become a *bona fide* long-term progenitor of the interfollicular epidermis.

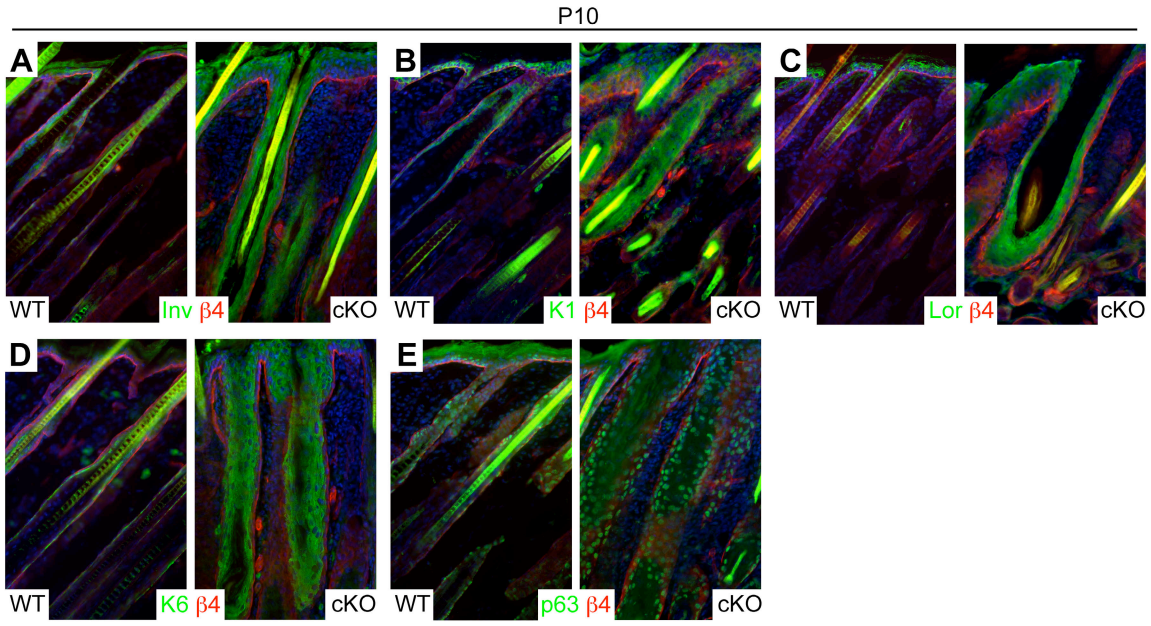

Figure 3.17. Hair follicles adopt epidermal markers in the absence of early SCs. (**A,B**) Involucrin and keratin 1 mark the spinous layer of the epidermis, and are also normally expressed in a single subrabasal layer in the HF. HFs from *Sox9* cKO mice display multiple involucrin and keratin 1 positive cell layers. (**C**) Loricrin, a marker of the granular layer of the IFE cornified envelope, is not expressed in WT HFs, but is present in multiple layers in cKO HFs. (**D**) Keratin 6 is normally expressed in the companion layer of the HF and is also induced in suprabasal layers of hyerproliferative IFE. In cKO follicles, multiple layers of keratin 6 positive cells are present in HFs, and extend above the normal location of the companion layer. (**E**) p63 is normally expressed in a single layer of proliferative basal cells in the IFE and ORS. In cKO HFs, multiple layers of p63 positive cells are present, indicative of a hyperproliferative state. β4, β4-Integrin.

Early bulge cells are required for formation of the adult bulge niche

While multiple markers of early bulge stem cells are absent or are not maintained in developing *Sox9* cKO hair follicles, a separate class of bulge stem cell markers do not appear in hair follicles until the beginning of the postnatal hair cycle at ~P20. Coupled with the morphological alterations of the bulge and its proximity to the dermal papilla at this time point, the synchronized appearance of these markers suggests that a specific developmental program is activated at this time to specify the features of the definitive

adult bulge stem cell population. Although the embryonic H2B-GFP pulse-chase data and *Sox9-Cre* genetic marking experiments demonstrated that cells in the adult bulge are descendants of the early follicle LRC bulge population, it remained possible that follicles might be able to specify an adult bulge population by some alternate mechanism when the normal population of early bulge SCs was absent.

To address this possibility, I evaluated the expression of a number of adult bulge stem cell markers in *Sox9* cKO backskin at P21, by which time the adult bulge niche has formed in WT skin (Figure 3.18). Consistent with a previous report, three of the four markers examined—CD34, Tenascin-C, and S100a6—were completely absent in the follicle remnants still present in cKO skin (Vidal et al., 2005). Keratin 15 was still present in follicle remnants, but was expressed at a uniform level throughout the follicles and interfollicular epidermis, in contrast to a normal bulge-preferred expression pattern in WT skin. This lack of adult bulge markers was consistent with the continued lack of a hair coat on older *Sox9* cKO mice. Taken together, this data suggested that the early bulge SC population in hair follicles not only contributes to formation of the adult bulge but is, in fact, essential for the formation of this population. In its absence, hair follicles cannot compensate by instructing other cells to fill the adult bulge niche.

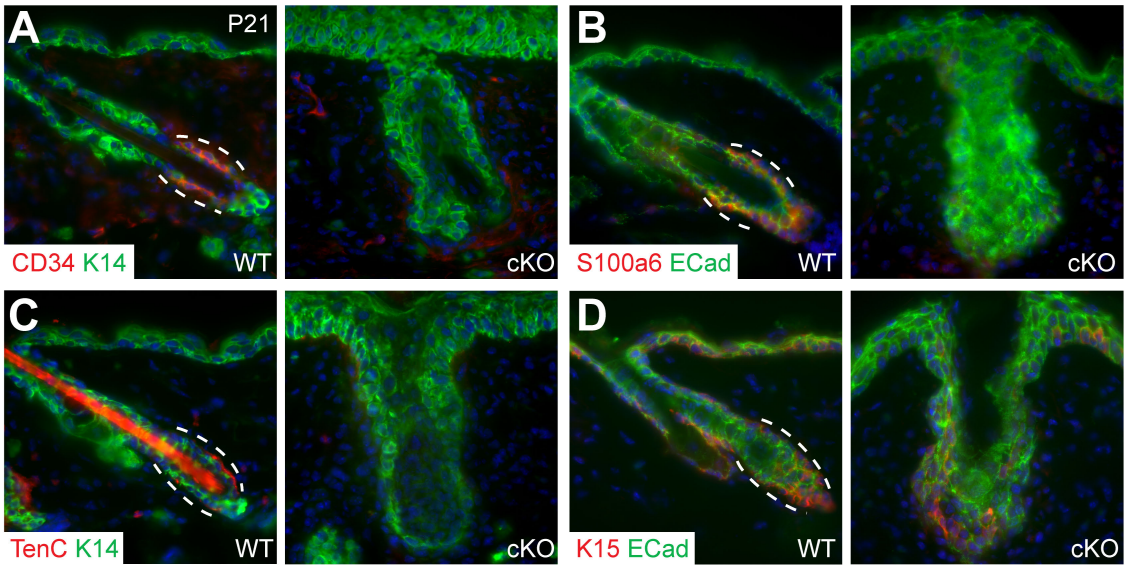

Figure 3.18. Early bulge SCs are required for formation of the adult bulge niche. **(A-D)** Backskin from P21 WT and *Sox9* cKO mice was analyzed by immunofluorescence for the presence of adult bulge niche markers (color-coded). In three of four cases (A-C), bulge markers are completely absent in the follicle remnants still present in cKO skin, but localize appropriately in the WT bulge (dotted white lines). Keratin 15 (K15) loses its bulge-preferred expression pattern in cKO skin and is uniformly expressed through the epidermis and follicle remnants.

Discussion

Characterizing the role of Sox9 in skin morphogenesis revealed that it is specifically required for the formation of a label-retaining, early stem cell population during hair follicle development. By analyzing the expression of Sox9 as well as tracking the progeny of Sox9-expressing cells, it was possible to demonstrate that the Sox9-positive cell population in developing follicles acts like a stem cell population in that it can give rise to all three epithelial lineages in the skin. Using *Sox9* cKO mice as a tool to ablate the early stem cell population, I was able to determine the function of early hair follicle stem cells in the skin and to show that they are essential for completion of skin

morphogenesis. Thus, not only does Sox9 mark both the early and adult stem cell populations in the skin, but in striking contrast to other known stem cell markers, it is essential for the formation of the follicle stem cell population (Horsley et al., 2008; Rhee et al., 2006; Trempus et al., 2007; Vidal et al., 2005).

By taking advantage of Sox9 as a marker of early LRCs, I was able to trace the origins of early bulge SCs to the hair placode. It is intriguing that placodes consist of two populations of cells that can be distinguished by their differential expression of Lhx2 and Sox9, since these two markers are later co-expressed not only by early bulge SCs but also adult bulge SCs. Notably, the existence of two distinct populations in the placode has never been reported, and most known placode marker genes appear to either label the entire placode or localize specifically in the P-cadherin/Lhx2 positive basal layer (DasGupta and Fuchs, 1999; Levy et al., 2005; Rhee et al., 2006). My Sox9 genetic marking studies suggest that the early basal placode cells expressing Lhx2 and P-cadherin are transient. They give rise to the initial hair bulb, but then seem to disappear entirely by ~P7. By contrast, the Sox9-expressing cell population which starts as only a few cells within the suprabasal layer of the placode gives rise not only to the long-lived, self-renewing SCs of the bulge but also the entire pilosebaceous unit, including the infundibulum. The ability of Sox9-positive cells, which first appear primarily in a suprabasal position, to act as long-term stem cells is somewhat intriguing given that contact with the basement membrane is commonly thought to be important for

maintaining stem cell character. However, a precedent for stem cell maintenance in a suprabasal niche can be found in the α6-Integrin^{Low}CD34^{Hi} population of adult bulge stem cells, which also express Sox9. The importance of basement membrane adherence, and especially the signaling pathways and cell division orientation which it can orchestrate, will be a worthwhile area of future investigation in regards to how the distinct cell populations in the placode migrate and proliferate to form the early follicle stem cell population.

In the adult follicle, the active, cycling portion is thought to originate from bulge SCs (Ito et al., 2004). How and why is a separate transit amplifying population specified during initial HF morphogenesis? While additional experiments will be necessary to fully elucidate the significance of this finding, it is interesting that a developmental paradigm of using separate TA and SC populations during morphogenesis has also been described in blood development, where hemogenic cells drive primitive hematopoiesis before long-term hematopoietic SCs commence definitive hematopoiesis (Orkin and Zon, 2008). Notably, the recognition of separate TA and SC compartments in developing follicles sheds new light on the function of currently known markers of early stem cells. For example, Lhx2 is first expressed in cells of the leading edge of placodes and hair germs, the population of cells which gives rise to the initial matrix, before later localizing to SCs in the upper ORS. In the *Sox9* cKO, Lhx2 is correctly expressed in the leading edge but never appears in the ORS. This suggests that Lhx2 may have multiple roles in the hair

follicle distinguished by their location, timing and dependence on Sox9 expression—a conjecture consistent with the pleiotropic nature of the *Lhx2*-null phenotype in the skin (Rhee et al., 2006). My studies now pave the way for examining expression patterns of other adult SC markers in these two placode residences and should allow us to predict how a given gene might function to control subsequent HF morphogenesis.

The existence of an initial pool of Sox9-independent matrix cells explains why HF morphogenesis and differentiation begin normally in *Sox9* cKO embryos. The premature exhaustion of these transient cells in the absence of subsequent input from Sox9-positive SCs further explains why HF maturation and hair production halt midstream during morphogenesis. These findings also demonstrate convincingly that the initial matrix relies upon input from early Sox9-positive SCs for its maturation, and that matrix cells cannot enhance their own self-renewal to compensate for a lack of early bulge SC input.

Some years ago, Oshima et al. (2001) observed that in the anagen phase of the adult rat whisker, bulge cells continue to migrate along the ORS to the hair follicle bulb, where they become matrix cells. Since this initial report, it has been widely debated whether this phenomenon is merely another feature unique to whisker follicles or whether backskin bulge SCs possess similar activity. My studies on the development of WT and *Sox9*-deficient backskin follicles not only provide compelling evidence in support of the Oshima studies, but also show that the fueling of the matrix by Sox9-

positive bulge cells is functionally required to maintain the matrix. In contrast to Lhx2 and Nfatc1, Sox9 also marks the trail of follicle SCs that appear to migrate from the bulge to the transit amplifying matrix during the HF growth phase. This pattern of expression is notably similar to that of early follicle H2B-GFP LRCs, which localize in a distinct cluster just below the sebaceous gland, but also extend a dimmer trail down the ORS towards the matrix (Chapter 2).

Another surprising finding that emerged from targeting *Sox9* ablation in the embryo was that SGs failed to form, even though Sox9 was not expressed in the SG lineage or its resident progenitors. The dependency of the SG lineage on Sox9-expressing cells was particularly intriguing considering that the emergence of Sox9-marked LRCs occurred just before that of sebaceous glands. Taken together, the inability of HF morphogenesis to proceed without Sox9-positive cells and the failure of SGs to form altogether establishes the early Sox9-expressing population as a multipotent SC pool essential for completing skin morphogenesis. These important conclusions could not be predicted from postnatal ablation of *Sox9* in the skin (Vidal et al., 2005), and they provide major new insights into the existence and usage of a follicle stem cell population at a stage and for a purpose that has hitherto been unanticipated.

Although nucleotide double-labeling experiments have detected HF-derived contributions to the IFE of young neonatal mice (Taylor et al., 2000), lineage tracing studies with a *Shh-Cre* reporter active in the developing placode suggest that the

development of HFs and IFE involves distinct progenitors (Levy et al., 2005). My *Sox9-Cre* lineage tracing experiments are consistent with *Shh-Cre* studies in showing that *Sox9-Cre* marked cells in the HF do not contribute to IFE either during its development or its subsequent homeostasis. However, my studies further revealed that in a wound response, *Sox9-Cre* marked HF cells in neonatal mice were robustly recruited to repair the IFE. This finding underscored the similarities between early bulge SCs and adult bulge SCs aiding in IFE repair (Ito et al., 2005; Levy et al., 2005; Levy et al., 2007a; Tumbar et al., 2004). The split thickness grafting approach allowed me to further measure the IFE reconstitution efficiency of early bulge SCs in a wound response and in long-term wound repair. Not only did HF-derived progeny repopulate the IFE with close to 100% efficiency, but these cells were also maintained stably over a four month period. In this regard, the early SC population may be more potent than the adult bulge population in terms of IFE repair capacity, since the adult bulge contribution to regenerated IFE appears to be transient and largely lost after a period of 3 weeks (Ito et al., 2005). Moreover, HFs from *Sox9* cKO mice lacking early SCs were highly impaired in regenerating IFE, suggesting that early SCs may be essential in order for follicles to participate in this process.

A model summarizing the roles of Sox9-dependent early SCs in skin morphogenesis is presented in Illustration 3.1. I've found that a quiescent SC population is formed during the earliest stages of HF morphogenesis and subsequently gives rise to

cells in the adult bulge SC niche. This early SC population is essential for normal morphogenesis of both HFs and SGs, and it robustly contributes to the IFE lineage in a wound environment. While I have identified a single gene, *Sox9*, which is required for early SC specification, these studies now set the foundation for identification of additional molecules and pathways involved in the formation and regulation of these early SCs. A comprehensive understanding of the embryonic origins of SC development is an essential first step not only for normal tissue biology but also for a wide variety of human diseases, including cancers, where SC and/or niche biology is genetically altered.

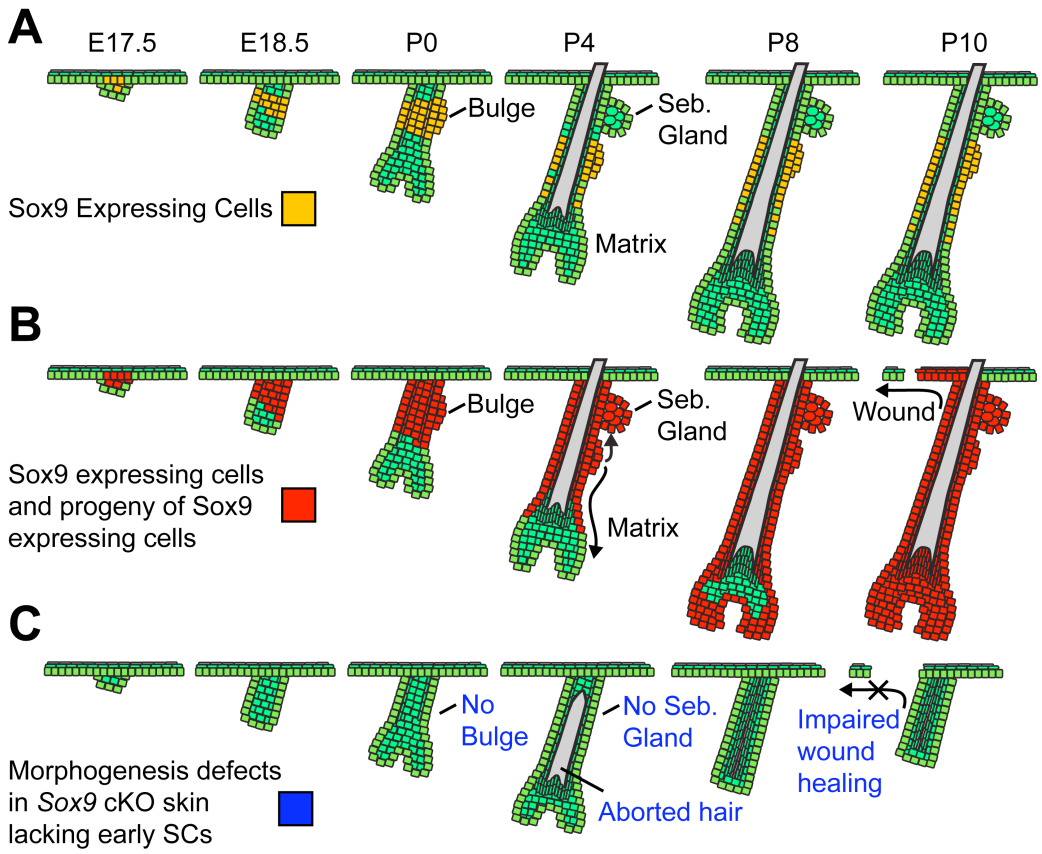

Illustration 3-1. A model for Sox9-dependent early stem cells in skin development. (**A**) Sox9 expression begins in the hair placode, where it marks a few suprabasal cells overlying PCad/Lhx2-positive basal cells at the leading edge. It persists in the upper ORS, where it overlaps with the quiescent LRCs that give rise to the adult bulge. (**B**) Genetic marking is consistent with the notion that Sox9 labels presumptive bulge stem cells within the upper ORS of the developing HF. As HF morphogenesis proceeds, Sox9-expressing cells give rise to the ORS that extends below the early bulge and also the emerging SG above the early bulge. Subsequently, Sox9-expressing cells move down the ORS and completely replace the initial matrix. Upon completion of morphogenesis, the entire HF is composed of Sox9-expressing cells and their progeny. In the presence of a wound stimulus, the progeny of Sox9-expressing cells can robustly contribute to IFE repair. (**C**) Conditional ablation of *Sox9* prior to HF morphogenesis reveals that in the absence of *Sox9*, an early bulge SC population never forms, and all three epithelial lineages are affected. HF differentiation is unimpaired, but hair shaft production is prematurely aborted. The sebaceous gland never forms in the absence of SCs, and HF contribution to wounded IFE is markedly impaired.

Materials and Methods

Mice and Labeling Experiments

BATGAL (Maretto et al., 2003). *Sox9-IRES-Cre* mice (Akiyama et al., 2005) were crossed to *ROSA26*$^{Flox\text{-}Stop\text{-}Flox\text{-}\beta geo}$ (R26R) mice (Mao et al., 1999). *Sox9*$^{flox/flox}$ mice (Akiyama et al., 2002) were crossed with *K14-Cre* mice (Vasioukhin et al., 1999). *K14-H2B-GFP* mice were previously described (Tumbar et al., 2004). All genotyping was performed by PCR using original primer sequences for each mouse strain. 5-Bromo-2'-deoxyuridine (BrdU) embryonic pulse-chase experiments were conducted by injecting pregnant females carrying E17.5 embryos with an intraperitoneal (IP) loading dose of 50μg/g BrdU in sterile PBS and adding BrdU to drinking water for a 24 hour period at 0.8mg/mL. Postnatal BrdU experiments were conducted by single IP injection of 50μg/g BrdU.

Engraftment Experiments

Full thickness grafts from newborn mice were performed as described (Rhee et al., 2006). For split thickness grafts, backskin from P0 mice was placed dermis-side down in 5mM EDTA in PBS for 1 hour at 37°C. The epidermis was then removed as a single sheet from HF/dermis, which was then grafted in the same manner as full thickness grafts. In all cases, paired WT and cKO tissues of identical size were grafted on a single *Nude* recipient. Bandages were removed 12-14 days after grafting. Graft area was

measured using a Canon Powershot S70 camera attached to a dissecting microscope and quantified using ImageJ software (NIH) and a calibrated standard area.

RNA Analysis

Epidermal cells were collected by trypsinization of either full thickness E16.5 skin, or dispase-separated epidermis from P0.5 and P4 skin. ORS, Mx, DP, DF and Mc populations were prepared as previously described (Rendl et al., 2005). Total RNA was isolated using the Absolutely RNA Micro-Prep Kit (Stratagene) and cDNA was synthesized from 100ng of purified total RNA using SuperScript III (Invitrogen). RT-PCR was performed on a LightCycler 480 (Roche) using SYBR Green I master mix. Sox9 mRNA expression levels were expressed as a function of GADPH mRNA calculcated using the comparative Ct method ($2^{-\Delta\Delta Ct}$).

Histology

Skin for immunofluorescence, hematoxylin/eosin staining and *in situ* hybridizations was harvested and processed for frozen sectioning as described in the methods section for Chapter 2. For XGal staining, frozen OCT sections were fixed in 2% glutaraldehye in PBS for 2 minutes, washed 3x5 minutes in PBS and incubated in XGal staining solution (100mM Na phosphate, pH 7.3, 1.3 mM $MgCl_2$, 3mM $K_3Fe(CN)_6$, 3 mM $K_4Fe(CN)_6$ and 1 mM XGal (Invitrogen)) at 37°C until color development reached a plateau. *In situ* hybridizations for mRNA detection were conducted as previously described (Byrne et al., 1994; Lowry et al., 2005). Alkaline

phosphatase detection in the dermal papilla was conducted on paraformaldehde-fixed frozen sections by reaction with BCIP/nitroblue tetrazolium in 100 mM Tris, pH 9.5, 100 mM NaCl, 50 mM $MgCl_2$, followed by subsequent immunofluorescence staining. For visualization of sebaceous gland morphology, 300mg of Oil Red-O were dissolved in 100ml of 99% 2-propanolol. A working stock was prepared by mixing 24ml of Oil Red-O/2-propanolol stock with 16mls of distilled water and filtering the stock through a 40μm filter. Paraformaldehyde-fixed frozen sections were incubated in working stock and destained by multiple washes in 60% 2-propanolol/PBS. BrdU incorporation was detected by incubating paraformaldehyde-fixed frozen sections in 1N HCl for 1 hour at 37°C before addition of primary antibody. Y-FISH analysis was performed on OCT sections using a Cy3 Star*FISH detection kit (Cambio). For immunohistochemistry, skins were fixed in paraformaldehyde and then dehydrated and embedded in paraffin. Antigen unmasking was performed using a Retriever 2100 for 20 min (Pick Cell Laboratories BV). Detection of immunohistochemical staining was performed using a Vectastain ABC kit (Vector Laboratories).

Additional primary antibodies used and not listed in Chapter 2 are: AE13 and AE15 (mouse, 1:50 and 1:20, T.T. Sun, New York University, New York), Blimp1 (mouse, 1:100, R. Tooze, University of Leeds, Leeds), BrdU (rat, 1:200, Abcam), active Caspase-3 (rabbit, 1:1000, R & D), CD34 (rat, 1:100, BD-Pharmingen), Cdk4 (rabbit, 1:200, Santa Cruz), P-Cadherin (rat, 1:100, M. Takeichi, RIKEN, Kobe), Gata-3

(mouse, 1:100, Santa Cruz), α6- and β4-Integrin (rat, 1:200, BD-Pharmingen), Involucrin (rabbit, 1:1000, Covance), K5 (rabbit, 1:2000, Fuchs Lab), K1 (rabbit, 1:250, Fuchs Lab), K6 (rabbit, 1:500, Fuchs Lab), K17 (rabbit, 1:4000, P. Coulombe, Johns Hopkins, Baltimore), Ki67 (rabbit, 1:500, NovoCastra), Lef1 (rabbit, 1:250, Fuchs Lab), Loricrin (rabbit, 1:300, Fuchs Lab), p63 (rabbit, 1:200, Santa Cruz), and PPARγ (rabbit, 1:200, Santa Cruz). Image acquisition was conducted as described in Chapter 2. In several cases, composite immunofluorescence images of HFs and skin (labeled Low Mag) were created by manually aligning overlapping images of adjacent skin sections.

HF length was quantified using MetaMorph software by measuring the linear distance along an in-plane follicle from the bottom of the leading edge/matrix to the epidermis. A minimum of 100 HFs from each genotype were analyzed for each time point. Developmental staging was performed according to standard classification (Schmidt-Ullrich and Paus, 2005) on 10 10x fields from 3 WT and 3 cKO mice. Quantification of proliferation in the upper ORS for BrdU pulse incorporation and Ki67 expression experiments was performed by analyzing the uppermost 20 cells on both sides of the K5/E-cadherin positive ORS for each follicle. Matrix size was measured by counting the number of Ki67 positive cells at the base of 20 HFs for WT and cKO at each time point. BrdU pulse-chase analysis of matrix proliferation and differentiation kinetics was performed on 15 HFs from WT and cKO mice at each time point in three separate labeling experiments. Hair keratin expression, detected by AE13 staining,

indicated the zone of differentiating cells, while ORS cells were recognized by their location at the edge of the follicle and unique elongated nuclear shape. Student's t-test was used to determine statistical significance.

Electron Microscopy

For scanning EM, samples were fixed in 2% glutaraldehyde, 4% PFA, and 2 mM $CaCl_2$ in 0.05 M sodium cacodylate buffer, pH 7.2, at RT for >1 h, dehydrated, critical-point dried, mounted, and sputter coated with gold-palladium. For transmission EM, samples were fixed as described for scanning EM, postfixed in 1% osmium tetroxide, and processed for Epon embedding; ultrathin sections (60–70 nm) were counterstained with uranyl acetate and lead citrate. Scanning EM images were obtained using a field emission scanning electron microscope (model 1550; LEO Electron Microscopy, Inc.), and transmission EM images were taken with a transmission electron microscope (Tecnai G2-12; FEI) equipped with a digital camera (model XR60; Advanced Microscopy Techniques, Corp.).

CHAPTER 4 MOLECULAR INSIGHT INTO STEM CELL SPECIFICATION

The recent development of numerous tools for isolation and genetic manipulation of adult bulge stem cells has led to advances in understanding how these cells function and what pathways regulate their activity. Notably, however, the factors required for initial specification and maintenance of stem cell identity are still largely unknown. Attempts to address these questions have been hampered by the unclear developmental origin of adult bulge cells and existing methods of stem cell isolation which do not function at early stages of skin development.

Together, results from embryonic H2B-GFP pulse-chase experiments (Chapter 2) along with results from Sox9 expression, genetic marking and conditional ablation experiments (Chapter 3) strongly suggest that the bulge stem cell population is specified during early stages of follicle development and participates actively in skin morphogenesis. Uncovering the origin and early identity of follicle SCs now permits an investigation into how SC identity is specified. In order to begin dissecting the molecular mechanisms required for initial stem cell specification as well as the functional properties of these early stem cells, I pursued two complementary approaches.

First, a microarray study was performed on purified outer root sheath cells isolated from WT and *Sox9* cKO mice. Because Sox9 is absolutely required for initial stem cell

specification, elucidation of its downstream transcriptional targets is an important first step in defining the regulatory network responsible for stem cell specification. Remarkably, less than 100 genes appear to be strongly regulated by Sox9 at the timepoint when the early stem cell population first appears. The majority of these Sox9 regulated genes are also specifically enriched in early stages of HF development or in the later adult bulge stem cell population, underscoring their potential roles in hair follicle development and stem cell function.

Second, a transgenic mouse tool was developed to allow for FACS identification and purification of Sox9-positive early stem cells in the K14-positive skin epithelium. As expected, FACS analysis revealed that Sox9-positive cells composed only a minority of the total cells within each hair follicle but displayed the highest colony forming efficiency when placed in culture—a feature consistent with a stem cell phenotype.

Further investigation of the transcriptional network regulated by Sox9 should yield new insight into the process of SC specification in the hair follicle. The ability to purify Sox9 expressing cells will provide a means to study a previously inaccessible early stem cell population and to further investigate its origins as well as its similarity to the adult bulge stem cell population.

Results

FACS isolation of outer root sheath cells from WT and Sox9 cKO mice

The dramatic phenotype seen in *Sox9* cKO mice unable to specify an early stem cell population suggested that Sox9 acts as a non-redundant transcriptional regulator in hair follicle morphogenesis. Although many transcriptional targets of Sox9 have been identified in other tissues, no Sox9 target genes are known in the skin (Lefebvre et al., 2007). Determining which genes are regulated by Sox9 in the skin would therefore provide insight into the transcriptional program necessary for early stem cell specification.

In order to identify Sox9-regulated genes, I conducted microarray expression profiling on purified outer root sheath cells from WT and *Sox9* cKO embryos. Genes that are directly regulated by Sox9, which is known to function as a transcriptional activator, would be expected to show decreased or absent expression in cKO ORS cells compared to WT ORS (Sudbeck et al., 1996). This approach would allow me to detect *in vivo* gene expression changes in the same cell population where *Sox9* is normally expressed and where phenotypic alterations first appear, maximizing the chance that the altered genes were the same ones responsible for the cKO phenotype. I chose to analyze mice at two time points, E18.5 and P0.5, which bracket the time when marker expression and slight phenotypic alterations first appear in *Sox9* cKO mice. Profiling expression at an early timepoint before gross phenotypic alterations increased the chance of detecting changes in direct Sox9 transcriptional targets, rather than later downstream

secondary changes. Analysis of two different time points served both as a measure of reproducibility for expected expression changes and also provided insight into the trend of gene expression changes over time.

In order to isolate a pure population of outer root sheath cells from E18.5 and P0.5 WT and cKO mice, I modified an existing protocol which was previously used to isolate outer root sheath and matrix from P4 mice (Rendl et al., 2005). In this system, skin from *K14-H2B-GFP* mice, which constitutively express H2B-GFP under control of the *keratin 14* promoter, is subjected to a series of enzymatic digestions and low-speed centrifugation to produce a cell suspension enriched in cells derived from the hair follicle. Separate populations of cells from the ORS and matrix can then be distinguished by FACS based on differential expression of *K14-H2B-GFP*, which is high in the ORS and low in the matrix. Non-epithelial cells do not express the *K14-H2B-GFP* transgene and can be easily excluded from analysis. Two modifications to this system made it possible to isolate ORS cells from younger mice in which hair follicles are much smaller and the matrix and ORS are not as well defined. Higher speed centrifugation increased the yield of the smaller hair follicles present at E18.5 and P0.5, and addition of an antibody directed against α6-Integrin increased the separation between ORS and Mx populations and allowed for more stringent population gating.

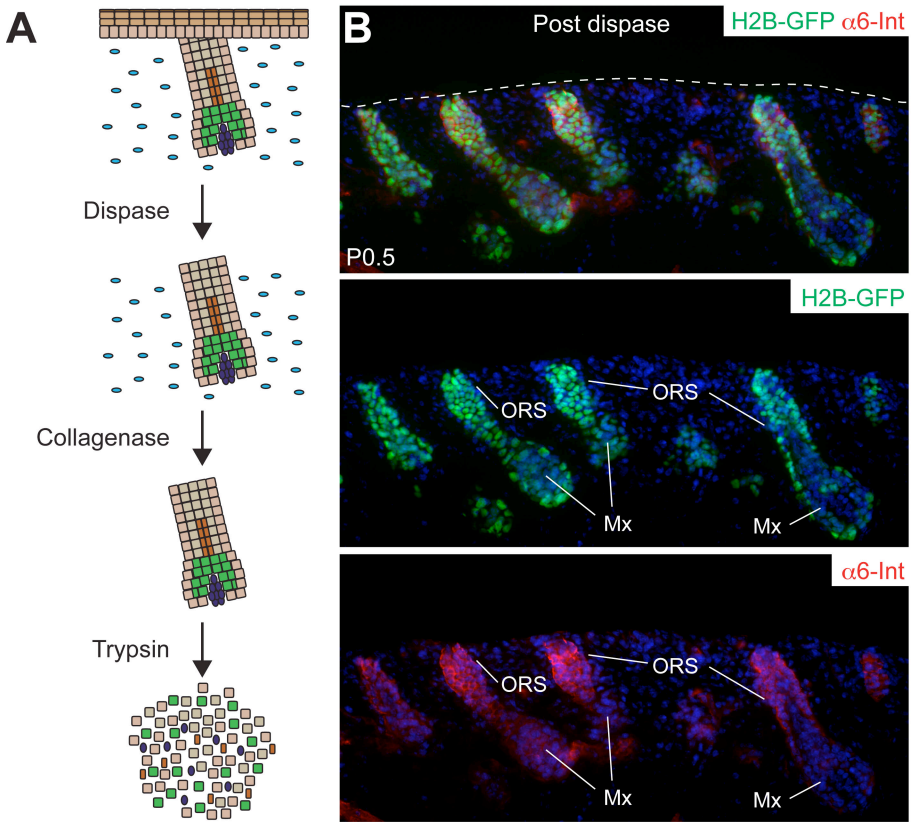

Figure 4.1. Schematic and markers for isolation of outer root sheath cells by FACS. (**A**) Sequential enzymatic treatments can be used to generate a single cell suspension enriched in ORS and matrix cells suitable for FACS. (**B**) Immunofluroescence analysis of *K14-H2B-GFP* and α6-Integrin expression in P0.5 backskin which has been dispase-treated to remove the overlying epidermis (junction marked by white dotted line in top panel). Note that H2B-GFP is expressed only in hair follicles, and is brighter in ORS cells than in the matrix. Similarly, α6-Integrin is highly expressed in the ORS and is low in the matrix.

Breeding *K14-H2B-GFP* mice with *K14-Cre/Sox9*$^{flox/+}$ mice yielded *K14-H2B-GFP/K14-Cre/Sox9*$^{flox/+}$ mice which could then be crossed with *Sox9*$^{flox/flox}$ mice to generate litters of *K14-H2B-GFP*-expressing WT and *Sox9* cKO mice. Mice harboring *K14-H2B-GFP* and *K14-Cre* but heterozygous for the *Sox9*-floxed allele were used as

WT controls. This approach avoided introducing a potential bias into the data due to phenotypic perturbances resulting from expression of Cre recombinase (Schmidt-Supprian and Rajewsky, 2007). While haploinsufficiency of *Sox*9 is sufficient to induce phenotypic alterations in some tissues (Bi et al., 1999; Wagner et al., 1994), no differences between the skins of *K14-Cre/Sox9*$^{flox/flox}$ and *K14-Cre/Sox9*$^{flox/+}$ were observed at either a gross or histological level, suggesting that skin which retains one functional copy of *Sox9* is similar to WT.

In order to validate this approach to identifying Sox9 target genes, it was first essential to determine whether the isolation procedure yielded comparable cell populations in WT and cKO mice. FACS analysis revealed that the distribution of H2B-GFP and α6-Integrin positive cells was quite similar for both WT and cKO at both E18.5 and P0.5 (Figure 4.2). As in the previous study, there was a greater that 10-fold difference between the brightest and dimmest H2B-GFP positive cells, and this entire population was cleanly separated from H2B-GFP negative cells (Rendl et al., 2005). Expression of α6-Integrin varied approximately 100-fold within this population, and was positively correlated with H2B-GFP expression, resulting in the appearance of two major cell populations, one GFP^{Hi}α6^{Hi} population representing K14 and a6-Integrin rich cells, presumably from the ORS, and one GFP^{Low}α6^{Low} population representing presumptive matrix cells. Notably, the number of cells in the GFP^{Low}α6^{Low} presumptive

matrix population increased in both the WT and cKO from E18.5 to P0.5, reflecting the progressive follicle maturation that occurs at this time.

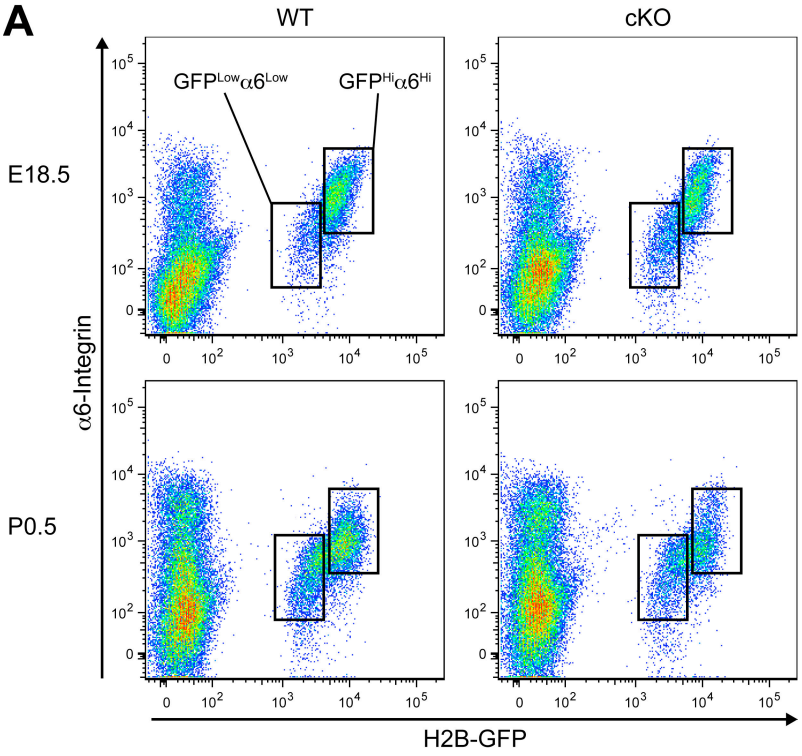

Figure 4.2. FACS isolation of ORS from WT and *Sox9* cKO hair follicles. (**A**) Cell suspensions enriched for hair follicle-derived cells were prepared from E18.5 and P0.5 *H2B-GFP* WT and *Sox9* cKO mice and stained with an antibody against α6-Integrin. FACS analysis reveals a discrete population of H2B-GFP-positive cells in all plots. Note that the H2B-GFP positive population can be subdivided into a $GFP^{Hi}\alpha6^{Hi}$ and a $GFP^{Low}\alpha6^{Low}$ population corresponding to presumptive ORS and matrix, respectively. H2B-GFP negative cells in all plots include dermal papilla, melanocytes, dermal fibroblasts and other cells that co-purify with hair follicle but are non-epithelial in origin.

In order to ensure that the $GFP^{Hi}\alpha6^{Hi}$ and $GFP^{Low}\alpha6^{Low}$ populations were reflective of cells from the ORS and matrix, both populations were sorted from WT and cKO mice at both time points and collected for RNA isolation. By employing previously defined gene expression signatures for P4 ORS and Mx, it was possible to assess the

identity of the FACS isolated cell populations (Rendl et al., 2005). RT-PCR analysis revealed that 6 of 8 ORS signature genes were enriched in the $GFP^{Hi}\alpha6^{Hi}$ population compared to $GFP^{Low}\alpha6^{Low}$ at E18.5 in both WT and cKO (Figure 4.3A). By P0.5, enrichment of ORS signature genes in the $GFP^{Hi}\alpha6^{Hi}$ became more apparent, and all 8 genes were now appropriately enriched in the $GFP^{Hi}\alpha6^{Hi}$ population, most by at least 4-fold. Analysis of matrix signature genes at E18.5 revealed that 5 of 8 genes were substantially enriched in the $GFP^{Low}\alpha6^{Low}$ population compared to the $GFP^{Hi}\alpha6^{Hi}$ population, with the three remaining genes showing either marginal enrichment or enrichment in the E18.5 $GFP^{Hi}\alpha6^{Hi}$ presumptive ORS population (Figure 4.3B). However, analysis of the matrix signature at P0.5 revealed that all eight signature genes subsequently became enriched in the $GFP^{Low}\alpha6^{Low}$ population.

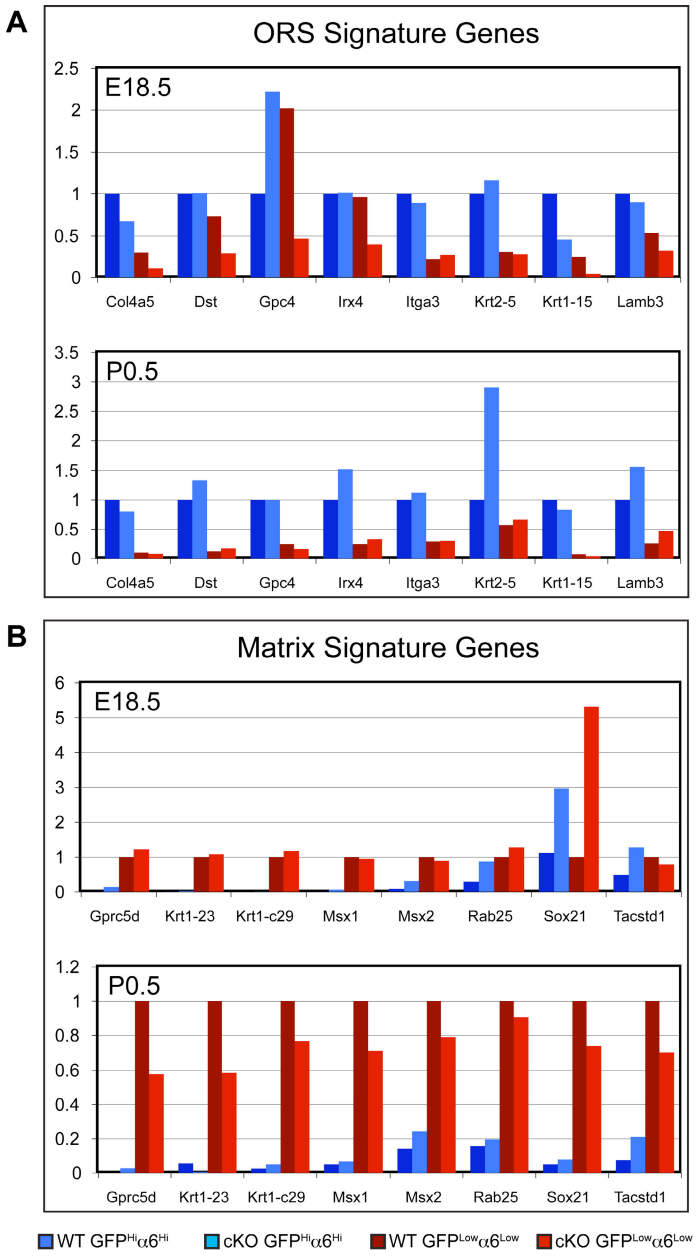

Figure 4.3. Expression of ORS and matrix signature genes in FACS isolated cells. FACS isolated $GFP^{Hi}\alpha6^{Hi}$ and $GFP^{Low}\alpha6^{Low}$ cells were isolated from WT and *Sox9* cKO mice at E18.5 and P0.5. RT-PCR was conducted on all populations for signature genes characteristic of the ORS (**A**) or matrix (**B**). Graph vertical axis indicates fold change. Note that ORS signature genes are enriched in the $GFP^{Hi}\alpha6^{Hi}$ population, while matrix signature genes are enriched in the $GFP^{Low}\alpha6^{Low}$ population. The enrichment becomes clearer at P0.5 compared to E18.5, reflecting the progressive development of ORS and matrix populations in growing hair follicles. Note that WT and *Sox9* cKO cell populations display similar enrichment trends at both timepoints.

Thus, despite the early developmental stage of follicles at E18.5 and P0.5, it was still possible to isolate separate cell populations reflective of the ORS and matrix components of the hair follicle. The more robust partitioning of both ORS and matrix signature genes at P0.5 compared to E18.5 is probably due to the progressive development of follicles at this time point and their increasing similarity to the P4 follicles which were used to generate the signature gene lists. Consistent with ORS development temporally preceding matrix development, the matrix signature was not as clearly partitioned between the $GFP^{Hi}\alpha6^{Hi}$ and $GFP^{Low}\alpha6^{Low}$ populations as was the ORS signature at E18.5. Crucially, expression of most ORS and Mx signature genes was quite similar between WT and cKO samples at both time points. This result, consistent with the lack of gross phenotypic alterations between WT and cKO at these time points, suggested that general ORS and matrix character had not been greatly disrupted by the absence of *Sox9*.

Once retention of general ORS character in the cKO had been established, I next determined whether RT-PCR could detect changes in the expression of genes that were already known to be altered in the cKO compared to WT. As expected, Sox9 was more highly expressed in WT ORS than matrix, and was virtually undetectable in both cKO populations at E18.5 and P0.5, confirming efficient knockout prior to the time of analysis. Although expression of Lhx2 and Tcf3 is lost at later developmental stages in cKO follicles, both genes were still abundantly expressed at E18.5 and P0.5, suggesting

that they are not direct transcriptional targets of Sox9. In contrast, Nfatc1 and PPARγ, two genes that never appeared at a protein level in cKO follicles, were substantially reduced at an mRNA level in the cKO at both time points. Thus, mRNA expression changes in WT and cKO FACS-isolated ORS and matrix populations corroborated protein level expression changes detected previously by immunofluorescence.

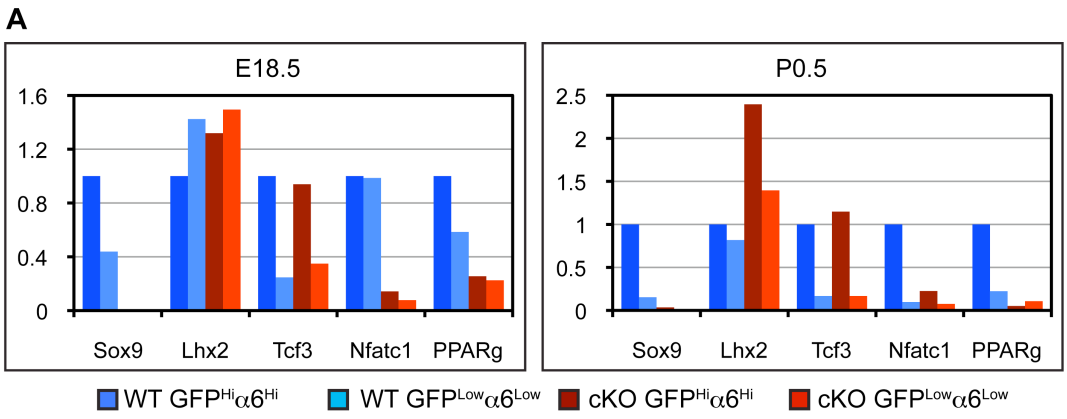

Figure 4.4. Validation of known expression changes in FACS isolated cells. (A) FACS isolated $GFP^{Hi}\alpha6^{Hi}$ and $GFP^{Low}\alpha6^{Low}$ cells were isolated from WT and *Sox9* cKO mice at E18.5 and P0.5. RT-PCR was conducted on all populations for genes that are known to be differentially expressed in developing WT and cKO HFs. Graph vertical axis indicates fold change. Sox9 expression was completely undetectable in all cKO populations, confirming effective ablation prior to E18.5. Tcf3 and Lhx2, which are initially expressed normally but subsequently lost in cKO follcles, do not yet display reduced expression at E18.5 and P0.5. In contrast, Nfatc1 and PPARγ, which are never expressed in cKO follicles, are markedly downregulated at both timepoints.

Identification of genes regulated by Sox9 in follicle morphogenesis

After validating the ability of the FACS isolation strategy to produce comparable populations of ORS cells from WT and cKO mice, and confirming that known gene expression changes between WT and cKO could be detected at an mRNA level in these cells, samples of total RNA from WT and cKO $GFP^{Hi}\alpha6^{Hi}$ cells at E18.5 and P0.5 were processed and hybridized to Affymetrix GeneChip Mouse Genome 430 2.0 arrays. Analysis of hybridization statistics revealed that all four samples had been processed, hybridized to gene chips and scanned with similar efficiency (Table 4.1). Background, noise values, and average signal values were comparable across all hybridizations, and

within normal limits defined by Affymetrix, indicative of efficient hybridization and scanning. The ratio of signal values from probes directed against either the 3′ or 5′ end of β-actin and GAPDH genes were also comparable across all hybridizations, indicating that input RNA sample quality was uniform. Finally, almost half of the 39,000 probes from each hybridization displayed detectable signal, reflecting the presence of mRNAs for many discrete genes in the input RNA samples.

Table 4.1 WT and *Sox9* cKO ORS microarray hybridization statistics. Affymetrix GeneChip Operating Software was used to analyze gene chip hybridization data from WT and cKO $GFP^{Hi}\alpha6^{Hi}$ ORS at E18.5 and P0.5. Ratios between 3′ and 5′ directed probes and the percentage of probes present in each hybridization demonstrate that all input RNA samples were of similar quality. Comparable background, noise and average signal values for all samples demonstrate consistent sample processing, hybridization and scanning.

		E18 WT	E18 cKO	P0 WT	P0 cKO
	Noise (RawQ)	1.85	1.85	1.96	1.94
	Scale Factor	3.456	3.22	3.547	3.324
Background	Average	57.52	54.44	57.52	58.25
	St. Dev.	1.08	1.39	0.35	0.72
	Min	56	51	56.4	56.5
	Max	60.9	59.4	58.6	60.2
Noise	Average	3.42	3.33	3.47	3.92
	St. Dev.	0.16	0.13	0.14	0.15
	Min	3.2	3	3.2	3.6
	Max	3.9	3.8	3.8	4.3
Signal (3′ / 5′)	β-actin	1.52	1.61	1.47	1.50
	GAPDH	0.79	0.76	0.67	0.66
Probe Calls	Present	48.2%	48.7%	48.0%	46.3%
	Absent	50.2%	49.6%	50.3%	51.7%
	Marginal	1.7%	1.7%	1.7%	2.0%
Average Signal	Present	1504.4	1569.2	1593.5	1519.1
	Absent	84.5	70.9	79.4	102.8
	Marginal	314.0	190.5	212.1	264.2
	All	772.4	802.8	808.1	761.4

An unfiltered comparison of all probe signals in WT and *Sox9* cKO ORS revealed that 93.2% of probes present at E18.5 and 92.3% of probes present at P0.5 remained unchanged between WT and cKO (Table 4.2), corroborating earlier analysis which suggested that general ORS character remained unchanged within WT and cKO hair follicles at early time points. At E18.5, 2.4% of probes showed increased expression in the cKO, while 3.9% showed decreased expression. Notably, only 37 of the increased probes displayed a 2-fold or greater change in signal, while 736 of the decreased probes were changed by at least 2-fold (Table 4.2). This highly asymmetric pattern of probe changes suggested not only that Sox9 functions as a transcriptional activator in the ORS, but that, at E18.5, many genes with decreased expression may reflect primary Sox9 transcriptional targets which are not expressed in the absence of Sox9. In contrast, changes in probe signal values were more symmetric at P0.5, with 3.7% of probes showing increased signal, 806 by at least 2-fold, and 3.3% of probes showing decreased signal, 310 by at least 2-fold. This more even balance between numbers of increased and decreased probes may reflect secondary expression changes that are not directly due to an absence of Sox9's transcriptional activity.

Table 4.2. WT and *Sox9* cKO ORS microarray raw comparison statistics. Affymetrix GeneChip Operating Software was used to compare probe signal values from WT and cKO $GFP^{Hi}\alpha6^{Hi}$ ORS at E18.5 and P0.5. Percentages are calculated as the fraction of total probes from each hybridization which displayed a given change behavior in the cKO compared to WT.

% of Probes	E18		P0	
Increase	2.40%		3.70%	
Decrease	3.90%		3.30%	
Marginal Increase	0.20%		0.50%	
Marginal Decrease	0.40%		0.20%	
No Change	93.20%		92.30%	
# of Probes	**Increase**	**Decrease**	**Increase**	**Decrease**
< 2 fold	1111	1420	1310	1340
>= 2 fold	30	506	582	232
>= 4 fold	5	142	203	53
>= 8 fold	1	63	71	20
>= 16 fold	0	25	20	5

In order to generate a list of gene expression changes which were most likely to reflect the direct transcriptional activity of Sox9, I focused on probes which displayed at least a 2-fold change in expression between WT and cKO at both time points, which were given a present call in at least one of the four samples, and had a calculated change p-value of ≤ 0.01. This filtering strategy resulted in a list of 110 probes representing 89 distinct genes (Table 4.3). Examination of the direction of change for these probes revealed that 91 out of 110 were decreased in the cKO at both E18.5 and P0.5, while only 11 probes were increased in the cKO at both time points (Figure 4.5). Only 8 probes switched the direction of their signal change between E18.5 and P0.5, indicating a relative stability in gene expression changes across time.

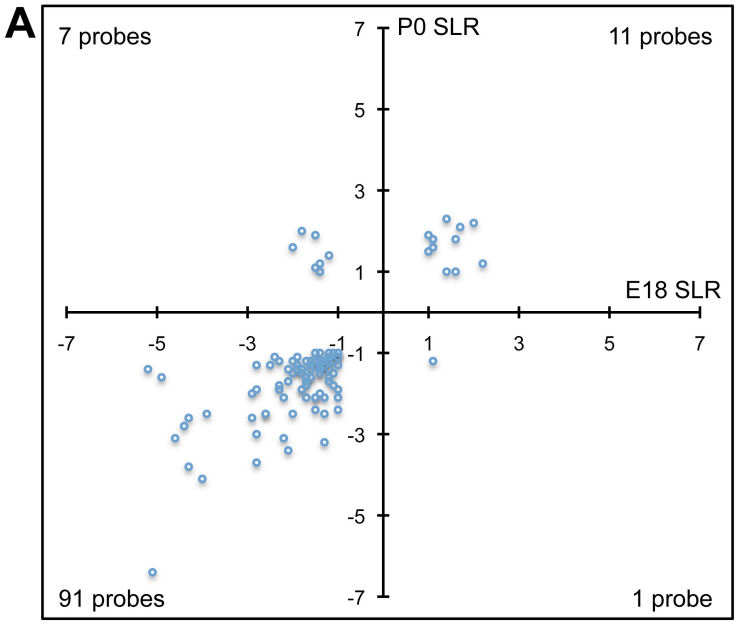

Figure 4.5. Correlation between array expression changes at E18.5 and P0.5. (A) Fold changes for probes which exhibited a 2-fold or greater change between WT and cKO at both E18.5 and P0.5 were $\log_2$ transformed to generate signal log ratios (SLRs). The scatter plot displays the SLRs for each probe at E18.5 and P0.5. The majority of probes exhibited negative SLRs at both E18.5 and P0.5, reflecting downregulation of their associated genes at both time points. Note that relatively few probes show split positive and negative SLRs, indicating that most probes are upregulated at both timepoints or downregulated at both timepoints.

Notably, all four genes which were never expressed in cKO follicles at any time point were contained in the list of filtered genes. Sox9 itself was one of the most highly downregulated genes at E18.5 (19.7×) and was also 6.1× downregulated at P0.5 (Table 4.3). Nfatc1, a maker of early bulge cells absent in cKO follicles, was detected by multiple probes as downregulated at both time points (4.9× and 3.7× at E18.5, 3.5× and 2.6× at P0.5). Finally, PPARγ and Blimp1/Prdm1, markers of the sebaceous lineage that fails to appear in cKO follicles, were also downregulated at both time points (PPARγ 19.7× at E18.5, 13.9× at P0.5; Prdm1 4.0× at E18.5, 2.8× at P0.5). In contrast, Lhx2 and Tcf3

which are initially expressed and then later lost in cKO follicles, did not score as changed in the filtered array gene list. These results suggested that the microarray approach was not only sensitive for detecting transcriptional changes in cKO follicles, since all genes known to have altered expression at a protein level were also detected by the array, but also relatively specific, since only 89 distinct genes were altered at both time points and later, secondary changes in cKO follicles were not present in the filtered array gene list.

While complete validation of the array data is beyond the scope of my thesis, it was interesting to note that the list of genes downregulated in cKO ORS included genes with a wide variety of known functions, including transcription factors, regulators of the cytoskeleton and cell adhesion, metabolic enzymes, and components of signaling pathways. This variety of genes indicates that many diverse cellular processes may have to be properly regulated for stem cell specification to occur, and suggests that stem cell-niche interactions may be crucial for this process (Fuchs et al., 2004).

While it is intriguing that a number of genes downregulated in the *Sox9* cKO ORS have previously reported roles in skin function, it is likely that the cKO phenotype represents the composite effects of many reduced or absent genes. Furthermore, the wide variety of genes affected by the loss of *Sox9* underscores the myriad signaling, transcriptional, and cytoskeletal changes which must be simultaneously orchestrated for hair follicle stem cell specification to occur. To gain further insight into which Sox9-regulated genes may be the most important for the stem cell specification process, I

compared the list of 110 probes altered in the *Sox9* cKO ORS with pre-existing microarray datasets in the laboratory, including P-cadherin positive placodes and hair germs from E17.5 skin, ORS from P4 mice, and CD34-positive bulge stem cells from both anagen and telogen hair follicles (Blanpain et al., 2004; Rendl et al., 2005; Rhee et al., 2006). Importantly, the previous array studies were performed using FACS purified cell populations from mice expressing GFP under control of the *K14* promoter, and were hybridized to very similar or identical microarrays from Affymetrix, thus minimizing the potentially confounding effects of isolation strategy differences and variable cell purity.

Remarkably, 78 of the 110 probes scored as significantly changed in at least one of the three comparison populations, with the vast majority of probes scoring as preferentially enriched. As expected, the greatest overlap occurred with genes enriched in the P4 ORS when compared to epidermis or matrix. However, a substantial number of genes were also present in the placode and adult bulge cell signature gene lists. Overall, 25 probes were significantly changed in at least two comparison populations, and a further 11 probes were significantly changed in all three populations. Much like Sox9 itself, which is expressed beginning in the placode and then continuously present in the ORS and adult bulge population, these genes would be especially strong candidates for key regulators involved in follicle stem cell specification. While elucidation of the transcriptional network regulated by Sox9 and required for stem cell specification will undoubtedly require several experimental approaches, knowledge of which genes are

differentially expressed in *Sox9* cKO ORS is an important starting point for future investigations. This full data set will be presented at a later date.

FACS isolation of Sox9-expressing cells from developing hair follicles

As a complementary approach to identifying genes potentially regulated by Sox9 in the outer root sheath, the ability to isolate Sox9-expressing early stem cells would allow for a more functional investigation of early stem cell properties and behavior. To facilitate this approach, a fluorescent transgenic mouse tool was developed for FACS isolation of Sox9-expressing cells within the skin epithelial population. This mouse tool consisted of two different transgenes driving—one driving expression of GFP in Sox9 positive cells and the other driving expression of RFP in K14 positive cells.

To determine whether the So*x9-EGFP* reporter accurately reflected Sox9 expression in hair follicles, So*x9-EGFP* mice were first mated to transgenic *K14-RFP* mice previously generated in the laboratory. This double fluorescent transgenic approach allowed for uniform, positive labeling of epithelial skin with RFP and enabled the extent of overlap with *Sox9-EGFP* expression to be carefully assessed. As expected, the skin of WT mice exhibited negligible GFP and RFP fluorescence (Figure 4.6A). In contrast, *Sox9-EGFP/K14-RFP* mice displayed broad RFP fluorescence throughout the epidermis, while GFP expression appeared in a punctate pattern characteristic of developing hair follicles (Figure 4.6A). This pattern of expression was especially clear in the whisker pads of newborn mice, where large whisker follicles were visible beneath the RFP marked

epidermis. Examination of backskin hair follicles from P4 skin confirmed that RFP was also broadly expressed in developing follicles, while GFP expression appeared restricted to subpopulation of cells within each follicle (Figure 4.6B).

FACS analysis of hair follicle derived cells from transgenic mice confirmed and extended the tissue-level expression results. Both *Sox9-EGFP* and *K14-RFP* mice exhibited expression of the respective fluorescent protein in a subset of hair follicle-derived cells (Figure 4.7A). Analysis of double transgenic mice further revealed that essentially all of the GFP positive cells expressed high levels of RFP, indicating their identity as epithelial cells from the outer root sheath, which is known to exhibit the highest *K14* promoter activity in hair follicles (Figure 4.7A) (Byrne et al., 1994). More specific analysis restricted to viable, RFP positive cells revealed three distinct epithelial populations. The first two populations exhibited comparably high levels of RFP fluorescence and were distinguished by the presence or absence of GFP expression (Figure 4.7B). These populations, designated $RFP^{Hi}GFP^{+}$ and $RFP^{Hi}GFP^{-}$, comprised approximately 10% and 16% of the total RFP population and represented Sox9-positive and negative cells in the ORS, respectively. The third population, designated RFP^{Low} and containing approximately 72% of the total cells, was characterized by a lack of GFP expression and a broader range of dimmer RFP expression than the first two populations, characteristic of cells from the hair follicle matrix (Rendl et al., 2005) (Figure 4.7B).

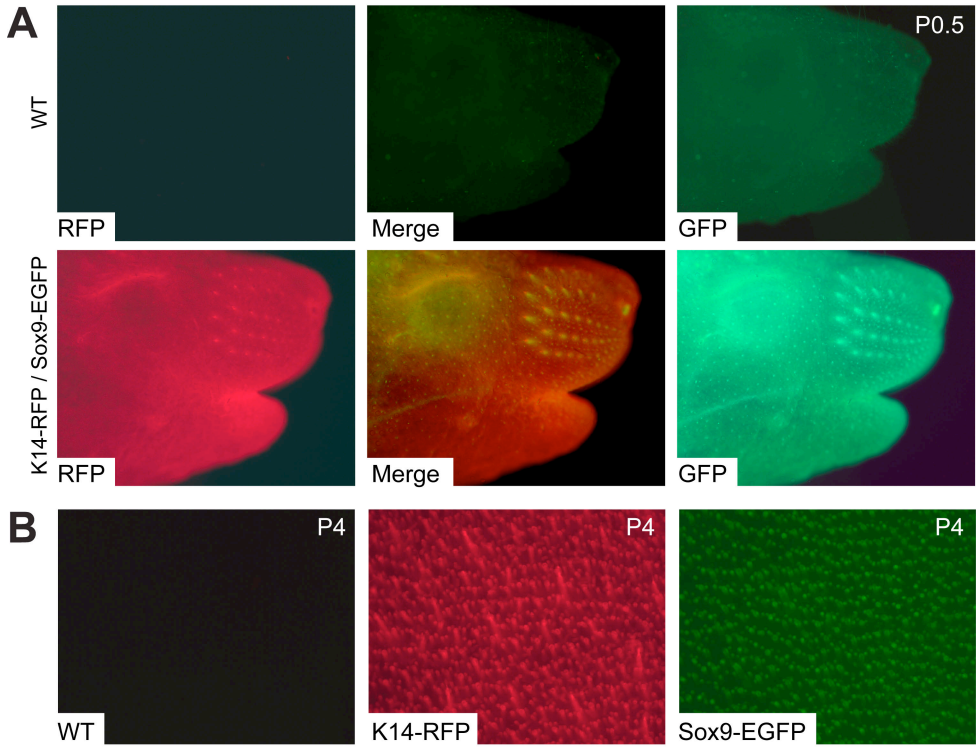

Figure 4.6. Expression of *Sox9-EGFP* and *K14-RFP* in the skin. A dissection scope equipped for fluorescent imaging was used to examine skin of WT and double transgenic *Sox9-EGFP/K14-RFP* mice. (**A**) Examination of P0.5 WT mice reveals near background levels of GFP and RFP fluorescence. In contrast, the skin of double transgenic mice was uniformly marked by RFP expression, with punctate GFP expression concentrating in developing hair follicles, readily distinguished in the whisker pad. (**B**) Skin from P4 single transgenic animals was enzymatically treated to remove the overlying interfollicular epidermis to permit top-down hair follicle visualization. Note that *K14-RFP* is expressed along the entire length of developing follicles, while *Sox9-EGFP* expression appears more restricted.

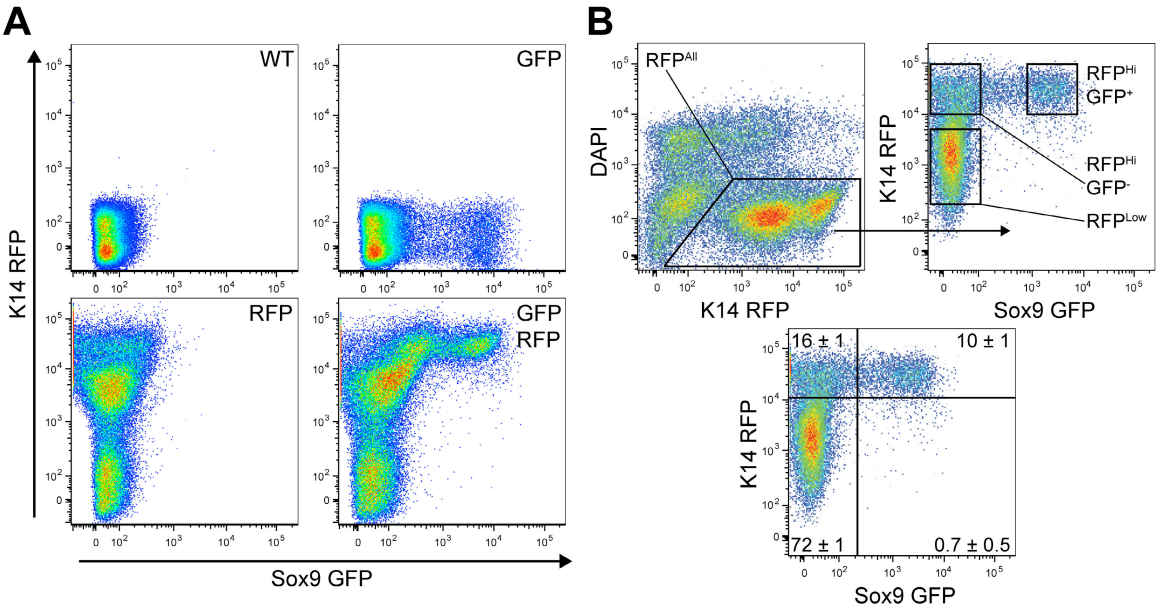

Figure 4.7. FACS analysis of *Sox9-EGFP/K14-RFP* hair follicle cells. Hair follicle cell preparations derived from P4 backskin were subjected to FACS analysis. (**A**) Specific fluorescence is detected in subpopulations of hair follicle cells from *Sox-EGFP* and *K14-RFP* single transgenic mice. Analysis of cells from double transgenic mice reveals that all GFP positive cells are strongly RFP positive. Note that a non-epithelial, K14-RFP negative subpopulation of cells, containing melanocytes, dermal papilla and dermal fibroblasts co-purifies with K14-RFP positive epithelial cells. (**B**) Specific gating for viable, RFP positive cells (RFP^{All}) reveals three distinct hair follicle epithelial cell populations differentiated by GFP and RFP expression—$RFP^{Hi}GFP^{+}$, $RFP^{Hi}GFP^{-}$, and RFP^{Low}. Quadrant gating of the RFP^{All} population reveals the relative distribution of cells within these populations. Corner numbers indicate percentage of cells in each quadrant.

Characterization of purified Sox9-expressing cells from developing hair follicles

As an initial functional characterization, cells from the GFP/RFP populations were FACS isolated and placed in culture to assess colony formation efficiency. Strikingly, after 14 days of culture, the $RFP^{Hi}GFP^{+}$ population had given rise to colonies with a far greater efficiency than either the $RFP^{Hi}GFP^{-}$ population or the RFP^{Low} population (Figure 4.8A,B). Thus, despite their relatively quiescent nature, these Sox9-positive cells can quickly be activated to proliferate extensively in culture, whereas the RFP^{Low} matrix population, composed of highly proliferative transit-amplifying matrix cells, exhibits poor colony formation in culture. The $RFP^{Hi}GFP^{-}$ population exhibited a colony formation efficiency in between that of the $RFP^{Hi}GFP^{+}$ and RFP^{Low} populations, suggesting that it may represent cells in the lower ORS which are transitioning from the $RFP^{Hi}GFP^{+}$ to the RFP^{Low} population. Taken together, the colony forming data clearly demonstrates functional differences between the GFP/RFP populations and furthermore suggests that the $RFP^{Hi}GFP^{+}$ population may harbor the greatest stem cell potential in the hair follicle.

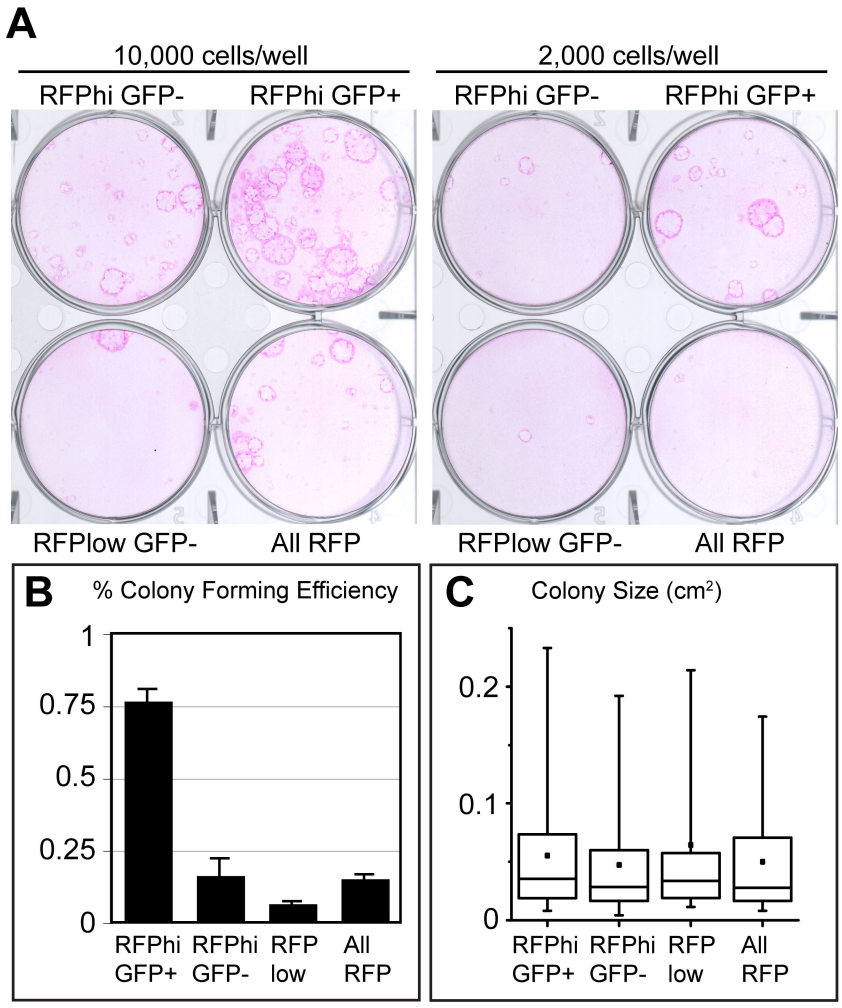

Figure 4.8. Growth of *Sox9-EGFP/K14-RFP* hair follicle cells in culture. Cells from indicated population were isolated by FACS and placed in culture at low density to assess colony forming efficiency. (**A**) Colonies formed after seeding 2,000 or 10,000 cells per well and culturing for 14 days. (**B**) Quantification of the colony forming efficiency reveals that cells from the $RFP^{Hi}GFP^{+}$ population form visible colonies much more readily than $RFP^{Hi}GFP^{-}$ or RFP^{Low} cells. (**C**) Quantification of colony area reveals no substantial difference in the size of colonies which do form from each of the isolated populations. Box and whisker plots quantify colony area (cm^2): min. and max. area are marked by whiskers; upper and lower box boundaries indicate quartile divisions; central line indicates median; square dot indicates mean area.

Discussion

A complete understanding of any population of cells within a tissue is predicated on knowing where the cells come from during development, what genes and pathways regulate their behavior, and what functional capacity the cell population harbors. Addressing these questions is especially important for stem cell populations, which by their very nature must integrate multiple signals from the environment with their own intrinsic regulatory mechanisms to self-renew and produce differentiated progeny. I took two approaches to begin addressing these issues for the early hair follicle stem cell population. By conducting microarray profiling on ORS cells isolated from WT and *Sox9* cKO hair follicles, it was possible to identify Sox9-regulated genes which may be required for early stem cell specification. By developing a double transgenic mouse system for isolation of Sox9 positive early stem cells, it was possible to begin conducting functional characterization of purified early stem cells. Moving forward, both of these resources will shed light not only on the early hair follicle stem cell population, but the entire process of hair follicle morphogenesis and the adult hair cycle.

Uncovering transcriptional changes in the outer root sheath of developing WT and *Sox9* cKO follicles not only confirmed the previously described histological alterations (Chapter 3), but provided insight into the entire set of genes which may be regulated by Sox9. Unexpectedly, a relatively small number of genes were substantially altered between the WT and cKO, suggesting that the array analysis was conducted early

enough to minimize potentially confounding secondary effects. Confirming Sox9's previously reported role as a transcriptional activator, almost all significantly changed genes at the E18.5 timepoint were downregulated. Together, these results suggest that Sox9's transcriptional role in the hair follicle is quite specific.

This short list of Sox9-regulated genes represents a pool of excellent candidates for future expression and mouse genetic studies, which are likely to lead to a better understanding of hair follicle stem function and specification. Given that the preferred DNA binding motif of Sox9 is known, it should be possible to perform a rapid bioinformatic screen to identify which of these genes are likely to be direct Sox9 transcriptional targets. The recent generation of a peptide-antigen, affinity-purified Sox9 antibody in the lab (unpublished data) will not only allow for chromatin immunoprecipitation (ChIP)-based confirmation of direct Sox9 binding in the promoters of these genes, but will also enable future ChIP-on-Chip or ChIP-Sequencing approaches for discovering direct Sox9 interactions with genomic DNA. These approaches would be complementary to the existing microarray data and could provide one of the first glimpses into genome-wide transcriptional regulation of epithelial stem cell function.

The use of double transgenic *Sox9-EGFP/K14-RFP* mice to isolate Sox9 expressing cells from the hair follicle will allow for better characterization of the early stem cell population at both a descriptive and functional level. Using the transgenic mice, it will be possible to isolate early Sox9-positive stem cells and compare their expression

profile both to the placode, where they may originate, and the adult bulge population, where they end up. This approach will be complementary to the microarray comparison of WT and *Sox9* cKO ORS because it should reveal all of the genes expressed in the early stem cell population, and not just those which are likely to be regulated by Sox9. In addition to microarray profiling, it should be possible to conduct large scale ChIP studies directly on *Sox9-EGFP/K14-RFP* sorted cells because a single mouse can yield up to $5x10^5$ $RFP^{Hi}GFP^+$ cells with a high viability that enables rapid FACS acqusition. Most importantly, however, will be the ability to perform functional culture and grafting assays on sorted cell populations. While initial culture experiments suggest that the $RFP^{Hi}GFP^+$ cells possess the highest colony forming capacity of all cells in the hair follicle, it will also be crucial to measure the long-term passaging potential, colony morphology, differentiation ability and growth rates of isolated populations placed in culture. Performing grafting experiments will provide more direct evidence about the multipotency and self-renewal ability of $RFP^{Hi}GFP^+$ cells. If these cells are specifically able to form and maintain an epidermis, hair follicles and sebaceous glands, this will be strong evidence that they function as *bona fide* stem cells.

Furthermore, it should be possible to use the *Sox9-EGFP/K14-RFP* mice to isolate *Sox9* expressing cells from multiple developmental time points and adult hair cycle stages. In combination with P-cadherin expression, these mice could be used to isolate the two distinct populations of cells (P-Cad/Lhx2-positive and Sox9-positive) which

reside in embryonic placodes and give rise to distinct parts of the hair follicle. Such a study could provide insight into what signaling events are necessary to specify these two populations during embryogenesis and how they function differentially during later steps of morphogenesis. The double transgenic mice could also be used in conjunction with CD34 to begin dissecting the overlap between adult stem cell markers. In this regard, Sox9-EGFP expression may be a useful tool for identifying the early progeny of adult bulge stem cells which have lost CD34 expression but still express Sox9 as they move down the ORS towards the matrix in anagen follicles. To date, no techniques exist to isolate distinct subpopulations of cells emanating from the adult bulge into the anagen ORS. Finally, the double transgenic mice should also make it possible to directly compare the functional capacity of early follicle SCs versus adult bulge SCs in culture, grafting and other assays. Preliminary data on wound healing in the interfollicular epidermis and colony formation activity suggest that early SCs may be more potent that adult SCs, but additional studies are needed to precisely quantify differences between these two stem cell populations (Blanpain et al., 2004; Ito et al., 2005).

Together, the microarray results on Sox9-regulated genes in the ORS and the development of *Sox9-EGFP/K14-RFP* mice for isolating Sox9-expressing cells not only provide a foundation for future molecular studies of the early stem cell population, but will help elucidate the entire process of hair follicle development and the role of stem cells at different stages of morphogenesis and adult hair cycling.

Materials and Methods

FACS isolation of outer root sheath cells

Sox9$^{flox/flox}$ mice (Akiyama et al., 2002) were crossed with *K14-Cre* mice (Vasioukhin et al., 1999) and *K14-H2B-GFP* mice (Tumbar et al., 2004). Timed matings were conducted to produce *K14-H2B-GFP/K14-Cre/Sox9*$^{flox/flox}$ and *K14-H2B-GFP/K14-Cre/Sox9*$^{flox/+}$ mice at either E18.5 or P0.5 one day prior to FACS isolation. Mice were visually assessed for WT or cKO phenotype based on the presence or absence of whiskers, uniform *K14-H2B-GFP* expression, and sex. *Sox9* genotype and sex were confirmed by PCR. Mice were pooled according to sex and genotype for subsequent cell isolation and FACS acquisition.

Hair follicles from E18.5 and P0.5 *K14-H2B-GFP* WT and *Sox9* cKO mice were isolated according to the method listed in Chapter 2 Materials and Methods, with the following alterations: 1) the low speed follicle isolation spin was conducted at 40g instead of 20g to facilitate harvesting the smaller hair follicles present at early time points; 2) cells were additionally stained with an antibody directed against α6-Integrin (rat PE-conjugated, 1:30, BD-Pharmingen) to facilitate detection of ORS and Mx populations.

RNA isolation and RT-PCR on sorted cell populations

Sorted cell populations were collected in sterile, RNase-free microfuge tubes. After collection, cells (typically 0.5-1.5x10^6) were pelleted by centrifugation at 300g for 5 minutes in a table-top centrifuge and lysed in 500uL of buffer from the Stratagene

RNAeasy Micro-Prep kit. Homogenized lysates were stored at -80°C for variable amounts of time before final processing according to kit protocol. Purified RNA was eluted in RNase-free water and stored for future array hybridization or used for cDNA synthesis and RT-PCR (Chapter 3 Materials and Methods). RT-PCR primers used for ORS and Mx signature genes, early bulge marker genes and sebaceous markers were previously described (Horsley et al., 2008; Nguyen et al., 2006; Rendl et al., 2005; Rhee et al., 2006).

Microarray hybridization and analysis

Skisn from 3-4 male *K14-H2B-GFP/K14-Cre/Sox9*$^{flox/flox}$ and *K14-H2B-GFP/K14-Cre/Sox9*$^{flox/+}$ pups or embryos was processed and subjected to FACS for isolation of ORS and Mx cells. WT and cKO samples were collected during a single sort for each time point. Upon RT-PCR verification of sorted populations and assessment of RNA quality and yield by Bio-Analyzer NanoChip (Agilent) and NanoDrop (Thermo Scientific), 2ug of total RNA from each ORS population was provided to the Genomics Core Laboratory at Memorial Sloan-Kettering Cancer Center for array hybridization. Samples were concentrated, annealed with oligo-dT-T7 primer and subjected to one round of reverse transcription before *in vitro* transcription using T7 RNA polymerase (Ambion). Labeled cRNA samples were hybridized to MOE 430 2.0 mouse expression arrays which were processed and analyzed according to standard Affymetrix protocols.

Microarray data files were imported into GeneChip Operating Software (GCOS 1.1.1.052, Affymetrix), scaled using data from all probe sets to a target signal value of 500, and summarized using the MAS5 algorithm. NetAffyx software was used to cross reference probe IDs with gene names and descriptions. Filtered comparisons between WT and cKO samples for each time point were performed by selecting for probes with minimum absolute fold change ≥ 2, a present call in at least one sample population, and a change p-value ≤ 0.01. Comparisons with previous microarray data were performed in Excel (Office Mac 2004, Microsoft) using existing filtered data sets (Blanpain and Fuchs, 2006; Rendl et al., 2005; Rhee et al., 2006).

FACS analysis of hair follicle cells from Sox9-EGFP/K14-RFP mice

Hair follicles from P4 mice were isolated according to the method listed in Chapter 2 Materials and Methods, except that 4',6-diamidino-2-phenylindole (DAPI) (1:10,000 working dilution of 1mg/ml stock; Molecular Probes) was used for dead cell exclusion instead of propidium iodide. Follicles from single transgenic and WT mice served as FACS compensation controls.

Culture of hair follicle cells from Sox9-EGFP/K14-RFP mice

Cells were collected by FACS under sterile conditions and stained with trypan blue (Sigma) to assess viability before quantification by hemocytometer. Equal numbers of viable cells from each population were seeded onto mitomycin-treated 3T3 fibroblast monolayers and fed every other day with E medium containing 15% serum and 0.3mM

calcium (Rheinwald and Green, 1977). To assess colony size and morphology, cells were fixed with 4% paraformaldehyde and stained with 1% Rhodamine B dye (Sigma). Colony number and area were determined by scanning stained plates on a flatbed scanner (Hewlett Packard) followed by quantification in ImageJ software (NIH).

CHAPTER 5
SUMMARY AND PERSPECTIVES

In order to fulfill its protective role throughout the lifetime of an organism, the mammalian skin epidermis undergoes constant regeneration. In addition to the epidermis itself, associated epithelial structures such as hair and nails, also growth continuously throughout an organism's lifetime. Stem cell populations have long postulated as the mechanism for maintaining this homeostasis (Leblond, 1964). While the regenerative power of epithelial stem cells was convincingly demonstrated decades ago by the treatment of burn patients with transplanted autologous keratinocytes expanded in culture (Gallico et al., 1984; Rheinwald and Green, 1975), the exact identity and location of epithelial stem cells in the skin has only recently become apparent. While multiple populations of stem or progenitor cells appear to exist within the adult skin, only bulge cells from the hair follicle are clearly multipotent, able to give rise to all skin epithelial lineages, and as such, they appear to be the most fully functional stem cells in the skin.

While the identity, roles and molecular regulatory mechanisms for these stem and progenitor populations are starting to become clear, less is known about where epithelial stem cells come from during development and what factors are necessary for their specification. These questions are germane not only to basic biology, which seeks to understand how tissues develop and function, but also to human health, where stem cell biology holds great promise for understanding and treating disease.

The role of stem cells in skin morphogenesis

The results which suggest that stem cells are specified early in hair follicle morphogenesis not only help to complete our current understanding of follicle development, but also highlight notable parallels between follicle morphogenesis and adult hair cycling. While both processes culminate in the same outcome—production of a differentiated hair—they begin at very different starting points. Embryonic follicles develop from an undifferentiated layer of basal epithelial cells that have already activated the program to produce a stratified epidermis. In striking contrast, adult follicles develop from the base of a pre-existing stem cell niche, an anatomically distinct region separate from the interfollicular epidermis and sebaceous glands and unique in its close contact with specialized mesenchymal dermal papilla.

Given these morphological differences, the participation of a stem cell population in embryonic follicle development was not intuitively obvious. However, the fact that both embryonic and adult follicles do appear to rely upon stem cells for proper function suggests that, rather than using separate mechanisms for follicle development and adult hair production, mammals have created a single morphogenetic program for follicle growth, and can activate it either to create a new hair follicle during development or to generate new hairs from an existing follicle later in life. In this regard, one main function of the earliest follicle development steps may simply be to specify an early stem cell population, which is then activated to complete the hair follicle morphogenesis program.

Beyond serving as a mechanism for hair follicle growth, the presence of a stem cell reservoir in the early follicle might also serve as an important backup in the context of injury to the interfollicular epidermis—a plausible occurrence given the lack of protection by a hair coat early in life. In this regard, it is notable that cells derived from early postnatal follicles appear to have a greater capacity to repair the interfollicular epidermis than adult bulge cells. While more definitive experiments using *in vivo* lineage tracing will be required to fully delineate this difference, the ability of cells from early follicles to make seemingly permanent contributions to the interfollicular epidermis suggests a greater developmental plasticity in early follicle stem cells and a greater potential for self-renewal. Determining why these features are lost as stem cells age should provide insight into the intrinsic and extrinsic mechanisms that control epithelial stem cell activity and potential.

While previous studies in the lab uncovered a remarkable similarity between cells in the embryonic placode, representing the first stage of hair follicle morphogenesis, and adult bulge stem cells (Rhee et al., 2006), it is now clear that two distinct populations of cells exist within the placode—one basal population marked by Lhx2 and P-cadherin and one primarily suprabasal population marked by Sox9. Based on genetic marking experiments, it appears that the Lhx2/P-cad cell population is merely transient, and that the Sox9-positive cells eventually give rise to the entire follicle. While both of these populations seem to appear simultaneously in any single placode, the lack of additional markers for the suprabasal Sox9 population and the rapidity of embryonic development

make it difficult to exclude the possibility that one population may give rise to the other. The ability of a *Shh-Cre* transgene, expressed primarily in the basal layer of the placode, to permanently mark most of the cells that give rise to the hair follicle (Levy et al., 2005) suggests that the Lhx2/P-Cad-positive basal population may give rise to the Sox9-positive population within the placode, but wide variability in the reported pattern of *Shh-Cre* transgene labeling leaves this possibility in need of further verification (Gritli-Linde et al., 2007). Examining the expression of additional placode markers with respect to both of these placode populations should provide more insight into the origins and functions of these discrete populations.

The fact that follicle development is initially unimpaired in *Sox9* cKO mice suggests that early SCs are not needed for the initial steps of follicle development and may not be fully specified until after morphogenesis begins. One possibility consistent with the temporal appearance of the cKO phenotype is that the stem population forms at the peg stage of follicle development, concomitant with the appearance of distinct ORS, IRS, and matrix populations. The peg stage is also likely to be the timepoint at which cells begin to migrate within the hair follicle itself, with ORS cells moving down to fuel the matrix, and proliferative matrix cells moving up and differentiating in the center of the follicle even as the whole structure grows deeper into the dermis. Notably, this is also the stage when the quiescence regulator Nfatc1 first appears in follicles, and is the earliest stage at which clear differences in label retention can be visualized in embryonic H2B-

GFP pulse-chase experiments. Given that failure to express Nfatc1 is the earliest detectable phenotype of *Sox9* cKO skin, the peg stage of follicle development is a reasonable starting point to begin future investigations of stem cell specification.

The process of follicle morphogenesis has many similarities to follicle growth in the postnatal hair cycle (Schmidt-Ullrich and Paus, 2005), and an organization similar to that of the two placode populations is reflected in the secondary hair germ and the adult bulge niche, two adjacent but distinct structures that both appear to contribute to postnatal follicle growth. Reflecting the organization of the placode, P-cadherin is highly expressed in the secondary hair germ, but is low in the bulge. While the relative contribution of both of these populations to adult hair growth awaits dissection with inducible lineage tracing tools specific for each population, it is notable that H2B-GFP label retaining studies show ongoing cell division in the bulge niche throughout anagen, suggesting that Sox9-positive adult bulge cells may function in a similar way as Sox9-positive cells in early follicle development. The ability to purify hair germ cells and to compare expression patterns between the two placode residences and the adult bulge and secondary hair germ should help to shed light on the possible similarities between these hair progenitor structures.

Molecular regulation of stem cell identity and activity

Although many genes are known to be important for proper hair follicle morphogenesis and the production of a hair coat, Sox9 is unique in that it is the first

known gene that specifically abrogates the participation of stem cells in follicle development. Furthermore, while numerous genes and signaling pathways have recently been identified which regulate adult stem cell quiescence and activity, Sox9 is the only gene that appears to regulate identity and not activity *per se*. The previously unrecognized finding that stem cells exist early in follicle morphogenesis and do not first appear with the commencement of the adult hair cycle may explain why few genes have been linked thus far to the stem cell specification process. Reassessment of existing follicle development phenotypes in light of this new information about the timing of stem cell specification may uncover previously unappreciated roles for known follicle development genes in SC regulation.

While the current molecular model of bulge stem cell regulation is far from complete, and many new genes will certainly be found to play a part in this process, an overall picture of the stem cell regulatory network is beginning to emerge. This network centers on a group of five transcription factors expressed both in early and adult bulge cells and also receives input from the Wnt and BMP signaling pathways. While Sox9 is essential for essential for stem cell specification, both Lhx2 and Nfatc1 help to maintain adult bulge cells in a quiescent state (Horsley et al., 2008; Rhee et al., 2006). In their absence, Sox9 is still nomally expressed and the bulge stem cell population exists, but shows decreased label retention capability, and accordingly, follicles enter the anagen stage of the hair cycle precociously. While *Nfatc1*-null bulge cells do not show any detectable

alterations in other known bulge markers, *Lhx2*-null bulge cells have greatly decreased CD34 expression. While the significance of CD34 is not yet clear, this result hints that *Lhx2*-null follicles may be impaired in the long term maintenance of established bulge niches. In contrast, Runx1 appears to be important for activation of adult bulge stem cells (Osorio et al., 2008). In its absence, the Sox9-positive bulge population is still present, but is excessively quiescent and cannot be spontaneously activated to drive follicles into anagen. Notably, expression of all three of these bulge cell quiescence regulators is diminished in *Sox9* cKO hair follicles, with Nfatc1 never appearing, Lhx2 gradually being lost and Runx1 being substantially downregulated at an RNA level by E18.5. Taken together, this data suggests that part of Sox9's stem cell specification function involves turning on a group of genes primarily involved in regulating stem cell quiescence and activation.

While functional redundancy and embryonic lethality have thus far precluded analysis of the role of Tcf3 and Tcf4 in bulge stem cells by genetic loss of function experiments, transgenic studies suggest that Tcf3 is an important functional regulator of stem cell identity. When inducibly expressed in early postnatal skin, Tcf3 inhibits the development and terminal differentiation of all three skin epithelial lineages and results in the interfollicular epidermis adopting a gene expression profile reminiscient of adult bulge stem cells. Consistent with a primary role for Tcf3 in repressing differentiation genes and maintaining stemness, the pattern of Sox9 expression was expanded by Tcf3 induced

in the hair follicle and interfollicular epidermis. Together with the fact that Tcf3 expression is gradually lost in *Sox9* cKO follicles, these results suggest a reciprocal regulation of Tcf3 and Sox9 by each other.

Beyond this core group of transcription factors, both Wnt and BMP signaling play specific roles in bulge regulation. In adult follicles, the bulge niche is normally a Wnt-inhibited environment (DasGupta and Fuchs, 1999). However, Wnt signaling appears to be transiently elevated in the bulge and secondary hair germ during the telogen to anagen transition (Merrill et al., 2001), and mice which mimic elevated Wnt signaling by expression of stabilized β-catenin show precocious stem cell activation (Lo Celso et al., 2004; Lowry et al., 2005). In this regard, Wnt signaling functions to periodically instruct bulge cells to enter an activated state to drive follicle growth. Consistent with this model, Sox9 was not detected in a screen for Wnt-regulated genes involved in bulge stem cell activation (Lowry et al., 2005).

In contrast to Wnt signaling, high levels of BMP signaling in the bulge help to maintain bulge quiescence and SC identity. When the BMP receptor gene *BMPr1a* is conditionally ablated in adult skin, otherwise quiescent bulge stem cells lose CD34 expression and begin to proliferate rapidly, expanding the size of the SC niche. While these abnormally activated cells start to express several early hair follicle lineage markers, including Sox4 and Shh (Kobielak et al., 2007), they are blocked in later stages of hair follicle differentiation, and cannot contribute to the hair shaft and IRS lineages (Andl et

al., 2004; Kobielak et al., 2003; Yuhki et al., 2004). Consistent with BMP signaling maintaining bulge cell quiescence, developing *BMPr1a*-null follicles never express the quiescence regulator Nfatc1 (Horsley et al., 2008), but instead display an expansion of Sox9-positive progenitors into the region where the matrix normally resides.

In sum, these results suggest an interdependent regulatory network where Nfatc1, Runx1, and Wnt signaling control stem quiescence, while Tcf3 and Sox9 control stem identity, and Lhx2 and BMP signaling contribute to both of these processes. Given that consensus binding sites for all of the transcription factors involved in this network are known, it should be possible to begin deducing the specific gene regulatory circuits required for stem cell specification and activation, as recently done in embryonic stem cells. While many notable advances have recently been made by studying global gene regulation and genetic reprogramming in embryonic stem cells (Boyer et al., 2005; Mikkelsen et al., 2008), the techniques underlying these advances have yet to be applied to *in vivo* stem cell populations on a large scale. Notably, the ability to isolate pure populations of Sox9-expressing early follicle stem cells using *Sox9-EGFP/K14-RFP* mice allows for recovery of sufficient *in vivo* cellular material to perform microarray and ChIP-on-Chip or ChIP-Seq experiments. By combining ChIP data for several transcription factors with microarray expression profiling of early stem cells, it should be possible to begin deducing the global genetic regulatory network required for hair follicle stem cell specification. Predicted components and relationships in this network could then be

tested by transgenic overexpression or genetic loss of experiments with hair coat formation as one rapidly scored phenotypic readout. While such a network will obviously be specific to skin hair follicle stem cells, it may help to shed light on possible stem cell populations in the wide variety of other epithelial tissues in the body. More generally, it will be interesting to determine how similar the organization of such networks is between different stem cell populations and whether, as is the case for ES cells, expression of a very small, select number of genes is sufficient to activate and stably maintain a complex stem cell identity program (Okita et al., 2007).

Sox9 and stem cells beyond the hair follicle

Beyond hair follicles, a wide variety of glands and structures develop from K14-positive stratified epithelium during embryogenesis. While stem cell populations have been conclusively identified in some of these tissues, such as mammary glands (Shackleton et al., 2006; Stingl et al., 2006), many epithelial tissues remain poorly characterized at the level of cellular homeostasis and regeneration. In contrast to other follicle stem cell markers such as CD34, preliminary observations reveal that Sox9 is expressed in distinct cellular subpopulations of many epithelial derived structures, including mammary glands, eccrine glands, salivary glands and the nail bed. Preliminary analysis of adult *Sox9* cKO mice has revealed a markedly hyperplastic nail phenotype and possible degenerative changes within eccrine glands. The smaller size and delayed milk spot acquisition of newborn cKO mice hints at possible defects in the K14-positive

portion of the digestive tract, which includes salivary glands. Using a combination of *Sox9* cKO, *Sox9-IRES-Cre*, and *Sox9-GFP* mice, it should be possible to determine whether Sox9 plays a functional role in other epithelial structures, and whether its expression generally correlates with stem cell populations or is highly variable and reflects distinct functions in each tissue.

As roles for adult stem cell populations in tissue homeostasis and regeneration become better characterized, recent attention has focused on the possible existence of cancer stem cells which may underlie the vast self-renewal capabilities of tumors. While links between stem cells and cancer have long been postulated in the skin (Ghadially, 1961; Perez-Losada and Balmain, 2003), a recent study has reported the existence of a CD34-positive cancer stem cell population in tumors trigged by a standard two-step DMBA/TPA mouse skin carcinogenesis protocol (Malanchi et al., 2008). Notably, these cancer stem cells, which efficiently reform tumors in transplantation assays, express a number of other bulge stem cells markers, including Sox9, and are dependent upon β-catenin signaling for maintenance of tumorigenic potential. Although the precise origin of these cancer stem cells is unknown, it appears that the molecular regulatory network that controls bulge stem cell behavior may be partially co-opted by stem cells within a skin epithelial tumor.

While DMBA/TPA treatment produces benign papillomas that occasionally progress to squamous cell carcinomas, activating mutations in Shh signaling are a

common cause of basal cell carcinomas (Dlugosz et al., 2002). Abnormal expression of Sox9 can be detected in both pre-malignant regions and within carcinomas generated by forced activation of Shh signaling in mouse skin (Vidal et al., 2005). Notably, Sox9 is also widely expressed in many subtypes of human basal cell carcinoma (Vidal et al., 2008), hinting at the possibility of stem cell populations within spontaneous human cancers. Together, the results that show Sox9 expression in both basal cell carcinomas and squamous cells carcinomas are somewhat surprising given that these two epithelial cancers have different morphologies, clinical behavior and are thought to originate from different cell populations within the skin (Dlugosz et al., 2002). Given Sox9's role as an essential regulatory of stem cell identity, it will be interesting to determine whether Sox9 plays a functional role or identifies stem cells in either basal cell or squamous cell carcinomas from humans.

Regardless of whether they are focused on hair follicles or other tissues in the body, future studies on the capabilities and identity of adult stem cell populations, as well as the molecular mechanisms which regulate them, will provide important insights into the basic biology of organismal development, homeostasis and aging. Perhaps more importantly, these insights will hopefully lead to an improved understanding of human disease as well as scientifically-guided therapies to advance medical care.

REFERENCES

Akiyama, H., Chaboissier, M.C., Martin, J.F., Schedl, A., and de Crombrugghe, B. (2002). The transcription factor Sox9 has essential roles in successive steps of the chondrocyte differentiation pathway and is required for expression of Sox5 and Sox6. Genes Dev *16*, 2813-2828.

Akiyama, H., Kim, J.E., Nakashima, K., Balmes, G., Iwai, N., Deng, J.M., Zhang, Z., Martin, J.F., Behringer, R.R., Nakamura, T., *et al*. (2005). Osteo-chondroprogenitor cells are derived from Sox9 expressing precursors. Proc Natl Acad Sci U S A *102*, 14665-14670.

Akiyama, H., Lyons, J.P., Mori-Akiyama, Y., Yang, X., Zhang, R., Zhang, Z., Deng, J.M., Taketo, M.M., Nakamura, T., Behringer, R.R., *et al*. (2004). Interactions between Sox9 and beta-catenin control chondrocyte differentiation. Genes Dev *18*, 1072-1087.

Alonso, L., and Fuchs, E. (2006). The hair cycle. J Cell Sci *119*, 391-393.

Alonso, L., Okada, H., Pasolli, H.A., Wakeham, A., You-Ten, A.I., Mak, T.W., and Fuchs, E. (2005). Sgk3 links growth factor signaling to maintenance of progenitor cells in the hair follicle. J Cell Biol *170*, 559-570.

Alonso, L.C., and Rosenfield, R.L. (2003). Molecular genetic and endocrine mechanisms of hair growth. Horm Res *60*, 1-13.

Andl, T., Ahn, K., Kairo, A., Chu, E.Y., Wine-Lee, L., Reddy, S.T., Croft, N.J., Cebra-Thomas, J.A., Metzger, D., Chambon, P., *et al*. (2004). Epithelial Bmpr1a regulates differentiation and proliferation in postnatal hair follicles and is essential for tooth development. Development *131*, 2257-2268.

Andl, T., Reddy, S.T., Gaddapara, T., and Millar, S.E. (2002). WNT signals are required for the initiation of hair follicle development. Dev Cell *2*, 643-653.

Arnold, I., and Watt, F.M. (2001). c-Myc activation in transgenic mouse epidermis results in mobilization of stem cells and differentiation of their progeny. Curr Biol *11*, 558-568.

Barrandon, Y., and Green, H. (1987). Three clonal types of keratinocyte with different capacities for multiplication. Proc Natl Acad Sci U S A *84*, 2302-2306.

Bi, W., Deng, J.M., Zhang, Z., Behringer, R.R., and de Crombrugghe, B. (1999). Sox9 is required for cartilage formation. Nat Genet *22*, 85-89.

Bickenbach, J.R. (1981). Identification and behavior of label-retaining cells in oral mucosa and skin. J Dent Res *60 Spec No C*, 1611-1620.

Birnbaum, K.D., and Sanchez Alvarado, A. (2008). Slicing across kingdoms: regeneration in plants and animals. Cell *132*, 697-710.

Blanpain, C., and Fuchs, E. (2006). Epidermal stem cells of the skin. Annual review of cell and developmental biology *22*, 339-373.

Blanpain, C., Horsley, V., and Fuchs, E. (2007). Epithelial Stem Cells: Turning over New Leaves. Cell *128*, 445-458.

Blanpain, C., Lowry, W.E., Geoghegan, A., Polak, L., and Fuchs, E. (2004). Self-renewal, multipotency, and the existence of two cell populations within an epithelial stem cell niche. Cell *118*, 635-648.

Botchkarev, V.A., Botchkareva, N.V., Nakamura, M., Huber, O., Funa, K., Lauster, R., Paus, R., and Gilchrest, B.A. (2001). Noggin is required for induction of the hair follicle growth phase in postnatal skin. Faseb J *15*, 2205-2214.

Botchkarev, V.A., Botchkareva, N.V., Roth, W., Nakamura, M., Chen, L.H., Herzog, W., Lindner, G., McMahon, J.A., Peters, C., Lauster, R., *et al*. (1999). Noggin is a mesenchymally derived stimulator of hair-follicle induction. Nat Cell Biol *1*, 158-164.

Bowles, J., Schepers, G., and Koopman, P. (2000). Phylogeny of the SOX family of developmental transcription factors based on sequence and structural indicators. Dev Biol *227*, 239-255.

Boyer, L.A., Lee, T.I., Cole, M.F., Johnstone, S.E., Levine, S.S., Zucker, J.P., Guenther, M.G., Kumar, R.M., Murray, H.L., Jenner, R.G., *et al*. (2005). Core transcriptional regulatory circuitry in human embryonic stem cells. Cell *122*, 947-956.

Braun, K.M., Niemann, C., Jensen, U.B., Sundberg, J.P., Silva-Vargas, V., and Watt, F.M. (2003). Manipulation of stem cell proliferation and lineage commitment: visualisation of label-retaining cells in wholemounts of mouse epidermis. Development *130*, 5241-5255.

Bullough, W.S. (1962a). Growth control in mammalian skin. Nature *193*, 520-523.

Bullough, W.S. (1962b). The control of mitotic activity in adult mammalian tissues. Biol Rev Camb Philos Soc *37*, 307-342.

Busslinger, M. (2004). Transcriptional control of early B cell development. Annu Rev Immunol *22*, 55-79.

Byrne, C., Tainsky, M., and Fuchs, E. (1994). Programming gene expression in developing epidermis. Development *120*, 2369-2383.

Chaboissier, M.C., Kobayashi, A., Vidal, V.I., Lutzkendorf, S., van de Kant, H.J., Wegner, M., de Rooij, D.G., Behringer, R.R., and Schedl, A. (2004). Functional analysis of Sox8 and Sox9 during sex determination in the mouse. Development *131*, 1891-1901.

Chase, H.B. (1954). Growth of the hair. Physiol Rev *34*, 113-126.

Chiang, C., Swan, R.Z., Grachtchouk, M., Bolinger, M., Litingtung, Y., Robertson, E.K., Cooper, M.K., Gaffield, W., Westphal, H., Beachy, P.A., *et al*. (1999). Essential role for Sonic hedgehog during hair follicle morphogenesis. Dev Biol *205*, 1-9.

Claudinot, S., Nicolas, M., Oshima, H., Rochat, A., and Barrandon, Y. (2005). Long-term renewal of hair follicles from clonogenic multipotent stem cells. Proc Natl Acad Sci U S A *102*, 14677-14682.

Clayton, E., Doupe, D.P., Klein, A.M., Winton, D.J., Simons, B.D., and Jones, P.H. (2007). A single type of progenitor cell maintains normal epidermis. Nature *446*, 185-189.

Cotsarelis, G. (2006). Epithelial stem cells: a folliculocentric view. J Invest Dermatol *126*, 1459-1468.

Cotsarelis, G., Sun, T.T., and Lavker, R.M. (1990). Label-retaining cells reside in the bulge area of pilosebaceous unit: implications for follicular stem cells, hair cycle, and skin carcinogenesis. Cell *61*, 1329-1337.

DasGupta, R., and Fuchs, E. (1999). Multiple roles for activated LEF/TCF transcription complexes during hair follicle development and differentiation. Development *126*, 4557-4568.

Dlugosz, A., Merlino, G., and Yuspa, S.H. (2002). Progress in cutaneous cancer research. J Investig Dermatol Symp Proc *7*, 17-26.

Dor, Y., Brown, J., Martinez, O.I., and Melton, D.A. (2004). Adult pancreatic beta-cells are formed by self-duplication rather than stem-cell differentiation. Nature *429*, 41-46.

Foster, J.W., Dominguez-Steglich, M.A., Guioli, S., Kowk, G., Weller, P.A., Stevanovic, M., Weissenbach, J., Mansour, S., Young, I.D., Goodfellow, P.N., *et al*. (1994). Campomelic dysplasia and autosomal sex reversal caused by mutations in an SRY-related gene. Nature *372*, 525-530.

Fuchs, E. (2007). Scratching the surface of skin development. Nature *445*, 834-842.

Fuchs, E. (2008). Skin stem cells: rising to the surface. J Cell Biol *180*, 273-284.

Fuchs, E., and Raghavan, S. (2002). Getting under the skin of epidermal morphogenesis. Nat Rev Genet *3*, 199-209.

Fuchs, E., Tumbar, T., and Guasch, G. (2004). Socializing with the neighbors: stem cells and their niche. Cell *116*, 769-778.

Gallico, G.G., 3rd, O'Connor, N.E., Compton, C.C., Kehinde, O., and Green, H. (1984). Permanent coverage of large burn wounds with autologous cultured human epithelium. N Engl J Med *311*, 448-451.

Gat, U., DasGupta, R., Degenstein, L., and Fuchs, E. (1998). De Novo hair follicle morphogenesis and hair tumors in mice expressing a truncated beta-catenin in skin. Cell *95*, 605-614.

Ghadially, F.N. (1961). The role of the hair follicle in the origin and evolution of some cutaneous neoplasms of man and experimental animals. Cancer *14*, 801-816.

Ghazizadeh, S., and Taichman, L.B. (2001). Multiple classes of stem cells in cutaneous epithelium: a lineage analysis of adult mouse skin. Embo J *20*, 1215-1222.

Gritli-Linde, A., Hallberg, K., Harfe, B.D., Reyahi, A., Kannius-Janson, M., Nilsson, J., Cobourne, M.T., Sharpe, P.T., McMahon, A.P., and Linde, A. (2007). Abnormal hair development and apparent follicular transformation to mammary gland in the absence of hedgehog signaling. Dev Cell *12*, 99-112.

Hardy, M.H. (1992). The secret life of the hair follicle. Trends Genet *8*, 55-61.

Hirai, Y., Nose, A., Kobayashi, S., and Takeichi, M. (1989). Expression and role of E- and P-cadherin adhesion molecules in embryonic histogenesis. II. Skin morphogenesis. Development *105*, 271-277.

Hong, C.S., and Saint-Jeannet, J.P. (2005). Sox proteins and neural crest development. Semin Cell Dev Biol *16*, 694-703.

Horsley, V., Aliprantis, A.O., Polak, L., Glimcher, L.H., and Fuchs, E. (2008). NFATc1 balances quiescence and proliferation of skin stem cells. Cell *132*, 299-310.

Horsley, V., O'Carroll, D., Tooze, R., Ohinata, Y., Saitou, M., Obukhanych, T., Nussenzweig, M., Tarakhovsky, A., and Fuchs, E. (2006). Blimp1 defines a progenitor population that governs cellular input to the sebaceous gland. Cell *126*, 597-609.

Huelsken, J., and Birchmeier, W. (2001). New aspects of Wnt signaling pathways in higher vertebrates. Curr Opin Genet Dev *11*, 547-553.

Huelsken, J., Vogel, R., Erdmann, B., Cotsarelis, G., and Birchmeier, W. (2001). beta-Catenin controls hair follicle morphogenesis and stem cell differentiation in the skin. Cell *105*, 533-545.

Ikeda, T., Kawaguchi, H., Kamekura, S., Ogata, N., Mori, Y., Nakamura, K., Ikegawa, S., and Chung, U.I. (2005). Distinct roles of Sox5, Sox6, and Sox9 in different stages of chondrogenic differentiation. J Bone Miner Metab *23*, 337-340.

Ito, M., Kizawa, K., Hamada, K., and Cotsarelis, G. (2004). Hair follicle stem cells in the lower bulge form the secondary germ, a biochemically distinct but functionally equivalent progenitor cell population, at the termination of catagen. Differentiation; research in biological diversity *72*, 548-557.

Ito, M., Liu, Y., Yang, Z., Nguyen, J., Liang, F., Morris, R.J., and Cotsarelis, G. (2005). Stem cells in the hair follicle bulge contribute to wound repair but not to homeostasis of the epidermis. Nature medicine *11*, 1351-1354.

Ito, M., Yang, Z., Andl, T., Cui, C., Kim, N., Millar, S.E., and Cotsarelis, G. (2007). Wnt-dependent de novo hair follicle regeneration in adult mouse skin after wounding. Nature *447*, 316-320.

Jahoda, C.A., Horne, K.A., and Oliver, R.F. (1984). Induction of hair growth by implantation of cultured dermal papilla cells. Nature *311*, 560-562.

Jamora, C., DasGupta, R., Kocieniewski, P., and Fuchs, E. (2003). Links between signal transduction, transcription and adhesion in epithelial bud development. Nature *422*, 317-322.

Joseph, N.M., and Morrison, S.J. (2005). Toward an understanding of the physiological function of Mammalian stem cells. Dev Cell *9*, 173-183.

Kanda, T., Sullivan, K.F., and Wahl, G.M. (1998). Histone-GFP fusion protein enables sensitive analysis of chromosome dynamics in living mammalian cells. Curr Biol *8*, 377-385.

Kligman, A.M. (1959). The human hair cycle. J Invest Dermatol *33*, 307-316.

Kobielak, K., Pasolli, H.A., Alonso, L., Polak, L., and Fuchs, E. (2003). Defining BMP functions in the hair follicle by conditional ablation of BMP receptor IA. J Cell Biol *163*, 609-623.

Kobielak, K., Stokes, N., de la Cruz, J., Polak, L., and Fuchs, E. (2007). Loss of a quiescent niche but not follicle stem cells in the absence of bone morphogenetic protein signaling. Proc Natl Acad Sci U S A *104*, 10063-10068.

Kopan, R., Lee, J., Lin, M.H., Syder, A.J., Kesterson, J., Crutchfield, N., Li, C.R., Wu, W., Books, J., and Gordon, J.I. (2002). Genetic mosaic analysis indicates that the bulb region of coat hair follicles contains a resident population of several active multipotent epithelial lineage progenitors. Dev Biol *242*, 44-57.

Langton, A.K., Herrick, S.E., and Headon, D.J. (2008). An extended epidermal response heals cutaneous wounds in the absence of a hair follicle stem cell contribution. J Invest Dermatol *128*, 1311-1318.

Laurikkala, J., Mikkola, M., Mustonen, T., Aberg, T., Koppinen, P., Pispa, J., Nieminen, P., Galceran, J., Grosschedl, R., and Thesleff, I. (2001). TNF signaling via the ligand-receptor pair ectodysplasin and edar controls the function of epithelial signaling centers and is regulated by Wnt and activin during tooth organogenesis. Dev Biol *229*, 443-455.

Leblond, C.P. (1964). Classification of Cell Populations on the Basis of Their Proliferative Behavior. Natl Cancer Inst Monogr *14*, 119-150.

Lechler, T., and Fuchs, E. (2005). Asymmetric cell divisions promote stratification and differentiation of mammalian skin. Nature *437*, 275-280.

Lefebvre, V., Dumitriu, B., Penzo-Mendez, A., Han, Y., and Pallavi, B. (2007). Control of cell fate and differentiation by Sry-related high-mobility-group box (Sox) transcription factors. Int J Biochem Cell Biol *39*, 2195-2214.

Levy, V., Lindon, C., Harfe, B.D., and Morgan, B.A. (2005). Distinct stem cell populations regenerate the follicle and interfollicular epidermis. Dev Cell *9*, 855-861.

Levy, V., Lindon, C., Zheng, Y., Harfe, B.D., and Morgan, B.A. (2007a). Epidermal stem cells arise from the hair follicle after wounding. Faseb J *21*, 1358-1366.

Levy, V., Lindon, C., Zheng, Y., Harfe, B.D., and Morgan, B.A. (2007b). Epidermal stem cells arise from the hair follicle after wounding. Faseb J *21*, 1-9.

Liu, Y., Lyle, S., Yang, Z., and Cotsarelis, G. (2003). Keratin 15 promoter targets putative epithelial stem cells in the hair follicle bulge. J Invest Dermatol *121*, 963-968.

Lo Celso, C., Prowse, D.M., and Watt, F.M. (2004). Transient activation of beta-catenin signalling in adult mouse epidermis is sufficient to induce new hair follicles but continuous activation is required to maintain hair follicle tumours. Development *131*, 1787-1799.

Logan, C.Y., and Nusse, R. (2004). The Wnt signaling pathway in development and disease. Annual review of cell and developmental biology *20*, 781-810.

Lowry, W.E., Blanpain, C., Nowak, J.A., Guasch, G., Lewis, L., and Fuchs, E. (2005). Defining the impact of beta-catenin/Tcf transactivation on epithelial stem cells. Genes Dev *19*, 1596-1611.

Luger, K., and Hansen, J.C. (2005). Nucleosome and chromatin fiber dynamics. Curr Opin Struct Biol *15*, 188-196.

Malanchi, I., Peinado, H., Kassen, D., Hussenet, T., Metzger, D., Chambon, P., Huber, M., Hohl, D., Cano, A., Birchmeier, W., *et al*. (2008). Cutaneous cancer stem cell maintenance is dependent on beta-catenin signalling. Nature *452*, 650-653.

Mao, X., Fujiwara, Y., and Orkin, S.H. (1999). Improved reporter strain for monitoring Cre recombinase-mediated DNA excisions in mice. Proc Natl Acad Sci U S A *96*, 5037-5042.

Maretto, S., Cordenonsi, M., Dupont, S., Braghetta, P., Broccoli, V., Hassan, A.B., Volpin, D., Bressan, G.M., and Piccolo, S. (2003). Mapping Wnt/beta-catenin signaling during mouse development and in colorectal tumors. Proc Natl Acad Sci U S A *100*, 3299-3304.

Merrill, B.J., Gat, U., DasGupta, R., and Fuchs, E. (2001). Tcf3 and Lef1 regulate lineage differentiation of multipotent stem cells in skin. Genes Dev *15*, 1688-1705.

Michalopoulos, G.K. (2007). Liver regeneration. J Cell Physiol *213*, 286-300.

Mikkelsen, T.S., Hanna, J., Zhang, X., Ku, M., Wernig, M., Schorderet, P., Bernstein, B.E., Jaenisch, R., Lander, E.S., and Meissner, A. (2008). Dissecting direct reprogramming through integrative genomic analysis. Nature *454*, 49-55.

Mikkola, M.L. (2007). Genetic basis of skin appendage development. Semin Cell Dev Biol *18*, 225-236.

Millar, S.E. (2002). Molecular mechanisms regulating hair follicle development. J Invest Dermatol *118*, 216-225.

Ming Kwan, K., Li, A.G., Wang, X.J., Wurst, W., and Behringer, R.R. (2004). Essential roles of BMPR-IA signaling in differentiation and growth of hair follicles and in skin tumorigenesis. Genesis *39*, 10-25.

Montagna, W., and Chase, H.B. (1956). Histology and cytochemistry of human skin. X. X-irradiation of the scalp. Am J Anat *99*, 415-445.

Morgan, B.A., Orkin, R.W., Noramly, S., and Perez, A. (1998). Stage-specific effects of sonic hedgehog expression in the epidermis. Dev Biol *201*, 1-12.

Morris, R.J., Liu, Y., Marles, L., Yang, Z., Trempus, C., Li, S., Lin, J.S., Sawicki, J.A., and Cotsarelis, G. (2004). Capturing and profiling adult hair follicle stem cells. Nat Biotechnol *22*, 411-417.

Morris, R.J., and Potten, C.S. (1999). Highly persistent label-retaining cells in the hair follicles of mice and their fate following induction of anagen. J Invest Dermatol *112*, 470-475.

Muller-Rover, S., Handjiski, B., van der Veen, C., Eichmuller, S., Foitzik, K., McKay, I.A., Stenn, K.S., and Paus, R. (2001). A comprehensive guide for the accurate classification of murine hair follicles in distinct hair cycle stages. J Invest Dermatol *117*, 3-15.

Nguyen, H., Rendl, M., and Fuchs, E. (2006). Tcf3 governs stem cell features and represses cell fate determination in skin. Cell *127*, 171-183.

Nowak, J.A., Polak, L., Pasolli, H.A., and Fuchs, E. (2008). Hair follicle stem cells are specified and function in early skin morphogenesis. Cell Stem Cell *3*, 33-43.

Okita, K., Ichisaka, T., and Yamanaka, S. (2007). Generation of germline-competent induced pluripotent stem cells. Nature *448*, 313-317.

Oliver, R.F. (1966a). Histological studies of whisker regeneration in the hooded rat. J Embryol Exp Morphol *16*, 231-244.

Oliver, R.F. (1966b). Whisker growth after removal of the dermal papilla and lengths of follicle in the hooded rat. J Embryol Exp Morphol *15*, 331-347.

Oliver, R.F. (1967). The experimental induction of whisker growth in the hooded rat by implantation of dermal papillae. J Embryol Exp Morphol *18*, 43-51.

Orkin, S.H., and Zon, L.I. (2008). Hematopoiesis: an evolving paradigm for stem cell biology. Cell *132*, 631-644.

Oro, A.E., and Higgins, K. (2003). Hair cycle regulation of Hedgehog signal reception. Dev Biol *255*, 238-248.

Oro, A.E., Higgins, K.M., Hu, Z., Bonifas, J.M., Epstein, E.H., Jr., and Scott, M.P. (1997). Basal cell carcinomas in mice overexpressing sonic hedgehog. Science *276*, 817-821.

Oshima, H., Rochat, A., Kedzia, C., Kobayashi, K., and Barrandon, Y. (2001). Morphogenesis and renewal of hair follicles from adult multipotent stem cells. Cell *104*, 233-245.

Osorio, K.M., Lee, S.E., McDermitt, D.J., Waghmare, S.K., Zhang, Y.V., Woo, H.N., and Tumbar, T. (2008). Runx1 modulates developmental, but not injury-driven, hair follicle stem cell activation. Development *135*, 1059-1068.

Panteleyev, A.A., Jahoda, C.A., and Christiano, A.M. (2001). Hair follicle predetermination. J Cell Sci *114*, 3419-3431.

Pelc, S.R. (1964). Labelling of DNA and Cell Division in So Called Non-Dividing Tissues. J Cell Biol *22*, 21-28.

Pellettieri, J., and Sanchez Alvarado, A. (2007). Cell turnover and adult tissue homeostasis: from humans to planarians. Annu Rev Genet *41*, 83-105.

Perez-Losada, J., and Balmain, A. (2003). Stem-cell hierarchy in skin cancer. Nat Rev Cancer *3*, 434-443.

Pinkus, H., Mehregan, A.H.H. (1981). A Guide to Dermatohistopathology (New York, Appleton Century Crafts).

Plikus, M.V., Mayer, J.A., de la Cruz, D., Baker, R.E., Maini, P.K., Maxson, R., and Chuong, C.M. (2008). Cyclic dermal BMP signalling regulates stem cell activation during hair regeneration. Nature *451*, 340-344.

Potten, C.S. (1974). The epidermal proliferative unit: the possible role of the central basal cell. Cell Tissue Kinet *7*, 77-88.

Potten, C.S. (1975). Epidermal transit times. The British journal of dermatology *93*, 649-658.

Potten, C.S., Jessup, B.A., and Croxson, M.B. (1971). Incorporation of tritiated thymidine into the skin and hair follicles. I. Oscillatory changes through the hair growth cycle. Cell Tissue Kinet *4*, 241-254.

Pummila, M., Fliniaux, I., Jaatinen, R., James, M.J., Laurikkala, J., Schneider, P., Thesleff, I., and Mikkola, M.L. (2007). Ectodysplasin has a dual role in ectodermal organogenesis: inhibition of Bmp activity and induction of Shh expression. Development *134*, 117-125.

Rando, T.A. (2006). Stem cells, ageing and the quest for immortality. Nature *441*, 1080-1086.

Rendl, M., Lewis, L., and Fuchs, E. (2005). Molecular dissection of mesenchymal-epithelial interactions in the hair follicle. PLoS Biol *3*, e331.

Rhee, H., Polak, L., and Fuchs, E. (2006). Lhx2 maintains stem cell character in hair follicles. Science *312*, 1946-1949.

Rheinwald, J.G., and Green, H. (1975). Serial cultivation of strains of human epidermal keratinocytes: the formation of keratinizing colonies from single cells. Cell *6*, 331-343.

Rheinwald, J.G., and Green, H. (1977). Epidermal growth factor and the multiplication of cultured human epidermal keratinocytes. Nature *265*, 421-424.

Sanchez Alvarado, A. (2000). Regeneration in the metazoans: why does it happen? Bioessays *22*, 578-590.

Schmidt-Supprian, M., and Rajewsky, K. (2007). Vagaries of conditional gene targeting. Nat Immunol *8*, 665-668.

Schmidt-Ullrich, R., and Paus, R. (2005). Molecular principles of hair follicle induction and morphogenesis. Bioessays *27*, 247-261.

Shackleton, M., Vaillant, F., Simpson, K.J., Stingl, J., Smyth, G.K., Asselin-Labat, M.L., Wu, L., Lindeman, G.J., and Visvader, J.E. (2006). Generation of a functional mammary gland from a single stem cell. Nature *439*, 84-88.

Sharov, A.A., Sharova, T.Y., Mardaryev, A.N., Tommasi di Vignano, A., Atoyan, R., Weiner, L., Yang, S., Brissette, J.L., Dotto, G.P., and Botchkarev, V.A. (2006). Bone morphogenetic protein signaling regulates the size of hair follicles and modulates the expression of cell cycle-associated genes. Proc Natl Acad Sci U S A *103*, 18166-18171.

Slominski, A., Wortsman, J., Plonka, P.M., Schallreuter, K.U., Paus, R., and Tobin, D.J. (2005). Hair follicle pigmentation. J Invest Dermatol *124*, 13-21.

St-Jacques, B., Dassule, H.R., Karavanova, I., Botchkarev, V.A., Li, J., Danielian, P.S., McMahon, J.A., Lewis, P.M., Paus, R., and McMahon, A.P. (1998). Sonic hedgehog signaling is essential for hair development. Curr Biol *8*, 1058-1068.

Stenn, K.S., and Paus, R. (2001). Controls of hair follicle cycling. Physiol Rev *81*, 449-494.

Stewart, M.E. (1992). Sebaceous gland lipids. Semin Dermatol *11*, 100-105.

Stingl, J., Eirew, P., Ricketson, I., Shackleton, M., Vaillant, F., Choi, D., Li, H.I., and Eaves, C.J. (2006). Purification and unique properties of mammary epithelial stem cells. Nature *439*, 993-997.

Sudbeck, P., Schmitz, M.L., Baeuerle, P.A., and Scherer, G. (1996). Sex reversal by loss of the C-terminal transactivation domain of human SOX9. Nat Genet *13*, 230-232.

Taylor, G., Lehrer, M.S., Jensen, P.J., Sun, T.T., and Lavker, R.M. (2000). Involvement of follicular stem cells in forming not only the follicle but also the epidermis. Cell *102*, 451-461.

Trempus, C.S., Morris, R.J., Bortner, C.D., Cotsarelis, G., Faircloth, R.S., Reece, J.M., and Tennant, R.W. (2003). Enrichment for living murine keratinocytes from the hair follicle bulge with the cell surface marker CD34. J Invest Dermatol *120*, 501-511.

Trempus, C.S., Morris, R.J., Ehinger, M., Elmore, A., Bortner, C.D., Ito, M., Cotsarelis, G., Nijhof, J.G., Peckham, J., Flagler, N., *et al*. (2007). CD34 expression by hair follicle stem cells is required for skin tumor development in mice. Cancer Res *67*, 4173-4181.

Tsonis, P.A. (2000). Regeneration in vertebrates. Dev Biol *221*, 273-284.

Tumbar, T., Guasch, G., Greco, V., Blanpain, C., Lowry, W.E., Rendl, M., and Fuchs, E. (2004). Defining the epithelial stem cell niche in skin. Science *303*, 359-363.

van Genderen, C., Okamura, R.M., Farinas, I., Quo, R.G., Parslow, T.G., Bruhn, L., and Grosschedl, R. (1994). Development of several organs that require inductive epithelial-mesenchymal interactions is impaired in LEF-1-deficient mice. Genes Dev *8*, 2691-2703.

Van Mater, D., Kolligs, F.T., Dlugosz, A.A., and Fearon, E.R. (2003). Transient activation of beta -catenin signaling in cutaneous keratinocytes is sufficient to trigger the active growth phase of the hair cycle in mice. Genes Dev *17*, 1219-1224.

Vasioukhin, V., Degenstein, L., Wise, B., and Fuchs, E. (1999). The magical touch: genome targeting in epidermal stem cells induced by tamoxifen application to mouse skin. Proc Natl Acad Sci U S A *96*, 8551-8556.

Vidal, V.P., Chaboissier, M.C., Lutzkendorf, S., Cotsarelis, G., Mill, P., Hui, C.C., Ortonne, N., Ortonne, J.P., and Schedl, A. (2005). Sox9 is essential for outer root sheath differentiation and the formation of the hair stem cell compartment. Curr Biol *15*, 1340-1351.

Vidal, V.P., Ortonne, N., and Schedl, A. (2008). SOX9 expression is a general marker of basal cell carcinoma and adnexal-related neoplasms. J Cutan Pathol *35*, 373-379.

Waghmare, S.K., Bansal, R., Lee, J., Zhang, Y.V., McDermitt, D.J., and Tumbar, T. (2008). Quantitative proliferation dynamics and random chromosome segregation of hair follicle stem cells. EMBO J *27*, 1309-1320.

Wagner, T., Wirth, J., Meyer, J., Zabel, B., Held, M., Zimmer, J., Pasantes, J., Bricarelli, F.D., Keutel, J., Hustert, E.*, et al*. (1994). Autosomal sex reversal and campomelic dysplasia are caused by mutations in and around the SRY-related gene SOX9. Cell *79*, 1111-1120.

Waikel, R.L., Kawachi, Y., Waikel, P.A., Wang, X.J., and Roop, D.R. (2001). Deregulated expression of c-Myc depletes epidermal stem cells. Nat Genet *28*, 165-168.

Wegner, M. (1999). From head to toes: the multiple facets of Sox proteins. Nucleic Acids Res *27*, 1409-1420.

Wegner, M., and Stolt, C.C. (2005). From stem cells to neurons and glia: a Soxist's view of neural development. Trends Neurosci *28*, 583-588.

Wilson, C., Cotsarelis, G., Wei, Z.G., Fryer, E., Margolis-Fryer, J., Ostead, M., Tokarek, R., Sun, T.T., and Lavker, R.M. (1994). Cells within the bulge region of mouse hair follicle transiently proliferate during early anagen: heterogeneity and functional differences of various hair cycles. Differentiation; research in biological diversity *55*, 127-136.

Yuhki, M., Yamada, M., Kawano, M., Iwasato, T., Itohara, S., Yoshida, H., Ogawa, M., and Mishina, Y. (2004). BMPR1A signaling is necessary for hair follicle cycling and hair shaft differentiation in mice. Development *131*, 1825-1833.

Zhang, J., He, X.C., Tong, W.G., Johnson, T., Wiedemann, L.M., Mishina, Y., Feng, J.Q., and Li, L. (2006). Bone morphogenetic protein signaling inhibits hair follicle anagen induction by restricting epithelial stem/progenitor cell activation and expansion. Stem Cells *24*, 2826-2839.

Zhou, P., Byrne, C., Jacobs, J., and Fuchs, E. (1995). Lymphoid enhancer factor 1 directs hair follicle patterning and epithelial cell fate. Genes Dev *9*, 700-713.